Evaluation of morphological and functional changes in placental villi and trophoblast cells in response to *Plasmodium falciparum* infection

CAROLINA LÓPEZ GUZMÁN

Thesis presented to qualify for the title of
Doctor in Basic Biomedical Sciences
with an emphasis on Microbiology and Parasitology

Evaluation of morphological and functional changes in placental villi and trophoblast cells in response to *Plasmodium falciparum* infection

CAROLINA LÓPEZ GUZMÁN

Thesis presented to qualify for the title of
Doctor in Basic Biomedical Sciences
with an emphasis on Microbiology and Parasitology

Ana Vásquez
Tutor

Tatiana Lopera
Cesar Segura
Julio Bueno
Gabriel Vélez
Miguel Ángel Mendivil
Tutorial Committee

Acknowledgments

To God, for never leaving me alone.

To my family, who are always my strength and support, especially my husband, my son, and my mother, who have been by my side in both good and not-so-good moments.

A special dedication to my son, the one who taught me that for God, nothing is impossible.

To the University of Antioquia, which opened the doors to this fascinating, challenging, and enriching academic world.

To the Malaria group for allowing me to be a member and learn with every experimental challenge that came with the doctoral journey.

To Professor Ana Vasquez, whom I consider an academic guide and a role model, always encouraging and supporting me to successfully achieve this dream.

To the tutorial committee, for their support every semester.

To my group mates who were a significant part of my growth as a person and a professional.

To Colciencias and Regalias for financing this academic and professional period.

Thank you very much!

Table of Contents

List of abbreviations and acronyms

cDNA: Complementary deoxyribonucleic acid.

AMPc: Cyclic adenosine monophosphate.

Ang 1/2: Angiopoietins 1 and 2

βhCG: Beta hCG subunit.

CTB: Cytotrophoblast cells, (BeWo CTB).

CM: Congenital malaria.

CSA: Chondroitin sulfate A.

DMSO: Dimethyl sulfoxide.

END: Endoglin.

ECM: Extracellular matrix.

ERVWE1: Syncytin 1 human fusogenic glycoprotein.

EVT: Extravillous trophoblast.

FSK: Forskolin

GM: Gestational malaria.

HPEs: Human placental explants.

hPL: Human placental lactogen.

Hz: Hemozoin.

iE: Erythrocytes infected with *P. falciparum*.

Ig: Immunoglobulin.

IL: Interleukin.

IFN-γ: Interferon gamma.

IUGR: Intrauterine growth restriction.

PM: Placental malaria.

LGALS13: Placental alkaline phosphatase.

LBW: Low Birth Weight.

MCP-1: Monocyte chemotactic protein-1.

MIP-1α, MIP-1β: Macrophage inflammatory proteins.

MN: Mononuclear.

NF-κB: Nuclear factor kappa-light-chain-enhancer of activated B cells.

NK: Natural killer.

STB: Syncytiotrophoblast, (BeWo STB).

PfEMP1: *P. falciparum* erythrocyte membrane protein 1.

PlGF: Placental growth factor.

PMN: Polymorphonuclear neutrophils.

qPCR: Quantitative real-time polymerase chain reaction.

RNA: Ribonucleic acid.

Th1/Th2: T lymphocytes (T helper 1/ T helper 2.

Th17: Proinflammatory subpopulation of CD4+ T lymphocytes, primarily producing IL-17.

Tie2: Tyrosine kinase receptors of angiopoietins.

TNF: Tumor necrosis factor.

Treg: T regulatory cells.

DV: Digestive vacuole.

VEGF: Vascular endothelial growth factor, also known as VEGF-A.

VEGFR-1: Vascular endothelial growth factor receptor 1, also known as FLT-1.

List of Figures

Figure 1. Life cycle of *Plasmodium* spp.

Figure 2. Maternal-fetal interface and placental barrier.

Figure 3. Molecular changes that occur during trophoblast differentiation down to the syncytiotrophoblast or extravillous trophoblast lineages.

Figure 4. Cytotrophoblasts in various stages of their life cycle: proliferating, differentiating, and fusing.

Figure 5. Sequestration of infected erythrocytes within the intervillous space of the placenta.

Figure 6. Placental malaria induces alterations in placental tissue and disrupts the normal balance of angiogenic and inflammatory mediators.

Figure 7. Proposed pathway of forskolin-mediated BeWo cell fusion.

Figure 8. Schematic representation of the FSK stimulus added to BeWo cells for syncytialization induction.

Figure 9. Mitochondrial activity assessed by the MTT assay is proportional to the number of cells present in the culture.

Figure 10. Production of βhCG increases in BeWo cells with forskolin stimulation.

Figure 11. Positive correlation between manual nucleus counts and automated count using MATLAB software.

Figure 12. Evaluation of syncytialization index through E-Cadherin expression.

Figure 13. The expression of Ki67 decreases in cells that have undergone differentiation into syncytiotrophoblast.

Figure 14. Increased apoptosis in differentiated cytotrophoblast cells transitioning to syncytiotrophoblast.

Figure 15. Expression levels of the SYN-1, SYN-2, and βhCG genes in treated cells compared to control cells evaluated by qPCR.

Figure 16. The expression of chondroitin sulfate A does not differ in cytotrophoblast and syncytiotrophoblast cells.

Figure 17. The differentiation model of cytotrophoblast to syncytiotrophoblast was optimized.

Figure 18. Exposures of BeWo cells to *P. falciparum.*

Figure 19. The cytoadherence of *P. falciparum*-CSA+ is supported by cytotrophoblast cells and syncytiotrophoblast.

Figure 20. BeWo cells syncytiotrophoblast exhibit significant changes in LDH activity when exposed to *P. falciparum*.

Figure 21. Measurement of hCG in syncytiotrophoblast in co-culture with erythrocytes parasitized by *P. falciparum* does not change compared to control.

Figure 22. Exposure to *P. falciparum* decreases syncytialization index in syncytiotrophoblast.

Figure 23. Frequency of Ki67-positive nuclei in syncytiotrophoblast cells exposed to *P. falciparum*-IE.

Figure 24. The expression of M30 does not change in syncytiotrophoblast cells exposed to *P. falciparum*-IE.

Figure 25. Expression levels of the SYN-1, SYN-2, and βhCG genes in treated cells versus control cells evaluated by qPCR.

Figure 26. The process of cell fusion was not carried out properly when CTB cells were simultaneously exposed to FSK and *P. falciparum*-IE.

Figure 27. Procedure for isolating human placenta villous.

Figure 28. Graphical description of co-culture of human placental explants with infected erythrocytes.

Figure 29. LDH activity and βhCG production in human placental explants exposed to *P. falciparum ex vivo.*

Figure 30. *P. falciparum* causes histological damage in human placental explants exposed *ex vivo*.

Figure 31. The exposure to *P. falciparum-iE* disrupts collagen in the villous stroma of human placental explants exposed *ex vivo* and induces an increase in regions with thickened trophoblast basal lamina.

Figure 32. The exposure to *P. falciparum*-iE does not significantly affect the cellular apoptosis of human placental explants exposed *ex vivo*.

Figure 33: Process for the natural hemozoin isolation using magnetic column.

Figure 34. Morphological characterization of natural hemozoin.

Figure 35. Natural hemozoin induces a downward trend in hCG but does not alter LDH activity in *ex vivo*-exposed Human placental explants.

Figure 36. Natural hemozoin increases histological damage in *ex vivo*-exposed Human placental explants.

Figure 37. Natural hemozoin disrupts the collagen distribution in the villous stroma of *ex vivo* exposed Human placental explants.

Figure 38. Natural hemozoin increases cellular apoptosis in *ex vivo* exposed human placental explants.

Figure 39. Description of study groups formed with tissues from naturally exposed pregnant women.

Figure 40. Classification of *P. falciparum* infection in the placenta.

Figure 41. The exposure to *P. falciparum*-iE causes histological damage in Human placental exposed *in vivo.*

Figure 42. The exposure to *P. falciparum*-iE disrupts collagen in the stroma of human placental exposed *in vivo.*

Figure 43. The exposure to *P. falciparum*-iE affects the cellular apoptosis of human placental exposed *in vivo.*

Figure 44. Possible mechanism of *P. falciparum* placental pathogenesis built from results obtained using various methodological approaches and supported by evidence from previous studies.

List of Tables

Table 1. Description of the key steps in the differentiation of the syncytiotrophoblast from the cytotrophoblast.

Table 2. Description of the main functions of the components produced by the syncytiotrophoblast.

Table 3. Classification of placental pathology.

Table 4. Description of the main types of models for studying the placenta.

Table 5. The primer sequences of the various syncytialization mediators used for qPCR.

Table 6. Scores for the analysis of the histopathological damage.

Table 7. Evaluation of placental villous integrity by histology.

Table 8. Evaluation of trophoblast epithelium through CK-7 staining.

Table 9. Score for the analysis of collagen organization in the villous stroma.

Table 10. Primer sequences for amplifying differentiation and inflammatory mediators.

Table 11. Production and release of cytokines and angiogenic factors by Human placental explants exposed *ex vivo* to *P. falciparum.*

Table 12. Characteristics of the pregnant women from the malaria-endemic region of Urabá included in the placental histology analysis.

List of Supplementary Files

Supplementary file 1. Article accepted by MDPI Methods and Protocols journal: "Assessment of the integrity and function of human term placental explants in short time culture: A rapid approach for modeling the effects of adverse conditions during pregnancy".

Supplementary file 2. Mail of received the manuscript titled "Assessment of the integrity and function of human term placental explants in short time culture: A rapid approach for modeling the effects of adverse conditions during pregnancy" on September 29, 2023. The submission is currently under review.

Supplementary file 3. Certificate for participation as a speaker in the oral presentation format at the XI International Congress of Neotropical Parasitology, Campeche, Mexico, November 13-18.

Supplementary file 4. Expression levels of syncytialization, angiogenesis, and inflammation mediators in human placental explant exposed *ex vivo* to *P. falciparum* evaluated by qPCR*.*

Supplementary file 5. Expression levels of syncytialization mediators in human placental explant exposed *ex vivo* to natural hemozoin evaluated by qPCR.

Supplementary file 6. Production and release of cytokines by Human placental explants exposed *ex vivo* to natural hemozoin evaluated by flow cytometry.

Supplementary file 7. Possible mechanism of *P. falciparum* pathogenesis on the placenta employing different methodological approaches.

Supplementary file 8. Article submitted to Malaria Journal: "*Plasmodium falciparum* alters the trophoblastic barrier and stroma villi organization of human placental villi explants".

Resumen

Este estudio investigó el impacto de los eritrocitos parasitados con *P. falciparum* (*P. falciparum*-iE) en el tejido placentario a través de tres modelos complementarios: un modelo *in vitro* con células BeWo, un modelo *ex vivo* con explantes placentarios humanos (HPEs) y una exposición *in vivo* que incorporó tejidos de gestantes naturalmente expuestas a la infección.

Se llevaron a cabo análisis cualitativos, semicuantitativos y cuantitativos en cada modelo para evaluar los posibles efectos fisiopatológicos de la malaria placentaria. Cada proceso se describió en detalle en la metodología específica por objetivos.

En el modelo *in vitro*, se observó un aumento en el daño celular, evidenciado por el incremento de la actividad de la LDH en células expuestas a *P. falciparum*-iE en comparación con las células control. Además, se registró disminución en la producción de la hormona hCG y una afectación en el proceso de diferenciación celular, especialmente en las células de citotrofoblasto expuestas a *P. falciparum*-iE, que no presentaron una adecuada fusión celular, como se reflejó en el análisis de la expresión de E-cadherina. Este fenómeno estuvo acompañado de una disminución en la expresión de mediadores clave para la sincitialización, como SYN-1, SYN-2 y hCG.

En el modelo *ex vivo*, se observó una disminución en la viabilidad celular y alteraciones en la integridad del tejido placentario, incluyendo daño en la membrana del trofoblasto, así como desorganización del colágeno en el estroma velloso acompañado de disminución en la distribución del Colágeno I y III. Además, se detectaron áreas de engrosamiento de la lámina basal, coincidiendo con zonas de desprendimiento y ruptura de la capa de trofoblasto. Por otro lado, se encontraron niveles elevados de mediadores inflamatorios, principalmente IL-6 e IL-10, en HPEs expuestos a *P. falciparum*-iE en comparación con HPEs control. Los mediadores angiogénicos evaluados no mostraron diferencias significativas entre los HPEs expuestos y control.

En el estudio *in vivo*, se identificaron cambios significativos en el daño del estroma velloso, con una reducción en la organización de las fibras de colágeno, similar a lo encontrado *ex vivo*. La membrana del trofoblasto se mantuvo íntegra en los tejidos y no se observaron regiones de engrosamiento en la lámina basal, diferenciándose así del modelo *ex vivo*. Estos hallazgos podrían relacionarse con el tiempo de exposición y los procesos de cicatrización y respuesta inmune materna que podrían estar participando en el modelo *in vivo*, pero no en el *ex vivo*.

Es esencial señalar que cada hallazgo debe interpretarse de acuerdo con las características del modelo específico, considerando los posibles efectos del tiempo de exposición a la infección en las células y el tejido evaluado. En general, estos resultados sugieren que la interacción de *P. falciparum*-iE con el citotrofoblasto y las vellosidades placentarias puede perturbar la integridad, la función y el perfil de factores producidos y liberados por estas células y tejidos, contribuyendo a la desregulación de diversos procesos en la interfaz materno-fetal.

Palabras clave: Malaria placentaria, *Plasmodium falciparum*, daño histológico, trofoblasto, citoquina, inflamación, angiogénesis, apoptosis.

Abstract

This study investigated the impact of *Plasmodium falciparum*-infected erythrocytes (*P. falciparum*-iE) on placental tissue through three complementary models: an *in vitro* model with BeWo cells, an *ex vivo* model with human placental explants (HPEs), and an *in vivo* exposition that incorporated tissues from naturally infected pregnant individuals. Qualitative, semiquantitative, and quantitative analyses were conducted in each model to assess the potential physiopathological effects of placental malaria. Each process was detailed extensively in the methodology specific to its objectives.

In the *in vitro* model, an increase in cellular damage was observed, evidenced by the elevation of LDH activity in cells exposed to *P. falciparum*-iE compared to control cells. Additionally, there was a decrease in hCG hormone production and an impairment in the cellular differentiation process, especially in citotrofoblast cells exposed to *P. falciparum*-iE, which exhibited inadequate cellular fusion, as reflected in the analysis of E-cadherin expression. This phenomenon was accompanied by a decrease in the expression of key mediators for syncytialization, such as SYN-1, SYN-2, and hCG.

In the *ex vivo* model, a decrease in cellular viability and alterations in placental tissue integrity were observed, including damage to the trophoblast membrane, disorganization of collagen in the villous stroma, and a decrease in the distribution of Collagen I and III. Additionally, areas of thickening of the basal lamina were detected, coinciding with regions of trophoblast detachment and rupture. Furthermore, elevated levels of inflammatory mediators, primarily IL-6 and IL-10, were found in HPEs exposed to *P. falciparum*-iE compared to control HPEs. The evaluated angiogenic mediators did not show significant differences between exposed HPEs and the control.

In the *in vivo* study, significant changes were identified in villous stromal damage, with a reduction in the organization of collagen fibers similar to what was found *ex vivo*. The trophoblast membrane remained intact in the tissues, and no regions of thickening in the basal lamina were observed, differentiating it from the *ex vivo* model. These findings could be related to the exposure time and maternal healing and immune response processes that might be involved in the *in vivo* model but not in the *ex vivo* model.

It is essential to note that each finding should be interpreted according to the characteristics of the specific model, considering the potential effects of the exposure time to infection on the evaluated cells and tissue. Overall, these results suggest that the interaction of *P. falciparum*-iE with cytotrophoblast and placental villi may disrupt the integrity, function, and profile of factors produced and released by these cells and tissues, contributing to the dysregulation of various processes in the maternal-fetal interface.

Keywords: Placental malaria, *Plasmodium falciparum*, histological damage, trophoblast, cytokine, inflammation, angiogenesis, apoptosis.

1. Introduction

1.1. Background

Malaria is one of the most significant parasitic diseases in humans. It is caused by *Plasmodium* spp and transmitted by *Anopheles* mosquitoes (1). Five species of *Plasmodium* affect humans: *P. falciparum*, *P. vivax*, *P. malariae*, *P. ovale*, and *P. knowlesi* (2); among these, *P. falciparum* and *P. vivax* are the most prevalent. The most vulnerable populations to infection are pregnant women and children under the age of five. Specifically, during pregnancy, *P. falciparum* leads to approximately 150,000 fetal deaths and 10,000 maternal deaths annually in malaria-endemic regions (3). Malaria during pregnancy, more commonly referred to as gestational malaria (GM), may manifest in the presence or absence of placental malaria (PM) and congenital malaria (CM). These different presentations of the infections have several risks to both the mother and the developing fetus. GM is demonstrated by the presence of *Plasmodium* spp in maternal peripheral blood. PM is identified by the presence of *Plasmodium* spp or hemozoin (Hz) in placental blood or placental tissue, and CM is indicated by the presence of *Plasmodium* spp in the umbilical cord at the time of delivery or in the peripheral blood from neonates within 30 days post-delivery (4).

The human placenta is a temporary organ that plays a crucial role in the successful development of the fetus. The placenta comprises two types of tissues - maternal and fetal. The decidua refers to the maternal tissue, while the chorionic villi refer to the fetal part. The chorionic villi include free-floating villi surrounded by maternal blood within the intervillous space. The chorionic villi serve as the functional unit of the placenta. They house the placental barrier and facilitate gas and nutrient exchange between mother and fetus (5).

The epithelial covering of the villous tree is the trophoblast, consisting of a proliferative basal layer known as cytotrophoblast (CTB) and a superficial syncytium formed by the Syncytiotrophoblast (STB). The trophoblast, the basal membrane, the villous stroma, and the fetal connective tissue containing fetal capillaries, form the placental barrier (6). The STB assumes crucial roles within the placental barrier, including the exchange of gases and nutrients, hormone production, immune tolerance toward the semi-allogeneic fetus, acting as

a physical barrier against pathogenic microorganisms, and contributing to the control of infections at the maternal-fetal interface (7).

The harmful effects of *P. falciparum* during pregnancy have been explained. These parasites can accumulate in the placenta due to the binding of the Chondroitin Sulfate A (CSA) receptor present on the STB and the parasitic antigen VAR2CSA expressed by the infected erythrocytes (iE) circulating in the placental intervillous space (8). Parasite sequestration in the placental villi and the inflammatory response induced by the parasite in the tissue have been considered the primary cause of adverse effects during pregnancy and histological alterations in the placenta (9-11). On the other hand, both the systemic deterioration of the mother and the placental involvement during the infection can lead to a series of complications affecting the fetus, such as intrauterine growth restriction (IUGR) (12), Low birth weight (LBW) (13), preterm birth (14), miscarriages, and stillbirths (15).

The presence of iE in the intervillous space of the placenta and other parasitic products, such as Hz leads to an increase in mononuclear and polymorphonuclear cells that infiltrate the tissue to control the local infection (16, 17). The STB also produces cytokines and chemokines to recruit maternal immune cells from peripheral blood, promoting an inflammatory environment. Simultaneously, it stimulates the production of antibodies and activates immune cells to clear parasites (16, 18, 19). Other findings associated with PM include the deposition of Hz in phagocytic leukocytes and within fibrin deposits in the intervillous space (20). Both sequestration and inflammation are considered two key elements that lead to disruptions in the exchange of gases and nutrients between the mother and fetus, as well as disturbances in angiogenic and endocrine mediators (12, 21).

Most studies related to PM have focused on assessing the impact of the infection on inflammatory mediators in maternal peripheral blood (22-24). Despite the existing information about the unfavorable pregnancy outcomes associated with PM caused by *P. falciparum*, it is necessary to investigate the direct effect of the parasite on the placental barrier. Furthermore, it is essential to assess the impact of infection on STB function, including the production of inflammatory, angiogenic, and endocrine mediators, which are crucial for fetal development as well as in their differentiation process beginning from CTB. Previously, the interaction

between *P. falciparum* and the STB was studied, and an inflammatory activation of these cells exposed to iE, or Hz was described (19, 25). However, despite current knowledge, the complete role of this activation in the adverse effects of placental infection, as well as the specific mechanisms that may lead to alterations on the STB, or additional components of placental villous, remains unclear.

Previous reports indicate that *P. falciparum* alters the trophoblast epithelium and increases the syncytial nodules, fibrin deposits, and infarction on placental tissue (11, 26, 27). However, many gaps still exist in our understanding of the effects of PM on key processes that are part of tissue structure and function, such as placental histoarchitecture, inflammation, angiogenesis, hormonal production, and cellular apoptosis (28, 29).

To better understand the molecular mechanisms behind placental damage and its impact on fetal development in the context of PM, it is essential to conduct further research. However, conducting studies that accurately replicate *in vivo* events is a challenge because: 1) studying the biology of the human placenta in remote endemic areas is experimentally very difficult, and 2) there is a lack of animal study models that closely resemble the human placenta.

Therefore, *in vitro* placental models based on cell cultures, such as syncytialization models (BeWo cells) and *ex vivo* models for studying the placenta function, such as the Human placental explants (HPEs) culture, that accurately recapitulate *in vivo* dynamics, represent experimental alternatives for comprehending the pathophysiological process during PM, facilitating research and future identification of molecular targets that helps to prevent the adverse effects of the infection.

HPEs have been used to study diverse placental pathologies and the impact of other parasite infections, including protozoan parasites such as *Trypanosoma cruzi* or *Toxoplasma gondii,* on placental tissue, not only at the level of the trophoblast membrane but also at the level of the villous stroma (30). The tissue damage triggered by these infections is significant and facilitates the entry of parasites into fetal circulation. Besides congenital transmission, tissue damage along with the dysregulation of the immune response and apoptosis may contribute to several

adverse effects in fetal development (28, 29). Specifically, for *P. falciparum* infection, the HPEs have allowed researchers to discern the cause of some adverse effects, such as IUGR (31).

What is intended to be done in the present study?

The primary goal of this study is to comprehensively assess the direct impact of *P. falciparum* on placental tissue and specific cells, such as STB, by employing three distinct models: *in vitro*, *ex vivo*, and *in vivo*. Given the crucial role of placental function in fetal development and pregnancy outcome, our study aims to fill a significant gap in the existing research. Understanding the pathophysiology of placental malaria is essential for developing effective interventions to prevent or treat this condition, ultimately reducing its devastating impact on pregnant women and their fetuses.

To assess the direct impact of *P. falciparum* on the cellular differentiation process of trophoblasts the *in vitro* syncytialization model with BeWo cells was used. This model is widely implemented to mimic the *in vivo* syncytialization of the villous trophoblast in the placenta (32). Moreover, considering the absence of an animal model that precisely reproduces the anatomy and function of the human placenta, an *ex vivo* model was included through the utilization of HPEs. Its primary advantage lies in preserving the structure of the placenta and the villous stromal component (33). Furthermore, an *in vivo* study was included, incorporating placental tissues from pregnant individuals naturally exposed to *P. falciparum* infection. This model presented a valuable opportunity to complement the findings from the previously mentioned models and validate the results obtained in various processes impacted by *P. falciparum* infection. Finally, additional evidence of the effect of Hz on placental tissue is included, considering that Hz plays a crucial role in the pathogenesis of PM caused by *P. falciparum*.

1.2. Theoretical Framework

<u>Epidemiology of Malaria: emphasis on pregnant women</u>

In 2021, almost half of the world's population was at risk of contracting malaria. During that year, there were 247 million cases of malaria reported globally. It is estimated that the disease caused the death of 619,000 individuals in the same year. The African region alone contributed to 95% of the reported malaria cases and 96% of the deaths resulting from the disease (3). During the peak of the COVID-19 pandemic from 2020 to 2021, there were around 13 million more cases of malaria and 63,000 more deaths from this disease. More than half of all malaria deaths worldwide were concentrated in just four African countries: Nigeria (31.3%), the Democratic Republic of the Congo (12.6%), the United Republic of Tanzania (4.1%), and Niger (3.9%) (3).

Around 125 million women globally are at risk of contracting malaria during pregnancy (34), with an estimated 25 million in high transmission areas of Africa, where *P. falciparum* is the most common species in these regions. Whereas, in Asia and Latin America, an estimated 77.4 and 4.3 million pregnant women are respectively at risk of infection, but in low transmission areas. The prevalent species in these areas are *P. falciparum* and *P. vivax* (34, 35). In 2022, 11.6 million pregnant women were exposed to *Plasmodium* spp infection during pregnancy, with a higher prevalence of exposure in West Africa (40%). Malaria in pregnancy is estimated to result in 819,000 LBW infants (3), and approximately 150,000 fetal deaths annually in malaria-endemic areas, as a consequence of LBW (35).

In Colombia, between 2007 and 2020, 380 cases of complicated malaria were reported in pregnant women (36). A meta-analysis published in 2021 regarding the prevalence of pregnancy-associated malaria in Colombia between 2000-2020 found a prevalence of GM detected by microscopy of 5.8%, and PM of 3.4%, which increases when diagnosed by PCR, reaching proportions of 16.7% and 11.0% respectively. This demonstrates a high prevalence of GM and PM in Colombia, emphasizing the need for attention and the implementation of more studies investigating the effect of malaria on the mother, the fetus, and the placenta (37).

Life cycle of *Plasmodium* spp

When a mosquito bites a person, it injects sporozoites into their bloodstream through its saliva. The sporozoites travel to the liver, where they multiply asexually and transform into merozoites. These merozoites then enter the bloodstream and infect red blood cells, where they multiply asexually forming new merozoites that invade new red blood cells. This cycle of invasion, replication, and rupture of infected cells, results in the symptoms of malaria, including fever, anemia, and organ dysfunction (38). Concurrently, certain merozoites within these cells develop into sexual forms known as gametocytes, which circulate in the bloodstream. These gametocytes play a crucial role in transmission, as they are acquired by the vector during blood feeding (39).

During asexual multiplication, infected erythrocytes with mature trophozoites and schizonts express on their membrane the *Plasmodium falciparum* erythrocyte membrane protein 1 (PfEMP1). These parasite proteins are cluster on the cell surface in structures known as knobs (40), and allows to the infected cells bind to several receptors on endothelial cells that lining capillaries, resulting in the sequestration of parasites from circulation. In the context of placental malaria, a specific PfEMP1 referred to as VAR2CSA (41), can bind to CSA segment of chondroitin sulfate A proteoglycans. The adherence of iE to placenta is observed in the apical lining of the STB and, notably, within the intervillous space, sometimes alongside monocytes and macrophages containing ingested Hz (11, 42).

As parasites growth, they use hemoglobin as a source of nutrients. Hemoglobin represents 90% of the cytosolic proteins of the red blood cell, and the parasite can consume up to 60-80% of it. The heme released from the catabolism of hemoglobin is chemically modified and stored in the form of Hz within the digestive vacuole (DV), also known as malaria pigment. Hz is an insoluble and non-degradable crystal, a waste product of the parasite's hemoglobin metabolism, found in mature stages of the asexual cycle (mature trophozoites and schizonts) and mature gametocytes. During the infected erythrocytes rupture, both merozoites and DV, along with the Hz release can induce the activation of inflammatory pathways, the intrinsic coagulation cascade and the alternative complement pathway (43). The Hz can be retained within the immune cells that phagocytosed them or on fibrin deposits in several tissues,

including the placenta (20). This is not only related to a constant stimulation of the immune response, since it has been reported that Hz can last up to 2 months in tissues, but also, and less explored could be a significant inducer of local tissue damage (44) (**Figure. 1**).
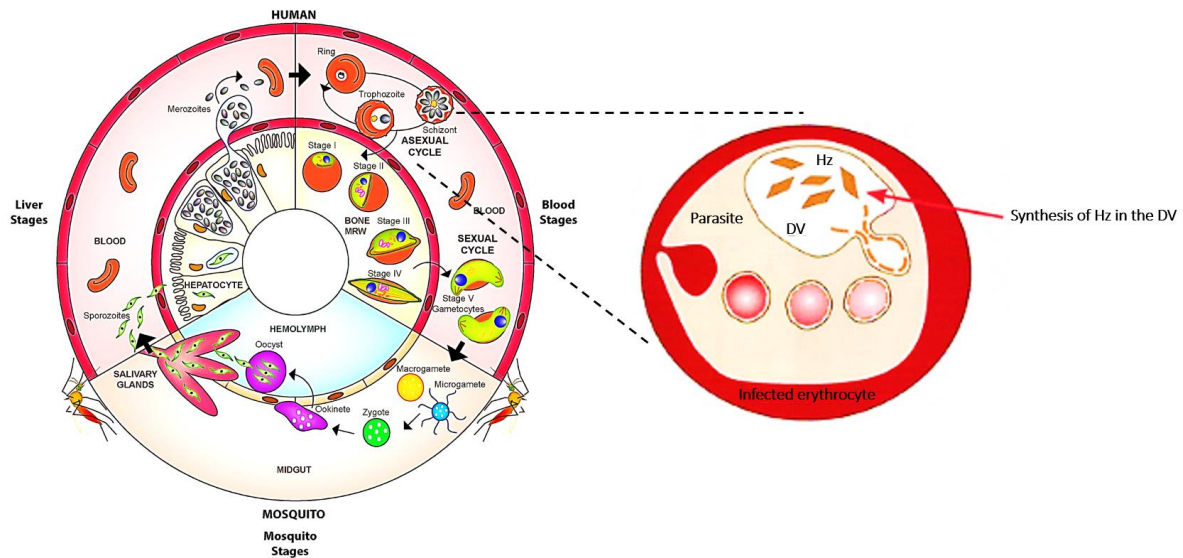

Figure 1. Life cycle of *Plasmodium* spp. Image from **(45)**

Pathophysiology of Gestational Malaria Caused by *P. falciparum.*

The adverse effects on the fetus and/or neonate arise due to the presence of the parasite in the placenta and its inflammatory response. Therefore, it is important to first understand the structure of the placenta under normal conditions without the presence of infectious processes to fully comprehend the mechanisms of damage and pathogenesis caused by *P. falciparum* in the tissue.

Healthy placental structure.

The placenta is a transient organ that forms during pregnancy formed by the maternal compartment, known as the basal decidua, and a fetal compartment, represented by the chorionic villi (5). The villi are covered by the STB, a syncytialized epithelium in direct contact with maternal blood. Beneath the STB and CTB, the villous stroma is formed by a variety of cells including endothelial cells, fetal vessels, mesenchymal cells, macrophages, and fibroblasts, as shown in **Figure 2**. The placenta is classified as hemochorial, meaning that maternal blood directly bathes the fetal villi, and it is a vital organ to sustain the proper fetal development.

21

The functions of the placenta include hormone production and metabolism, hemodynamic adaptations, and acting as a physical barrier between maternal and fetal circulations. The placental barrier allows for the diffusion of nutrients, gases, and waste between maternal and fetal bloodstreams. It also plays a crucial role in immune tolerance toward the fetal semi-allograft, acts as a physical barrier against pathogenic microorganisms, and contributes to innate infections control at the maternal-fetal interface. (7, 46).
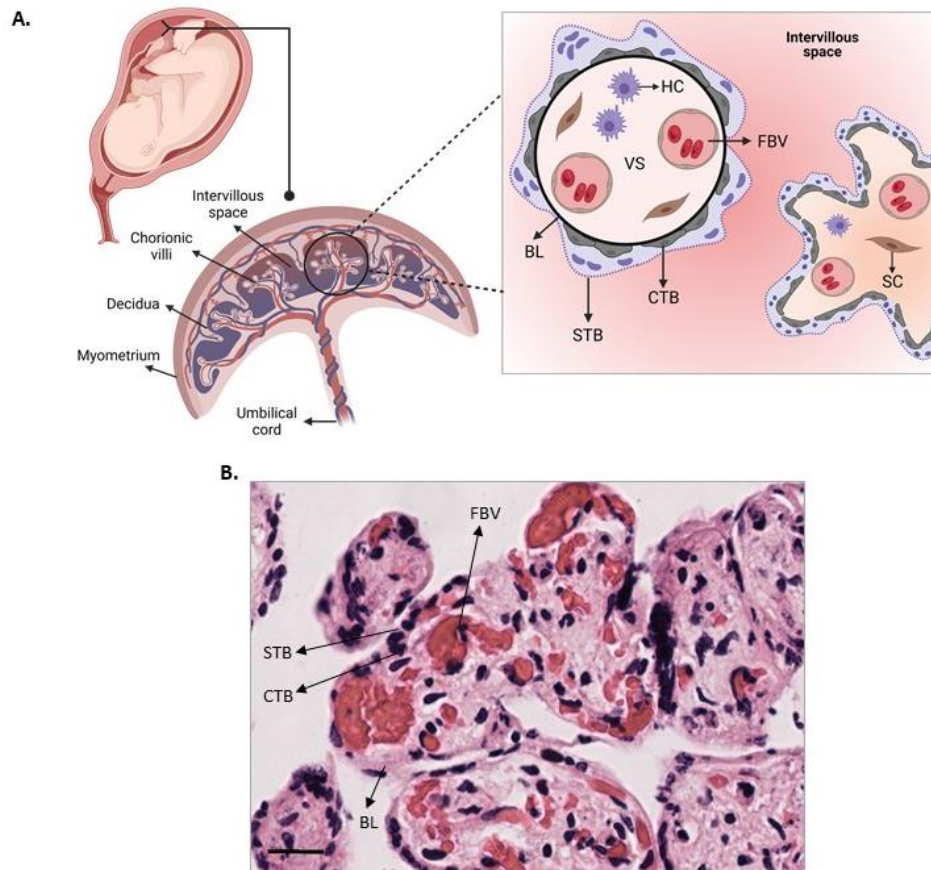

Figure 2. Maternal-fetal interface and placental barrier. A. To the left, there's placental tissue and the fetus while to the right, there's placental villus with a multinucleated layer of STB and an underlying mononuclear layer of CTB. The STB can form nodes as part of the final stage of the cell cycle of epithelial differentiation. The fetal blood vessels (FBV) are positioned close to the trophoblast. The compartments of placental tissue are decidua, villus, and intervillous space. BL represents basal lamina, VS represents villous stroma, HC represents Hofbauer cells, and SC represents stromal cells. In **B**, a cross-section of HPEs stained with H&E identifies the different regions and cells in the scheme in A. The image has a scale bar of 20 μm and a magnification of 400X. The illustration was created with a BioRender license.

During the development of the placenta, the CTB cells undergo two distinct differentiation pathways, in a process regulated at molecular level by the expression of several molecules

(**Figure 3**). One pathway involves the formation of extravillous trophoblast (EVTs). These cells move deeply into the uterus, reaching up to the first third of the myometrium. They replace the endothelium and vascular wall of spiral arteries by invading them. The process of invasion is at its highest level at 12 weeks of gestation and then quickly decreases. This indicates that the invasion is regulated spatially and temporally, which is different from tumor invasion (47).
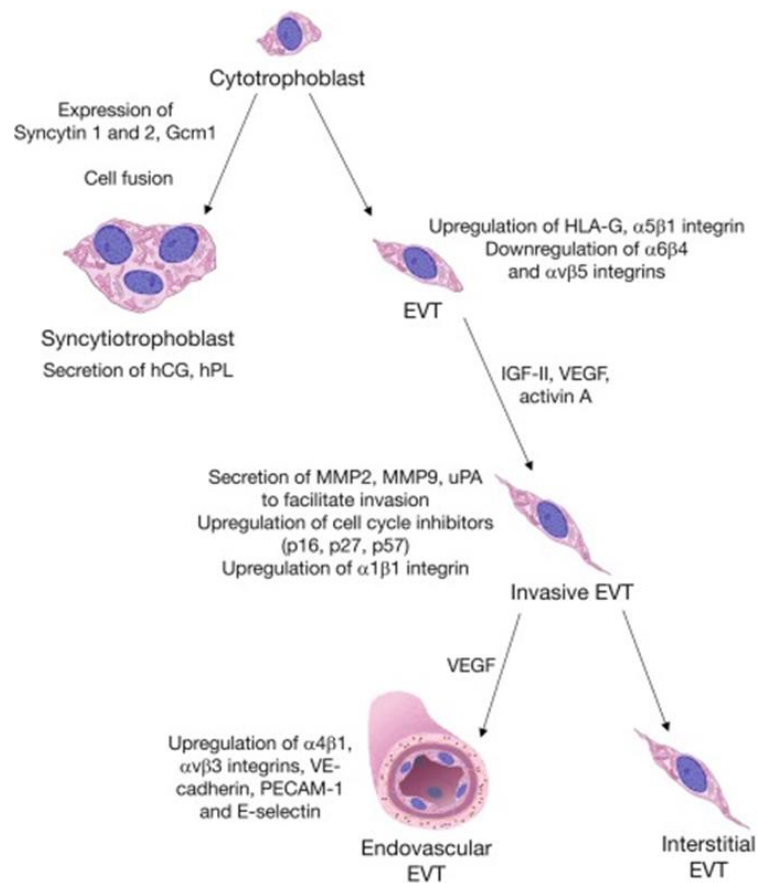

Figure 3. Molecular changes that occur during trophoblast differentiation down to the syncytiotrophoblast or extravillous trophoblast lineages. Image from (48).

The second differentiation pathway of CTB corresponds to the formation of the villous trophoblast, specifically the STB. The majority of CTB cells in both floating and anchoring villi undergo fusion to create the STB layer, a unique multinucleated syncytium comprising millions of nuclei connected by a continuous cytoplasm (**Figure. 4**). The fusion and conversion from a mononuclear state to syncytial are crucial for a successful pregnancy (49), proteins involved in this process include fusion proteins such as syncytins (50). **Table 1** provides a comprehensive description of the molecular mediators that are involved in each step of cellular differentiation.
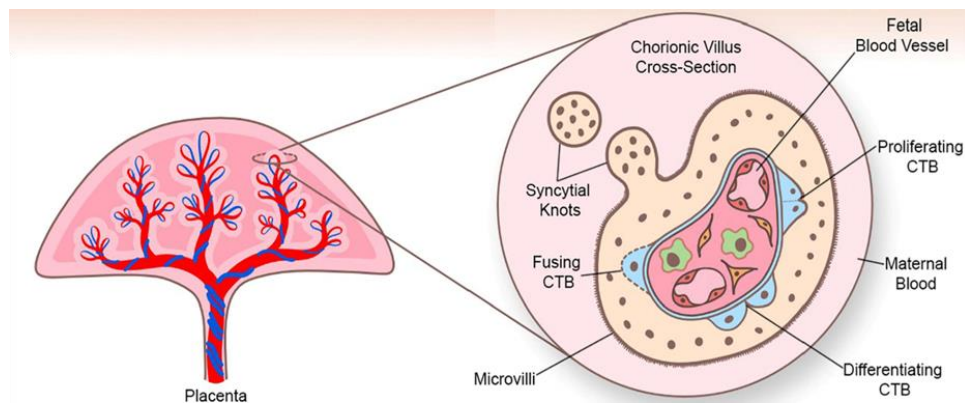
Figure 4. Cytotrophoblasts in various stages of their life cycle: proliferating, differentiating, and fusing. The STB barrier is crucial for a functional placenta. It undergoes a differentiation process that involves CTB cell proliferation, cell cycle arrest for differentiation, cellular fusion, and apoptosis. This process forms the multinucleated syncytium of the STB, which is composed of apoptotic syncytial nuclei that form syncytial knots. These knots are crucial for maternal-fetal interaction and proper pregnancy development. The events are intricately regulated to ensure optimal placental formation and function. Image from (51).

Table 1. Description of the key steps in the differentiation of the syncytiotrophoblast from the cytotrophoblast.

Key steps in the trophoblast differentiation process		Molecular mediators	Study markers	Ref.
CTB Proliferation	CTB cells actively undergo cell division through processes of cellular proliferation. A specific trophoblast marker is CK-7, which covers both CTB and STB.	ACTN4	Nuclear antigen Ki67 involved in eukaryotic proliferation.	(52-54)
Cellular fusion CTB and STB formation	The multinucleated layer results from CTB fusion. DNA and RNA synthesis does not occur in STB, implying that syncytial nuclei are unable to replicate.	EGF, hPL, CSF, GM-CSF, ERVW-1 and HERV-FRD.	Detecting the expression of desmoplakin or E-cadherin, hCG production, or Syn-1 and Syn-2 gene expression.	(50, 55-57)
Synthesis of Specific Products	The resulting STB is capable of synthesizing and secreting specific products, such as hormones and proteins, essential for sustaining pregnancy and communication with maternal tissues.	hCG, estradiol, and EG, pro-opiomelanocortin-derived peptides, including β-lipotropin, β-endorphin, and α-melanocyte-stimulating hormone, cortisol.	Several hormones and growth factors.	(58, 59)

Cellular Apoptosis	Caspase 8 and caspase-9 can be activated, initiating intracellular signaling cascades. Morphological changes characteristic of apoptosis, such as nuclear condensation and formation of apoptotic bodies.	Expression of cytokeratin 18 neo-epitope – clone M30, Caspase 8, Fas/CD95, FasL.	The cellular DNA fragments as part of the apoptotic process and can be determined using the TUNEL assay. Similarly, mitochondrial inactivity in cells assessed by the MTT assay allows for the detection of cell death or damage.	(60-62)
Syncytial Knots Formation	During the fusion process and STB formation, nodules containing apoptotic syncytial nuclei are generated and syncytial knots reflect placental maturation.	pUBF, PCNA.	true nucleus marker knots: 8-oxo-deoxyguanosine.	(63-65)

EGF: Epidermal growth factor; hPL: human placental lactogen, CSF: Colony stimulating factor, GM-CSF: granulocyte-macrophage colony-stimulating factor, ERVW-1: Syncytin 1, HERV-FRD: Syncytin 2. FasL: FasL: Fas ligand, ACTN4: Actinin alpha 4, Ki67: Nuclear protein whose general function is the regulation of cellular, pUBF: Phospho–upstream binding protein, PCNA: Proliferating cell nuclear antigen.

In humans, the STB facilitates implantation and eventually covers chorionic villi, immersing itself in maternal blood. Several molecules produce by the STB, as well vesicles and waste material enter maternal circulation, playing crucial roles in modulating maternal physiology and offering diagnostic potential for fetal-placental abnormalities and pregnancy-related diseases. Indeed, this pathway is relevant for the current study, since the iE by *P. falciparum* can bind to the STB. The STB plays a crucial role in nutrient and gas exchange between the mother and fetus. Additionally, it secretes hormones such as hCG, essential for pregnancy maintenance. The STB also releases angiogenic factors like vascular endothelial growth factor (VEGF) and placental growth factor (PlGF) to stimulate blood vessel formation. Furthermore, it produces immunological factors, including macrophage migration inhibitory factor (MIF) and interleukin-10 (IL-10), modulating immune responses at the maternal-fetal interface (66).

Syncytiotrophoblast as the primary provider of endocrine, angiogenic, and immunologic mediators.

The STB not only establishes structural and biochemical barriers between maternal and fetal compartments during pregnancy but also serves as a significant endocrine organ that produces numerous growth factors and hormones supporting and regulating placental and fetal development and growth (58, 67, 68). In normal conditions, the production of estrogen and progesterone promotes the humoral immune response, which is beneficial for the pregnancy.

Estrogens, influential in immune modulation, enhance antibody production, alter T lymphocyte activity, increase regulatory T lymphocytes (Treg), and affect various immune cells. Progesterone, on the other hand, inhibits lymphocyte activation and proliferation, influences apoptosis, and modulates the activity of immune cells, playing a role in graft survival. It induces the production of immunomodulatory factors such as Progesterone-Induced Blocking Factor (PIBF), Progesterone-Associated Endometrial Protein 14 (PP14), and galectin-1 (Gal-1) (69, 70).

The placental angiogenic pattern, crucial for tissue and fetal development, relies on endothelial cells as functional units. These cells play pivotal roles in maintaining vascular integrity, regulating thrombotic status, and responding to local stimuli. Inadequate placental vascularization is linked to histological changes, including infarction, fibrin deposits, necrosis, and thrombosis, with consequential adverse fetal effects such as increased embryonic mortality, preeclampsia, LBW, and IUGR (71). Various endocrine, angiogenic, and immunological mediators contribute to these intricate processes are detailed in **Table 2**.

Table. 2. Description of the main functions of the components produced by the syncytiotrophoblast.

Function of the mediators produced by the syncytiotrophoblast	
Mediators	Function
Endocrine	
Human chorionic gonadotropin (hCG)	hCG hormone is synthesized before implantation, maintains the maternal corpus luteum, and is the basis for early pregnancy tests. It induces the blockade of maternal macrophages, regulates uterine NK cells through IL-10, and decreases the proinflammatory response through the production of IDO enzyme (72).
Estrogens and progesterone	During pregnancy, the placenta produces progesterone and estrogen to maintain the pregnancy without relying on cholesterol precursors. Progesterone levels increase throughout gestation and promote Th2 cytokines production. Progesterone-Induced Blocking Factor (PIBF) has

	immunosuppressive properties that prevent the activation of NF-κB in NK cells (73).
Human placental lactogen (hPL) or human chorionic somatomammotropin	HPL is a hormone with similarities to growth hormone and prolactin. It plays a role in growth, maternal mammary duct proliferation, lipid and carbohydrate metabolism, cell differentiation, trophoblastic regulation and growth, angiogenesis, and immune regulation. It production increases towards the end of pregnancy (72).
Human placental growth hormone	Throughout pregnancy, a hormone distinct from pituitary growth hormone is gradually produced in the mother's body. Starting from 15 weeks until the end of pregnancy, this hormone takes on the role of maternal pituitary GH. Its primary function is to regulate the mother's blood glucose levels, which guarantees that the fetus receives an adequate supply of nutrients.
Endoglin	It is a component of the TGFb receptor complex that binds to the b1 and b3 isoforms and is also transiently up-regulated in extravillous trophoblasts differentiating along the invasive pathway (74).
Angiogenic	
Insulin-like growth factors	Stimulates proliferation and differentiation of cytotrophoblasts.
Endothelial growth factor	Start to produce this hormone by 4 -5-week after conception. It stimulates proliferation of trophoblasts.
VEGF	During placental and fetal vascular development, several pathways are involved. Among them, the most extensively studied ones are regulated by VEGF, and the angiopoietins 1 and 2 axis, along with their receptor tyrosine kinase angiopoietins (Ang 1/2 – Tie2) (75).
Angiopoietins 1 and 2	
PlGF	VEGF, along with other pro-angiogenic factors such as PlGF, works together with anti-angiogenic mediators like the soluble VEGF receptor 1 (sVEGFR-1 or sFLT-1) to control the growth and alteration of blood vessels. It captures circulating VEGF and produces an anti-angiogenic effect (75). The soluble form of vascular endothelial growth factor receptor-1 (sVEGFR-1) binds to circulating VEGF and PlGF, preventing their interaction with endogenous receptors, mainly VEGFR (76). In case of an imbalance in the expression of angiogenic factors, placental vascularization is disrupted, hindering proper gestational development (76).
sVEGFR-1	
TGF-β	TGF is comprised of three isoforms: TGF-β1, TGF-β2, and TGF-β3. TGF-β1 is a cytokine that regulates immune cells, their functions, and immune homeostasis. (77).
immunologic	
IL-10	Stimulates B lymphocyte, thymocyte, and mast cell proliferation. Enhances IgA secretion in cooperation with TGF-β. Also, it has anti-inflammatory properties and inhibits Th1 cell generation.
IL-6	It is produced by EVTs and CTBs, regulates migration, invasion, differentiation, and proliferation of trophoblast cells (78).
IL-17	IL-17A induces the secretion of proinflammatory cytokines such as IL-6, TNF-α, and IL-1β, as well as granulocyte-macrophage colony-stimulating

	factor, promoting the local accumulation of neutrophils and other inflammatory cells (79).
TNF-*α*	Regulates immune and inflammatory functions, cell growth, and differentiation. It has cytotoxic effects on some cells and promotes angiogenesis, bone resorption, and thrombotic processes. Also suppresses lipogenic metabolism.

Adapted and modified table from (80).

Collagen Fibers and extracellular matrix in the villous stroma

The production of extracellular matrix (ECM) is significantly contributed by resident mesenchymal cells, which play a crucial role in stromal architecture (81). Collagens, laminins, and fibronectin are present in the stroma of chorionic villi (82, 83). Increasing evidence suggests that ECM significantly impacts trophoblasts' behavior, function, and cellular differentiation (83). Castellucci et al. 1990 demonstrated that the ECM, particularly collagen, influences the synthesis of products such as hormones and proteins by trophoblastic cells (84).

Placental villi have a highly organized collagenous fibrillar scaffold that supports fetal chorionic vessels and the trophoblastic layer and are associated to the functional activity of term placentas (85, 86). Different types of collagens—types I, III, IV, and V—are found in the stroma and basal lamina of human placenta, type I and type IV being the most abundant (85). Type I collagen provides strength to tissues, including placental and umbilical cord membranes. Type IV collagen is a crucial component of the basal membrane of placental villi and plays a role in the placental barrier.(87).

Placental barrier

The maternofetal barrier comprises the STB, CTB cells, fetal connective tissue within the villous stroma, fetal capillary, and basal lamina situated between the villous stroma and trophoblast, as well as around the fetal endothelium (88). During pregnancy, several pathogens can cross the placental barrier and infect both the placenta and the fetus. These include human immunodeficiency virus (HIV), hepatitis B and C, varicella-zoster virus, rubella, parvovirus B19, and cytomegalovirus (89). Additionally, infections by other parasites have been reported, aside from *T. cruzi*. Notable among these are infections caused by *P. falciparum* (20), *Schistosoma* (90), *Toxoplasma gondii* (91) y *Trypanosoma brucei* (92).

Physiopathology of placental malaria caused by *P. falciparum*

During pregnancy, *P. falciparum* parasites can cause sequestration of iE in the intervillous space of the placenta, through the interaction between the parasitic protein VAR2CSA on the erythrocyte surface and the glycosaminoglycan CSA, which is expressed by the STB (**Figure 5**) (41). This sequestration of parasites can lead to the infiltration of immune cells, such as monocytes and macrophages, into the placenta (93). Stimulation of maternal macrophages leads to expression of monocyte chemotactic protein (MCP-1) and macrophage inflammatory proteins (MIP-1α and MIP-1β), which attract inflammatory mediators and initiate the inflammatory cascade (94). Additionally, production of proinflammatory cytokines such as TNF and IFN-γ is also induced to control placental infection, but contributing, in turn, to adverse outcomes associated with the product of gestation (95).
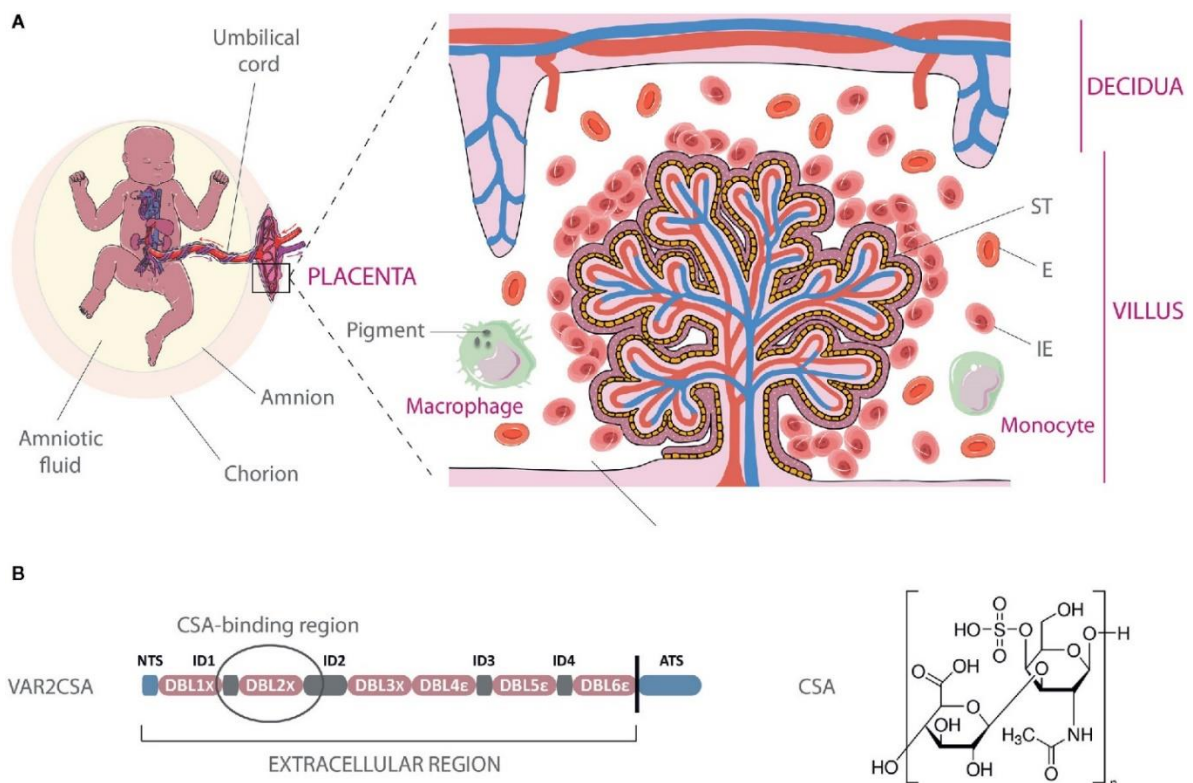

Figure 5. Sequestration of infected erythrocytes within the intervillous space of the placenta. A. Schematic representation of iE adhering to the STB lining of fetal villi, with an increased presence of macrophages and monocytes in maternal blood. Hz remains visible in macrophages after the phagocytosis of iEs. The natural transfer of gases and nutrients between maternal blood in the intervillous space and fetal blood circulating in the villi is affected by the sequestration of IE. **B.** Architecture of the VAR2CSA protein and chemical structure of chondroitin-4-sulfate A. The region enclosed in a circle within VAR2CSA (ID1-ID2a) represents the chondroitin sulfate A-binding domain. Image from (96).

The local and systemic inflammation is characterized by the infiltration of monocytes and macrophages in placenta, as well the increased production of pro-inflammatory cytokines, chemokines, and complement proteins, and reduced levels of critical angiogenic and placental growth factors (97). Collectively, these factors have the potential to disrupt placental development if the infection occurs early in pregnancy, affecting shallow spiral artery development and increasing intrauterine arterial resistance (**Figure. 6**). It is important to mention that the induction of inflammatory processes is not specific to *P. falciparum*; proinflammatory and hypoxic mediators have been found increased in PM caused by *P. vivax* as well (98).

PM caused by *P. falciparum* increases risk of adverse effects for pregnant women especially in the first trimester, coinciding with placental growth and maturation. Anomalies observed in the placenta during infection encompass persistent damage to structures such as compromised STB, basement membrane thickening, heightened syncytial knot formation, increased areas of fibrinoid necrosis, and dysregulated trophoblast apoptosis (**Figure 6**). These alterations can lead to placental insufficiency, which increases the risk of IUGR, LBW, and pre-eclampsia (13).
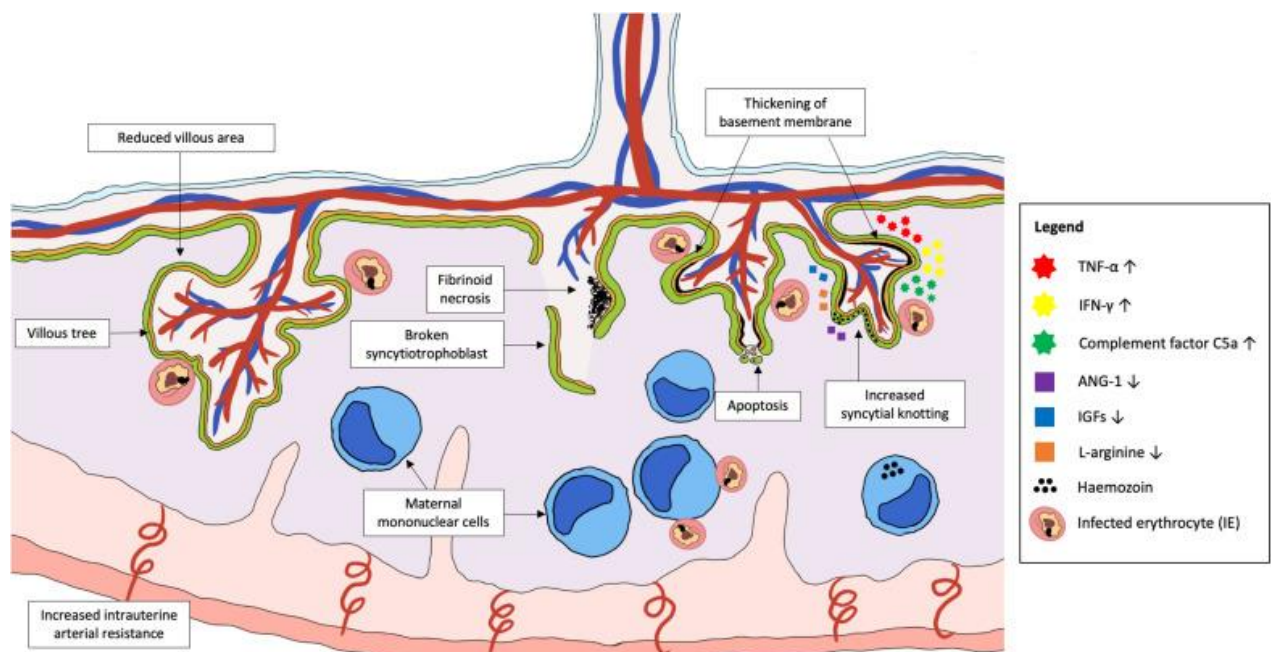

Figure 6. Placental malaria induces alterations in placental tissue and disrupts the normal balance of angiogenic and inflammatory mediators. Image from (9).

The Hz found in infected placentas worsens placental damage due to its immunomodulatory properties, however, the specific changes within the host and altered pathological pathways associated with the persistence of Hz remain insufficiently understood. Hz may persist in the placenta even after the parasites have been eliminated, so its pathological effect could extend even after the infection is resolved.

Hz is commonly found in infected placentas, either entrapped in fibrin or residing within maternal macrophages (99) and their presence in this tissue is used to classify PM in different categories as shown in **Table 3** (20). The persistent Hz may exacerbate placental damage due to its immunomodulatory and cytotoxic properties, for example, could worsen placental inflammation by reducing the ability of phagocytes to clear parasites and increasing cytokine secretion (100).

Classification	Description
Not infected	No evidence of parasites or malaria pigment (hemozoin)
Active infection	Parasites present without (acute) or with presence of pigment deposition within fibrin (chronic).
Past infection	Presence of pigment with no parasites

Table 3. **Classification of placental pathology** from (20).

Study Models of Trophoblast and Placental Tissue

To explore the biology and function of the placenta, various approaches can be employed, including specifically BeWo cells (ATCC-98) (52, 101), primary trophoblasts (102), placental explants in culture, and organoids. In this study, an *in vitro* model was utilized using the cell line BeWo, an *ex vivo* model with HPEs, and an *in vivo* study of natural exposure to *P. falciparum* infection (tissue from donors naturally exposed to the infection).

Briefly, the BeWo cell line, a choriocarcinoma cell line, representative of CTB, undergoes intercellular fusion upon stimulation with forskolin (FSK), a cyclic adenosine monophosphate (cAMP) inducer (54), as depicted in **Figure 7**. This cell line proves a useful model to study the fusion process between trophoblasts (32). Treatment of BeWo cells with FSK leads to the

formation of multinucleated syncytia and an upregulation in the expression of human chorionic gonadotropin (hCG). The syncytialization process can be observed through staining with membrane-associated proteins like E-cadherin or desmoplakin.

One notable advantage of working with the BeWo cell line is its capacity to evaluate diverse exposure scenarios, including exposure to *P. falciparum*, within a controlled laboratory environment. This allows for the determination of the direct impact of infection on trophoblast cells. However, a significant limitation is that the BeWo cell line lacks intrinsic components present in tissues, including those constituting the extracellular matrix. This divergence from *in vivo* conditions poses a challenge in accurately replicating the complexities involved in the infectious process.
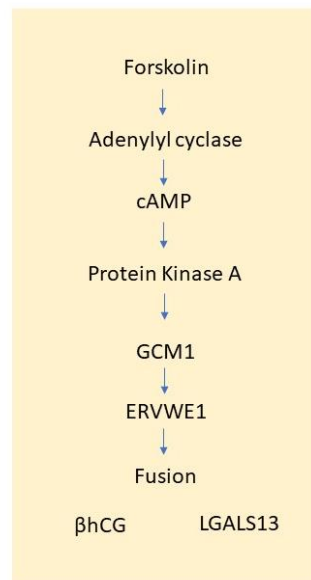

Figure 7. Proposed pathway of forskolin-mediated BeWo cell fusion. The accepted pathway of forskolin-mediated cell fusion and expression of βhCG and LGALS13. LGALS13, as well as βhCG, are expressed only after the fusion of BeWo cells. Image adapted from (54).

HPEs are widely used to study cellular proliferation and differentiation, as well several placental functions (103). Two main experimental approaches involve villous explants: 1. using explants from normal pregnancies to assess how external factors impact on tissue survival and function, and, 2. comparing explants from placentas with documented pathologies (e.g., preeclampsia, intrauterine growth restriction) to age-matched controls (104). HPEs from healthy donors are

particularly valuable, providing a platform to introduce specific conditions for comprehensive assessment, such as simulating infections with pathogenic agents.

This approach allows for a more physiological context, surrounded by placental immune cells, blood cells, endothelial cells, and various mesenchymal stromal cells. HPEs cultivation, lasting several days, proves to be a suitable *ex vivo* model for studying placental tissue. However, caution is warranted in attributing specific activities to individual cell types due to the complex co-culturing dynamics. A notable limitation in villous explant culture lies in the challenge of obtaining fresh material for culturing, restricting the utilization of placental tissue to immediate post-delivery periods, and posing a reproducibility obstacle. Attempting to replicate explant cultures from a single placenta later is unfeasible. Cryopreservation of explants presents a potential solution to these issues, but the freeze-thaw procedure introduces added complexity to tissue analysis (105).

Finally, it should be mentioned that the *in vivo* study of placentas naturally exposed to infection, in this case, *P. falciparum*, allows for a general understanding, although not specific, of the damage that the infection can exert on placental tissue. Results derived from this model must be interpreted with caution, as the placental tissue, comprising not only cellular elements but also maternal and fetal immune components, may have various elements influencing the identified effects of an infectious process and the associated immune response. Different study types complement each other, making their inclusion in a research project intricate, and results must be interpreted judiciously based on each model's nature. The key characteristics of various study models included in this work are detailed in **Table 4**.

Table 4. Description of the main types of models for studying the placenta

Study Models	Cellular	Human placental explants	Tissues/Placentas
	Células BeWo ATCC® CCL-98TM	Healthy placentas	Naturally exposed pregnant placentas
Differentiation	X	X	
Apoptosis	X	X	X
Production of Molecules	X	X	
Tissue Integrity		X	X
	Allows assessing the direct impact of *P. falciparum* on the STB and its differentiation process	Ex vivo infection in the context of extracellular stromal cell without maternal innate immune response. Biological variability	*In vivo* infection Maternal innate immune response context Biological variability

The cellular model, human placental explant model, and natural placentas exhibit different possibilities based on their nature for studying various conditions inherent to the process of cellular differentiation.

2. Objectives

2.1. General objective

To evaluate the integrity of placental tissue and identify changes in cellular differentiation processes, endocrine function, inflammatory response, and apoptosis in cells and tissues exposed to *Plasmodium falciparum*.

2.2. Specific Objectives

In Trophoblast Cell Line

1. To induce the differentiation of cytotrophoblast cells to syncytiotrophoblast in the *in vitro* model of syncytialization.
2. To assess the effect of *P. falciparum* on syncytiotrophoblasts viability, proliferation, differentiation, and apoptosis.

In Placental Tissues

3. To establish a viable and integral culture of human placental explants (HPEs) from third-trimester placentas of healthy pregnant women.

4. To evaluate changes in the tissue integrity and production of various physiological mediators in HPEs from healthy donors exposed to *P. falciparum ex vivo*.

5. To evaluate changes in the tissue integrity and production of various physiological mediators of HPEs from healthy donors exposed to natural hemozoin *ex vivo*.

6. To compare the effect of *P. falciparum*-iE *ex vivo* exposure of HPEs with placentas from pregnant women with malaria (*in vivo* exposure), using histological and immunohistochemical analysis.

Hypothesis

The exposure of STB and placental tissue to *Plasmodium falciparum* disrupts their integrity, and contributes to the dysregulation of endocrine, angiogenic, inflammatory, and apoptotic processes.

3. Methodology and Results

The methodology will be presented along with the results and conclusions corresponding to each study objective. Finally, there will be a comprehensive discussion and overall conclusion, summarizing the findings for each objective.

3.1. Specific objective 1.   To induce the differentiation of cytotrophoblast cells to syncytiotrophoblast in the *in vitro* model of syncytialization

3.1.1.   Methods

3.1.1.1.   BeWo Cell culture

The human choriocarcinoma cell line BeWo (CCL-98) was obtained from the American Type Culture Collection (ATCC). The cell line was maintained in Ham F-12K medium (Sigma Aldrich), supplemented with 10% Fetal Bovine Serum (F0926-500mL) and 1% (v/v) penicillin/streptomycin/B-amphotericin (Sigma Aldrich), following the ATCC recommendations (106). The cell cultures were kept at 37˚C with 5% CO_2. When cultures reached 70-80% confluence were washed three times with phosphate-buffered saline (PBS) 1X sterile (0780-50L VWR Chemicals Avantika) before detaching the cells with 0.25% trypsin-EDTA (Gibco) for subculture.

3.1.1.2.   Induction of syncytialization

Cells were seeded in 96-well culture plates, 8-well Lab-Teck™ chamber (Thermo Scientific) or in 6-well culture plates at densities of 20,000, 50,000 or 500,000 cells per well, respectively, and allowed to adhere and adapt overnight before initiating treatment. To induce syncytialization, the cells were exposed to 12.5 μM, 25 μM, or 50 μM FSK for 48 hours. The media was replaced daily, and fresh FSK was added to every media change. After 48 hours, the supernatants were collected and kept at -20°C for ELISA analysis. The cells were then washed with PBS and fixed in 4% paraformaldehyde for immunofluorescent staining. In other

experiments, the cells were detached using trypsin, and the RNA was extracted and stored at -80°C for gene expression analysis using RT-PCR. A schematic representation of the treatments is provided (**Figure 8**).
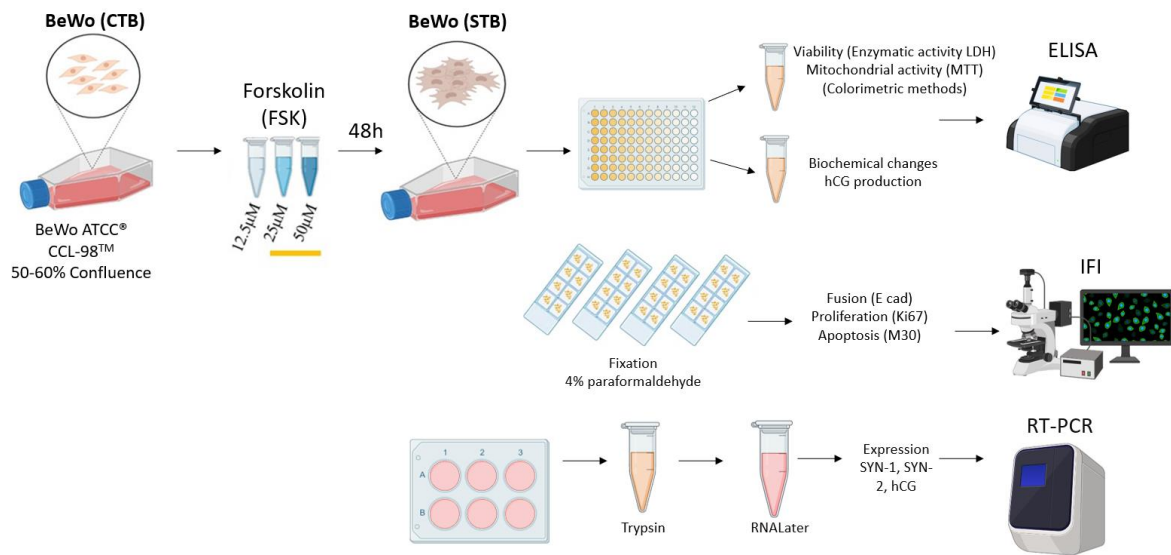

Figure 8. Schematic representation of the FSK stimulus added to BeWo cells for syncytialization induction. To induce syncytialization in BeWo cells, an increasing dose of FSK was used. After 48 hours, supernatants were collected for measuring LDH and hCG, and RNA from cells was extracted to measure gene expression of syncytialization mediators using qPCR. Some cells were seeded in a slide chamber to stain structural markers like E-cad, while others were used for detecting proliferative (Ki-67) and apoptotic (M30) processes.

3.1.1.3. Cell fusion and differentiation markers

To evaluate cell fusion and differentiation, various variables were measured. Initially, cell viability was determined through MTT reduction assay and measurement of Lactate Dehydrogenase activity. Subsequently, the production of β-hCG in the cellular milieu was quantified using ELISA to assess biochemical differentiation. Cell membrane fusion was evaluated employing an anti-human E-cadherin antibody for immunofluorescence and Hoechst for nuclei staining to evaluate morphological differentiation. Proliferation was assessed via immunostaining with an antibody against Ki67. Apoptosis was investigated through immunostaining for cytokeratin 18 fragment using the M30 monoclonal antibody. Finally, the gene expression of key molecules was quantified using qPCR.

3.1.1.4. Cell viability

3.1.1.4.1. MTT reduction assay to assess viability of BeWo cells

This test determines the ability of healthy cells to reduce MTT (the mitochondrial activity) (3-[4,5-dimethylthiazol-2-yl]-2,5-diphenyltetrazolium bromide) to formazan, as an indicator of mitochondrial activity. BeWo cells were seeded at a density of 20,000 cells per well in 96-well plastic plates and allowed to grow. Treatments were added as previously described. After incubation, 10 µL of 5 mg/mL MTT solution in PBS was added to each well and incubated at 37°C for 4 hours. Then, the culture medium was removed, and 130 µL of dimethyl sulfoxide (DMSO) was added to dissolve the formazan crystals. Finally, the absorbance in each well was measured at 570 nm using a spectrophotometric microplate reader.

3.1.1.4.2. Lactate Dehydrogenase activity to assess cellular viability

The activity of the Lactate Dehydrogenase (LDH) is a cytosolic enzyme, and its release into the extracellular environment is an indicator of cell damage or lysis. The "Cytotoxicity detection kit" (Roche Diagnostics GmbH, Mannheim, Germany) was used to detect the enzymatic activity. After 24 hours of HPEs culture, 100 µL of the supernatant was transferred to a 96-well plate in triplicate. Then, 100 µL of the reaction mixture (catalyst and dye solution) from the kit was added to each well. The plate was incubated in darkness at room temperature for 30 minutes. After that, 50 µL of 2N sulfuric acid (R&D Systems) was added to stop the reaction. The optical density (OD) was measured at 450 nm using a microplate reader (Multiskan™ FC Microplate Photometer, Thermo Scientific™ Massachusetts, United States). Triton X-lysed tissue was used as a positive control, to validate the technique, representing 100% LDH release.

3.1.1.5. Detection of hCG in culture supernatants

The secretion of hCG hormone was measure by using the DuoSet ELISA enzymatic immunoassay kit (R&D Systems), to detect free protein in culture supernatant. In brief, a 96-well microplate was coated with 50 µL of capture antibody and left overnight at room temperature. The plate was then washed three times with buffer and dried with a clean towel. Next, the plate was blocked with 150 µL of blocking buffer and left to incubate for one hour at room temperature, followed by more washes. Samples were added in a 1:1 (v/v) ratio, with a final volume of 100 µL in each well and incubated for 2 hours. The plate was then washed

again, and 50 µL of Detection Antibody was added to each well and incubated for another 2 hours, followed by more washing. Finally, 50 µL of Streptavidin-HRP solution was added to each well and left to incubate for 20 minutes at room temperature. After that, 50 µL of substrate solution was added to each well and left to incubate for another 20 minutes at room temperature. The reaction was stopped by adding 50 µL of stop solution. The absorbances were measured in a Microplate Photometer (Multiskan™ FC Thermo Scientific™) at 450 nm OD, and the concentration was determined in pg/mL by extrapolating the OD data into a standard curve.

3.1.1.6. Immunofluorescence staining to study cell membrane fusion, proliferation, and apoptosis

The following primary antibodies were used for immunofluorescence staining: **anti-E-Cadherin** monoclonal antibody from mouse (Anti-human E-cadherin, HECD-1) from R&D Systems (Abingdon, UK) at a concentration of 2 µg/ml to examine cell fusion, **anti-Ki67** monoclonal antibody from mouse (clone MIB-1) from Dako Cytomation (Glostrup Denmark) at a concentration of 4 µg/ml to examine proliferation, **anti-M30** monoclonal antibody from mouse against the M30 epitope of cytokeratin 18 from Boehringer Mannheim GmbH (Mannheim, Germany) at a concentration of 4 µg/ml to study apoptosis, and **anti-CSA** monoclonal antibody (1:200, ab11570; Abcam) to confirm CSA expression on the cell surface.

Cells were initially seeded at a confluence of 50,000 cells per well using Lab-Tek® II (Chamber Slide w/Cover RS Glass Slide Sterile, Brand Products. Thermo Fisher Scientific, United States), featuring eight wells with covers, for multi-marker staining. Following a growth period of 24-48 hours to achieve an 80% confluence, cells underwent two rounds of washing with 250 µL of PBS 1X per well. After seeding, cells were fixed with 4% paraformaldehyde (Thermo Scientific, United States) for 15 minutes at room temperature without removing the lab Lab-Tek plastic cover. Paraformaldehyde was subsequently eliminated with PBS 1X in a double wash (2 times). If immediate staining was not required, cells were stored in a humid chamber with PBS 1X in the refrigerator. The following washing steps consisted of 3 cycles with PBS, each lasting 3 minutes. To streamline the process, cells were simultaneously permeabilized and blocked with Triton X100 (0.2%) and PBS-BSA 10% in PBS 1X, using 150 µL per well for 10 minutes. The permeabilization/blocking solution was then completely removed, and a diluted Primary

Antibody PBS-BSA 1%, 150 µL per well, was added. The primary antibody was added at the concentrations specified before, and cells were incubated for 2 hours at 37°C or overnight in a humid chamber in the refrigerator.

Following the incubation period, a triple wash with PBS (5 minutes each wash) was performed. Subsequently, cells were incubated with Secondary Antibody, specifically Alexa Fluor 488-labeled (goat polyclonal anti-mouse IgG; Abcam, United Kingdom), FIT-C (goat polyclonal anti-mouse IgG; Sigma-Aldrich, German), or CSA Secondary (goat polyclonal anti-mouse IgG; Abcam United Kingdom). Simultaneously, nuclear counterstaining with Hoechst (Sigma) was conducted, allowing it to incubate for 1 hour in the dark. The final step involved a set of three PBS washes, each lasting 5 minutes. Staining observations were made using a fluorescence microscope. Staining preservation with Fluorsave® (Sigma-Aldrich, German) was employed if images were not captured on the same day with the fluorescence microscope. Note: permeabilization was deemed unnecessary for E-cadherin and CSA staining, but it was crucial for Ki67 and M30 staining, both of which are intracellular. The incubation period for M30 extended to 72 hours, acknowledging the extended time required for the cellular apoptosis process to manifest.

3.1.1.7. Analysis of IF staining

3.1.1.7.1. <u>Cellular fusion:</u> The number of total nuclei and nuclei in a syncytium were counted in five fields. A syncytium was defined as a multinuclear cell containing two or more nuclei without E-cadherin-stained membranes. The fusion index (FI) was calculated as follows: the total number of nuclei in syncytium divided by the total number of nuclei present, multiplied by 100 (107).

3.1.1.7.2. <u>Cell proliferation and cell death:</u> The percentage of cells positive for Ki67 and M30 was determined by counting how many cells emitted fluorescence from the total number of stained nuclei.

3.1.1.8. Ribonucleic acid extraction and complementary deoxyribonucleic acid synthesis

BeWo cells were seeded in 6-well plates at 500,000 cells per well in 2 mL of culture medium. The cells were allowed to attach for 24 hours before any treatment was administered. Once treated, the medium was removed and stored, and the cells were subjected to RNA extraction

using the RNeasy PLUS Mini Kit from Qiagen, following the manufacturer's instructions. The RNA concentration and purity were studied using a Nanodrop 2000 UV-Vis Spectrophotometer (Thermo Fisher Scientific). The RNA was then stored at -80 °C until used. To synthesize cDNA, 1 µg of total RNA was used, and reverse transcription was done using the qScriptTM SuperMIX® cDNA synthesis kit from QuantaBio as per the manufacturer's protocol. The thermic profile of the reaction was 5 min at 22°C followed by 30 min at 42°C and 5 min at 85°C, then a cool down to 4°C. The cDNA was stored at -20°C until further use.

3.1.1.9. Real-time PCR

The HOT FIREPol® EvaGreen® qPCR Supermix was used for the PCR reaction under universal amplification conditions. The reaction was carried out on the AriaMx Real-Time PCR System and included the following steps: 12 minutes at 95°C, followed by 15 seconds at 95°C, 30 seconds at 62°C, and 30 seconds at 72°C. The final reaction volume was 20 µL, consisting of 2 µL of cDNA, 12.5 µL of Master mix (Solis Biodyne), and 1.125 µL of primers, adjusted with 5.25 µL of water. The delta-delta CT method was used to determine the relative expression, with GAPDH as the normalization gene. The primer sequences are shown in **Table 5**.

Gen	Sequences (5'-3')
ERVW-1 (Syncityn-1)	F- GCA ACC ACG AAC GGA CAT C R- GTA TCC AAG ACT CCA CTC CAG C
ERVFRD-1 (Syncytin-2)	F- CGG ATA CCT TCC CTA GTG CC R- AGC TGA GGT TGC TGG TTC TG
βhCG	F- GCT ACT GCC CCA CCA TGA CC R- ATG GAC TCG AAG CGC ACA TC
GAPDH	F- GGT GTG AAC CAT GAG AAG R- CCA CGA TAC CAA AGT TGT C

Table 5. The primer sequences of the syncytialization mediators used for qPCR.

3.1.1.10. Statistical Analyses

The experimental data were presented as the mean ± standard error of the mean (SEM). This included measurements of LDH, hCG, and factors released in the culture supernatants of BeWo cells. A repeated measures ANOVA test was utilized for group comparisons. A *p-value* < 0.05 was considered statistically significant. The descriptive statistics and Dunnett's post hoc test

were applied to compare different conditions. Graphs and statistical analyses were performed using GraphPad Prism version 10.

3.1.2.   Results and Analysis

Mitochondrial activity assessed by the MTT assay is proportional to the number of cells present in the culture

After performing the MTT assay, it was observed that nearly half of the cells showed a decrease in mitochondrial activity compared to the control cells or unstimulated (CTB) cells. This observation could have two possible explanations. Firstly, FSK may be causing cell death. Secondly, FSK might be triggering cellular differentiation, which could result in a decrease in cell proliferation and a proportional reduction in mitochondrial activity. Notably, the number of active mitochondria is directly proportional to the number of cells in the assay. Hence, a higher number of cells would result in a greater number of active mitochondria. As mentioned earlier, cellular differentiation from CTB to STB involves cell cycle arrest, and after that, cell fusion is associated with the non-replicative differentiation of STB (**Figure 9A**). To determine if FSK impacted cell viability, we measured LDH activity. The results showed no significant differences in LDH activity, in the supernatants of cells exposed to the treatment versus control cells. Therefore, it is suggested that the observed decrease in mitochondrial activity in the MTT assay was not due to cell death or damage. Instead, it probably resulted from the cell differentiation process (**Figure 9B**).
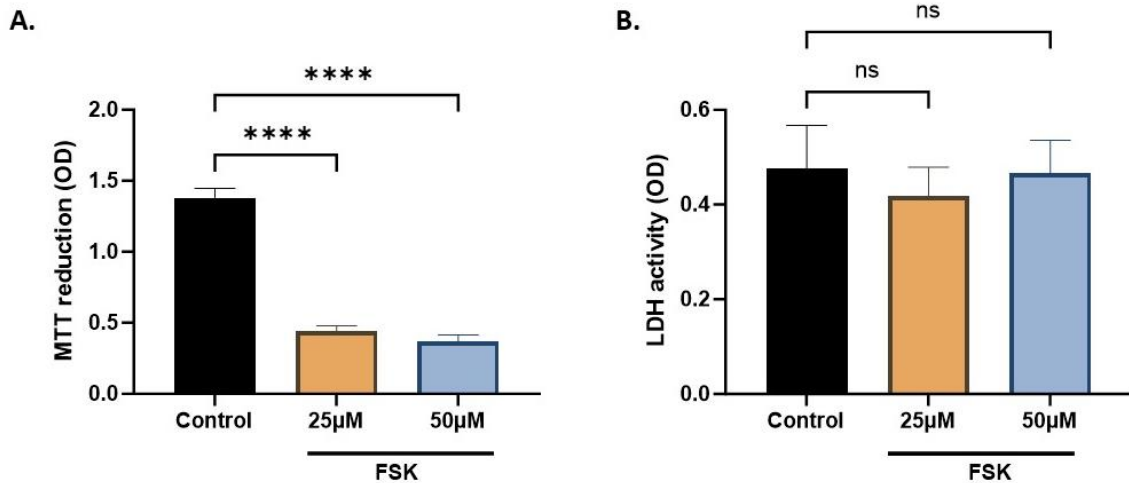
Figure 9. Mitochondrial activity assessed by the MTT assay is proportional to the number of cells present in the culture. **A.** MTT reduction as an indicator of mitochondrial activity and cell proliferation. (n=3). ANOVA *p-value*: <0.0001. **B.** Measurement of lactate dehydrogenase activity as an indicator of cell viability. OD: Optical densities of control and treated cells. (n=3). ANOVA *p-value*: 0.846.

3.1.2.1.   The production of βhCG increases in BeWo cells stimulated with Forskolin

Differentiated STB produced an average of 157,382 $\pm$ 45,483 pg/mL of hCG compared to CTB cells, which produced an average of 17,104 $\pm$ 8,336 pg/mL of this hormone. These data suggest that the STB are actively performing their function in the specific case associated with the production of the hormone hCG, a primary characteristic of well-differentiated STB, data shown in the **Figure 10**.
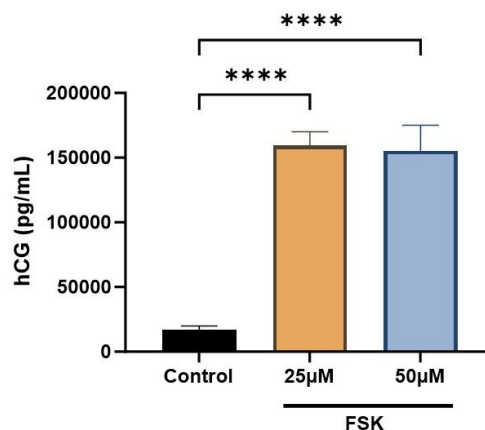

Figure 10. Production of βhCG increases in BeWo cells with forskolin stimulation. Comparison of βhCG production in pg/mL based on the concentration of FSK stimulus used in STB vs. control CTB cells (n=3). ANOVA *p-value*: (****): <0.0001.

3.1.2.2.   The syncytialization index increases in cells treated with forskolin

Prior to analyze the induction of syncytialization, a comparison of manual and automatic cell count was performed using MATLAB software, to estimate the quantity of nuclei that formed syncytia. Both methodologies demonstrated a positive correlation and were employed to cross-verify counts of individual nuclei and nuclei within syncytia (**Figure 11**).
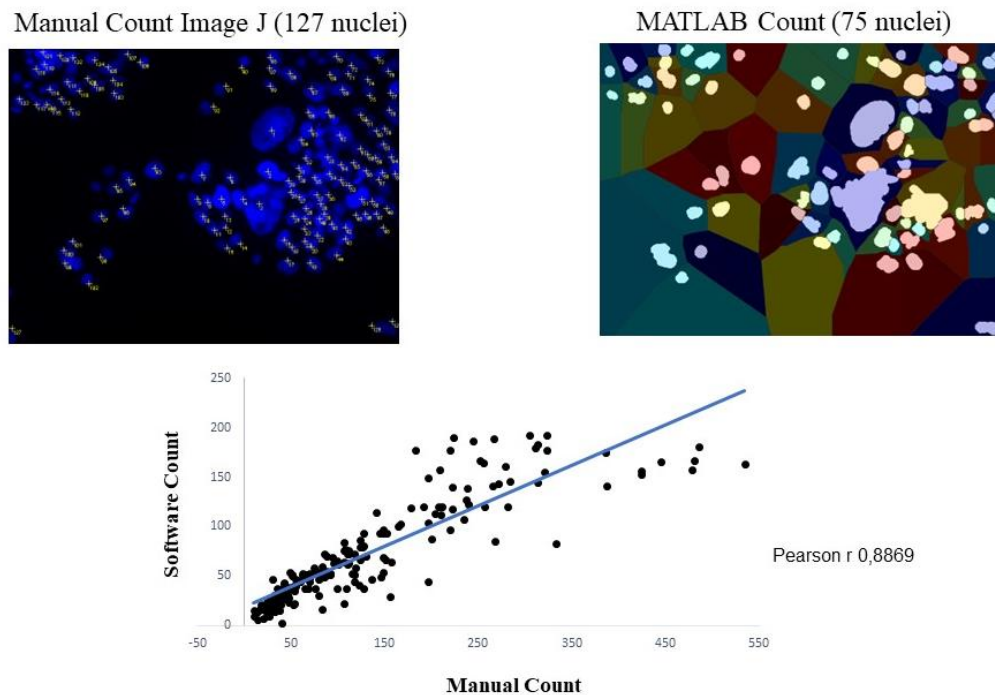

Figure 11. Positive correlation between manual nucleus counts and automated count using MATLAB software.

E-Cadherin immunostaining was used to evaluate cell membrane fusion, which is indicated by the reduction of intercellular junctions and nuclear fusion, under treatment with FSK as an inductor of the differentiation process of CTB into STB. Syncytium formation was determined by the fusion of three or more nuclei and was calculated using the fusion index. The results showed that the formation of STB was induced by FSK. As illustrated in **Figure 12**, both FSK concentrations of 25 µM and 50 µM led to a decrease in E-Cadherin expression, accompanied by the distinctive nuclear fusion characteristic of STB. No significant difference was observed between the two concentrations. It was found that both concentrations of FSK significantly induce nuclear fusion, demonstrated by an increased fusion index (around 30%) in FSK-stimulated BeWo cells compared to control CTB cells (around 10%). Additionally, this was corroborated by the significantly decreased expression of E-cadherin in fused layer or STB.
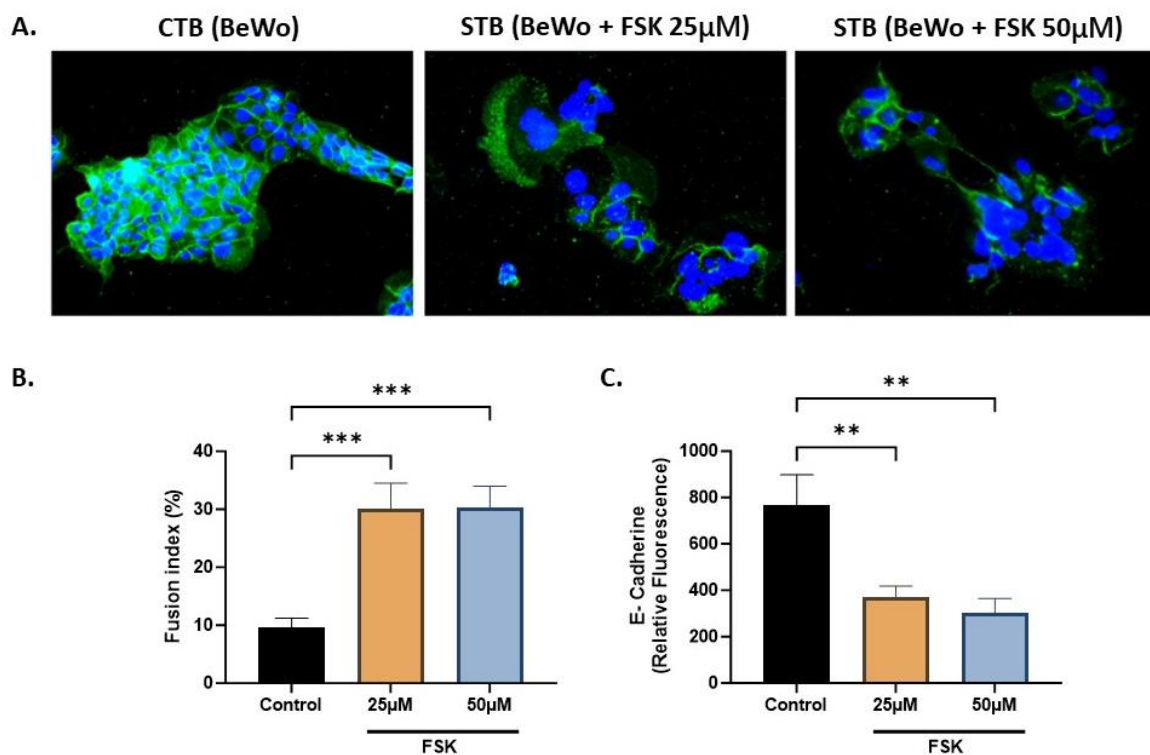
Figure 12. Evaluation of syncytialization index through E-Cadherin expression. A. Photographic record from the fluorescence microscope at a total magnification of 200X. Expression of E-Cadherin in control CTB cells and in STB with different FSK treatments (25μM and 50μM). In green: staining with Alexa Fluor-488 for E-Cadherin, in blue: Hoechst for nuclei. **B.** Mean fluorescence intensity of E-Cadherin in control cells and FSK treatments. **C.** Syncytialization index in control cells and FSK treatments. (n=3). ANOVA *p-value*: (*): <0.0001; (): 0.0013.

After confirming the cellular differentiation process, which was verified through the syncytialization index by manual and systematic nucleus counting as well as the decrease in E-Cadherin expression, the next step was to determine whether FSK had any cytotoxic effects on the cells. In order to do this, we conducted an MTT reduction assay and measured the LDH activity in cells both, with and without FSK stimulus.

3.1.2.3. Decreased proliferation in cells that differentiate into syncytiotrophoblast

The impact of FSK stimulation on the cellular proliferation process was assessed, and it was found that, as expected, when CTB differentiated into STB given that the latter is non-proliferative Ki67 expression decreased. A significant reduction in expression of Ki67 with FSK was observed, the presented data correspond to three independent assays conducted on different days. (**Figure 13**).
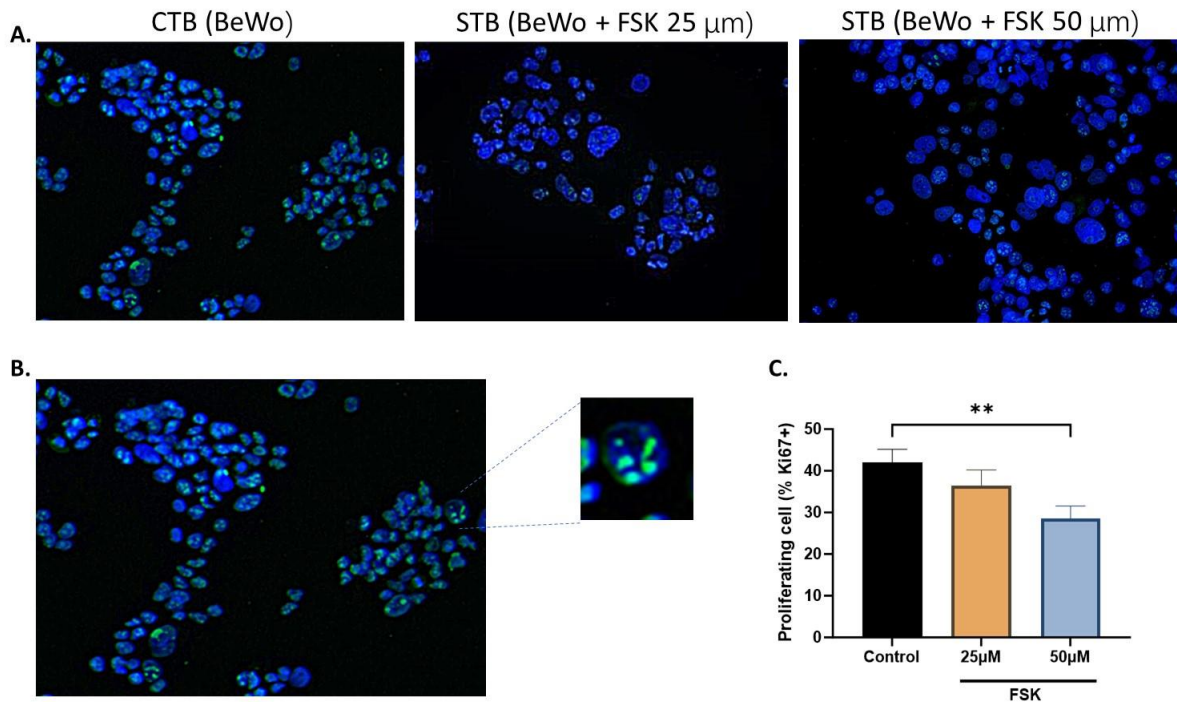
Figure 13. The expression of Ki67 decreases in cells that have undergone differentiation into syncytiotrophoblast. **A.** Photographic panel of treatment conditions to assess cell proliferation in BeWo cells. **B.** Enlarged microphotograph to depict the appearance of nuclei stained with Ki67. **C.** Frequency of Ki67 expression in the various evaluated conditions, (n=3).

3.1.2.4. Incremented apoptosis in differentiated cytotrophoblast cells leading to syncytiotrophoblast formation

In the final step of cell differentiation, non-proliferative STB undergoes cell death. To determine the frequency of cells undergoing apoptosis, M30 staining was employed. M30 staining detects a neoepitope that results from cytokeratin 18 cleavage during cell death. The study found that as STB differentiates, cell death increases, as expected in the final differentiation process. There was a significant increase in M30 expression in differentiated cells, with an average of apoptotic cells at 45% ± 2.06, compared to the control with an average of apoptotic cells at 20.26% ± 10.1 (*p-value* < 0.0001) (**Figure 14**).
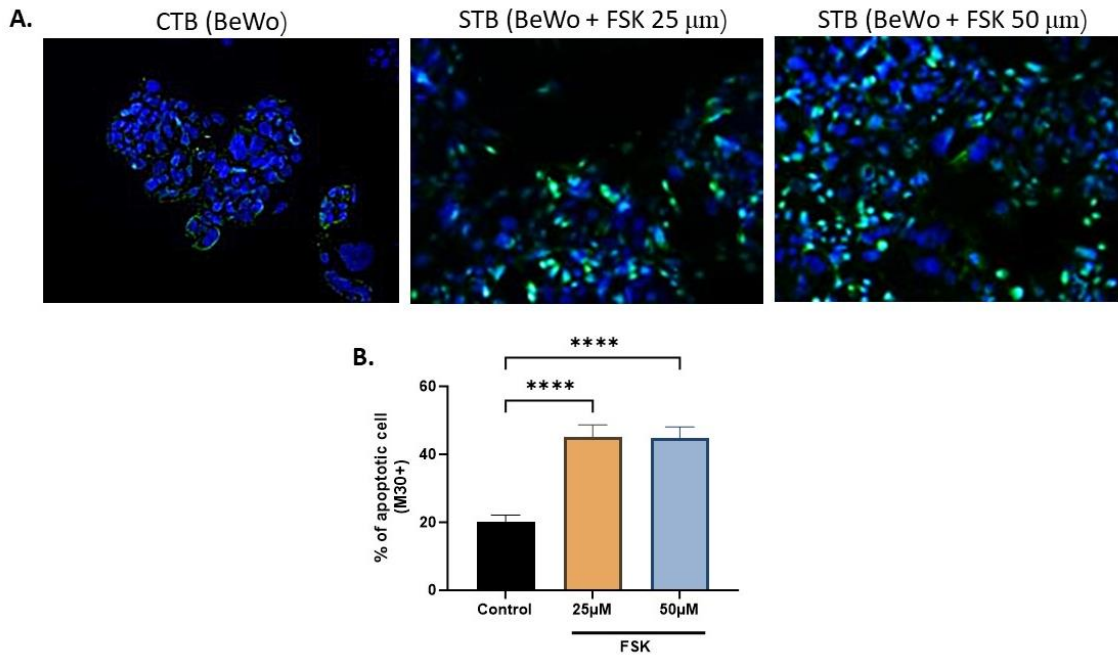
Figure 14. Increased apoptosis in differentiated cytotrophoblast cells transitioning to syncytiotrophoblast. A. Photographic panel of M30 expression in CTB cells differentiated to STB. **B.** Frequency of M30 expression under different study conditions (n=3).

3.1.2.5. Stimulation with Forskolin significantly increases the expression of syncytialization mediators in BeWo cells

Three specific genes were chosen to examine the involvement of molecular mediators in syncytialization: SYN-1, SYN-2, and βhCG genes. The expression of these genes suggests a considerable increase in their expression when BeWo cells were exposed to 50 μM of FSK (Figure 15).
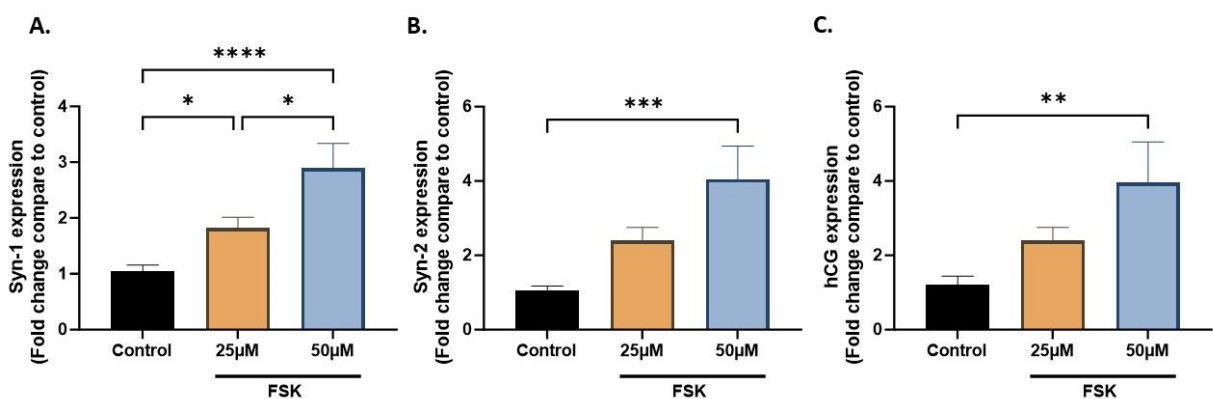

Figure 15. Expression levels of the SYN-1, SYN-2, and βhCG genes in treated cells compared to control cells evaluated by qPCR. **A.** On average, the SYN-1 gene exhibited a 2.65-fold increase in expression in cells treated with 50 μM FSK compared to the control, B. The SYN-2 gene

showed a 4.04-fold increase in expression, C. The βhCG gene demonstrated a 3.32-fold increase in expression (n= 3). ANOVA s: (**): 0.0082; (*): 0.0174.

3.1.2.6. Syncytiotrophoblast differentiation does not affect the expression of the chondroitin sulfate A receptor

To demonstrate that FSK-mediated cellular differentiation does not affect the expression of the receptor used by *P. falciparum* for adherence, chondroitin sulfate A receptor (CSA), immunofluorescence labeling of CSA was performed as previously described in the methodology section. The expression of CSA was similar for the different treatments, including the control CTB cells, five replicates of BeWo cell cultures stimulated with concentrations of 25 and 50 μM of FSK were conducted, each with its respective control of unstimulated cells, namely CTB (**Figure 16.A**). For the analysis, the mean fluorescence for CSA was determined using the Fiji program. The results showed a mean fluorescence of 19 ± 2.23 for CTB, 16.4 ± 2.30 for STB (25 μM), and 20.20 ± 2.17 for STB (50 μM). This led to the conclusion of FSK does not induce changes in CSA expression (**Figure 16.B**).
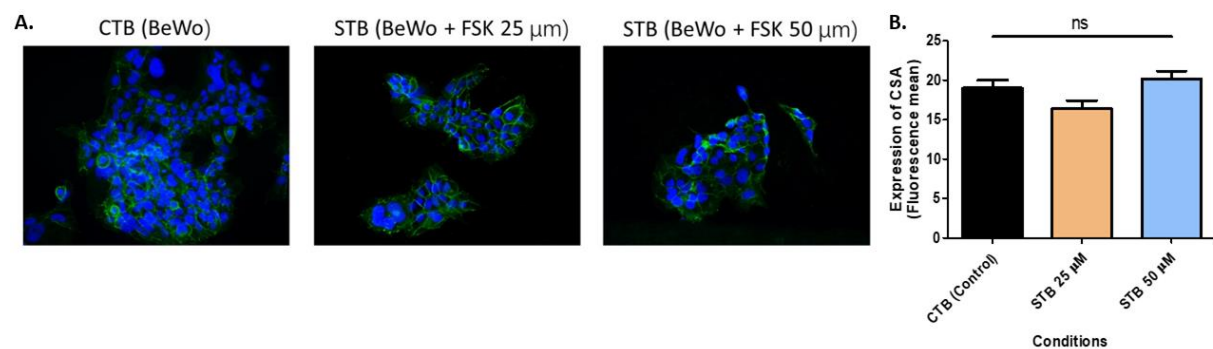

Figure 16. The expression of chondroitin sulfate A does not differ in cytotrophoblast and syncytiotrophoblast cells. **A.** Immunofluorescence staining images of CSA are presented. **B.** The mean and standard deviation of the mean are shown in control and syncytialized cells expressing CSA.

3.1.3. Graphical summary of results
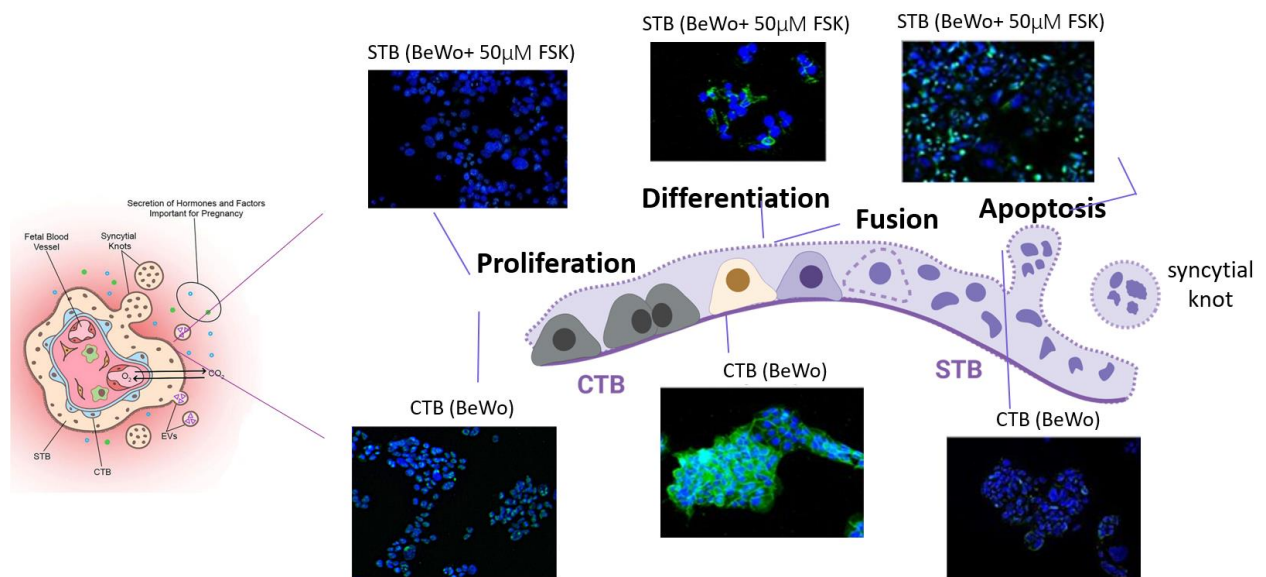
Figure 17. The differentiation model of cytotrophoblast to syncytiotrophoblast was optimized. The different processes associated with the differentiation of CTB to STB were carried out appropriately: proliferation, differentiation-fusion, and cellular apoptosis.

3.1.4. Conclusion

Various methodological strategies used to assess the viability and different stages of cell differentiation, such as proliferation, syncytialization, and apoptosis, collectively allowed us to conclude that the *in vitro* differentiation of CTB cells to STB was successfully established using FSK stimulation. Cells differentiated *in vitro* replicated various steps of the process and expressed CSA, a key molecule used by *P. falciparum* as a cytoadherence receptor for sequestration in the placenta. The next step is to evaluate changes in differentiation and the expression of molecules in trophoblast cells exposed to *P. falciparum.*

3.2. Specific objective 2. To assess the effect of *P. falciparum* on trophoblast proliferation, differentiation, viability, and apoptosis

3.2.1. Methods

Does *Plasmodium falciparum* have any effect on the differentiation of BeWo cells?

Once the optimal conditions were standardized to study the various differentiation processes from CTB to STB, we proceeded to investigate how *P. falciparum* affects or interferes with these processes. Methods related to BeWo cells parameters were described in Objective 1 methods section. The methodologic approach of *P. falciparum* culture and co-incubation conditions with the cells, is outlined below.

3.2.1.1. Culture of *P. falciparum* strain adherent to CSA (FCB1CSA)

The FCB1CSA strain was grown in A+ erythrocytes using RPMI-1640 medium, which was supplemented with 25 mM HEPES, 21.6 mM $NaHCO_3$, 16 µg/L of gentamicin, 0.2 mM of hypoxanthine (Sigma), and 10% A+ human serum. The continuous culture was maintained according to previous studies, at a hematocrit (Hto) of 5% and in a gas mixture of 5% CO_2, 5% O_2, and 90% N_2 at a temperature of 37°C. (108). The parasitemia was monitored daily, and the medium was changed every 24 hours. Healthy erythrocytes were added three times a week until a parasitemia level of 5-7% was achieved (108).

3.2.1.2. Concentration of mature forms of *P. falciparum* by gelatin

Mature forms of *P. falciparum* (trophozoites and schizonts) were concentrated using the gelatin flotation protocol. The *P. falciparum* cultures were centrifuged at 2,500 rpm for 5 minutes in conical tubes. The culture supernatant was removed, and 1% porcine gelatin solution (Sigma) in incomplete RPMI-1640 was added to the *P-falciparum*-IE pellet (1 volume of IE pellet/10 volumes of gelatin). The mixture was incubated at 37°C for 40 minutes, allowing separation into two phases. The upper phase, containing the mature stages, was then transferred to a new 15 mL conical tube, and washed twice with incomplete RPMI-1640 by centrifugation at 2,500 rpm for 5 minutes. The parasitemia of the pellet was estimated by counting *P. falciparum*-IE in a thin blood smear (108).

3.2.1.3. Maintenance of *P. falciparum* adhesive (CSA) phenotype

Parasites adherent to CSA (FCB1CSA strain) were selected every four weeks to maintain the parasite's phenotype. Briefly, the culture flask was coated with soluble CSA for 2 hours at 37°C with agitation. After a series of PBS 1X washes and the application of a blocking solution, the parasite suspension was added to CSA-coated flasks and incubated for 2 hours at 37°C on a shaker. The medium was removed, and non-parasitized and non-adherent erythrocytes were eliminated by washing with 5 mL of incomplete RPMI 1640. Following this, 5 mL of complete RPMI 1640 culture medium (10% human serum and 3.5% sodium bicarbonate) and non-infected erythrocytes at a hematocrit of 2.5% were added. Finally, the flasks were incubated at 37°C with a gas mixture suitable for *P. falciparum* until the following day. The next day, the culture was transferred to new bottles, and cultivation continued until the parasites were ready for the repeat selection procedure (16).

3.2.1.4. *Plasmodium falciparum* cytoadherence assay

Cytoadherence assays were conducted to measure the amount of adherent iEs to BeWo cells using static conditions. The cells were grown in 8-well Lab-Tek® II chambers (Nunc®, St. Louis, MO, United States). The cells were grown until they reached a confluence of 50-80% over a period of 2-5 days. Following this, they were washed using an adhesion medium of RPMI 1640 supplemented with 0.5% BSA (Sigma-Aldrich, St. Louis, MO, United States) at pH 6.7. Subsequently, they were incubated with 300 μL of a mature stage iEs suspension that had a parasitemia of 10% and hematocrit of 1% in an adhesion medium. The incubation was carried out for one hour at room temperature with constant agitation (100 rpm). After incubation, non-adherent erythrocytes were removed by washing the slides four times with an adhesion medium. The adhered iEs were fixed overnight in 2% glutaraldehyde and then stained for 45 minutes with 1% Giemsa. The level of adhesion was quantified microscopically by counting the number of attached iEs to a total of 500 STB nuclei. The experiments were repeated on a minimum of three different occasions, each time being conducted twice.

3.2.1.5. Exposures of BeWo cells to *Plasmodium falciparum*

The impact of *P. falciparum* on BeWo cells was assessed by co-exposing the cells to *P. falciparum*-IE and FSK. Unsyncytialized BeWo cells were used as a control (CTBs). Cells were plated and allowed to adhere to culture plates overnight. The following day, they were exposed to iE and treated with FSK simultaneously by 24 hours. Subsequently, parasites were removed, and the cells were incubated once again for an additional 24 hours with a new FSK treatment to complete the 48-hour differentiation process. **Figure 18.**
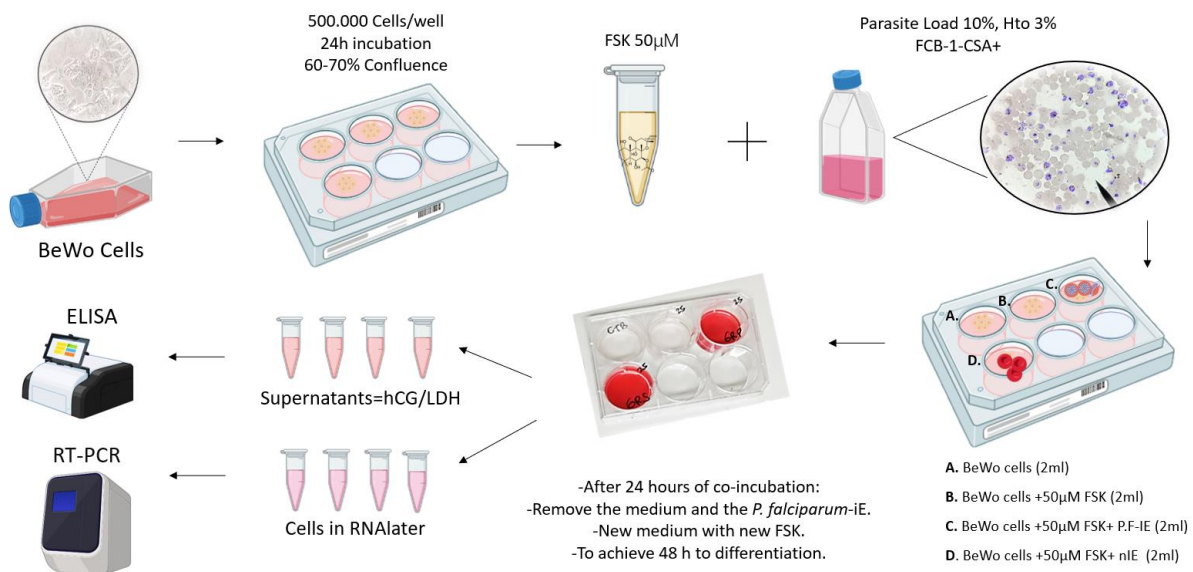

Figure 18. Exposure of BeWo cells to *P. falciparum*. For these assays, 500,000 BeWo cells were placed in each well and incubated for 24 hours until they reached 50-60% confluence. Then, FSK at concentrations of 50μM were added along with parasites having a parasitemia of 10% and gelatin with Hct 3%. After 24 hours, the parasites were removed, and FSK was added again with a complete F-12 medium to complete the 48-hour differentiation. LDH activity (Absorbance) and G production (ELISA) were measured from the supernatants. The treatment with trypsin helped to detach the cell monolayer, and RNA was extracted from it to measure the expression of syncytialization-associated mediators such as SYN-1 and SYN-2 (qPCR).

3.2.1.6. Statistical Analyses

The experimental data were presented as the mean ± standard error of the mean (SEM). A repeated measures ANOVA test was employed to compare groups. A *p-value* < 0.05 was considered statistically significant. The descriptive statistics and Dunnett's post hoc test were applied to compare different conditions. Graphs and statistical analyses were performed using GraphPad Prism version 10.

3.2.2. Results and Analysis

3.2.2.1. Syncytiotrophoblast and cytotrophoblast cells support *P. falciparum* cytoadherence, through chondroitin sulfate A

The first step was determining if the CTB and STB supported the adherence of the *P. falciparum* strain FCB1CSA cultured and selected for the CSA cytoadherence phenotype and confirm if the adherence was specific to CSA, by performing a prior coincubation with soluble chondroitin sulfate (CSA-S) as a specificity control, used to competitively block the parasite antigen (**Figure 19**). It was observed that in cells with the CSA receptor blocked, the cytoadherence of infected erythrocytes (iE) significantly decreased, compared to cells with unblocked CSA receptor (**Figure 19**). This led to the conclusion that the cytoadherence of iE to cells in these experimental conditions was specifically mediated by CSA. This finding laid a crucial foundation for subsequent experiments aimed at assessing the damage caused by *P. falciparum* to the cellular differentiation process, as outlined in Objective 2.
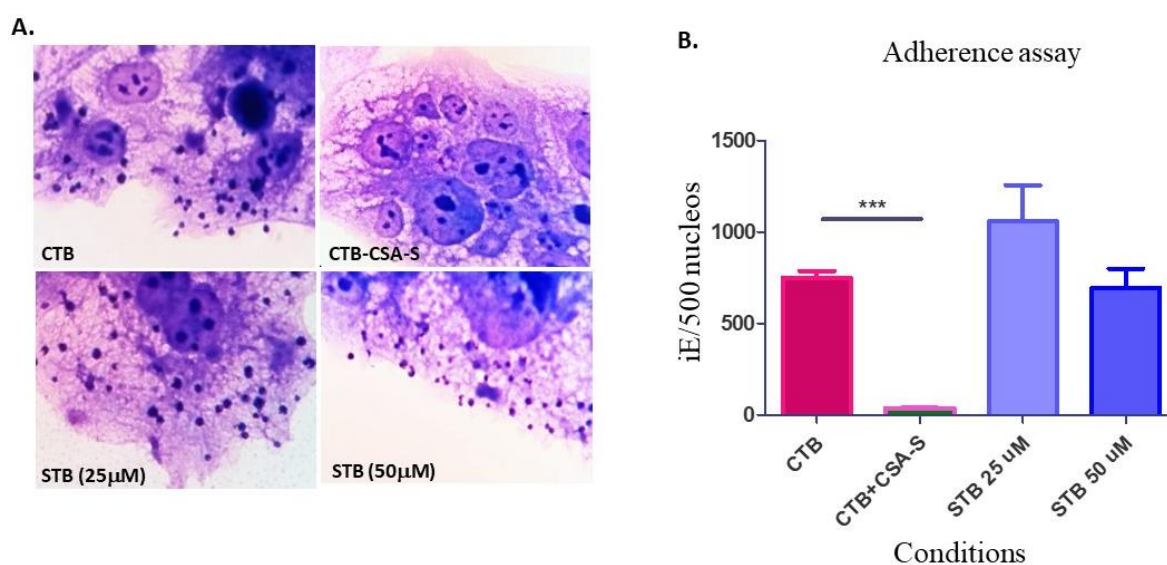
Figure 19. The cytoadherence of *P. falciparum*-CSA+ is supported by cytotrophoblast cells and syncytiotrophoblast. **A.** Representative images of *P. falciparum* FCB1-CSA cytoadherence on BeWo cells treated with 25μM and 50μM forskolin (STB), untreated control cells (CTB), and specificity control cells with preincubation of soluble CSA, stained with Giemsa. **B.** Statistical analysis of the cytoadherence assay, using soluble CSA as the specificity control (CTB+Soluble CSA). (Total magnification of 1000X). Test: ANOVA *p-value*: < 0.05.

3.2.2.2. Increase in LDH activity when CTB and STB exposed to *Plasmodium falciparum*

We evaluated *P. falciparum*-induced cell damage by measuring LDH levels. Our findings revealed a significant role of the parasite in inducing cellular damage in STB, as evidenced by an optical density (OD) of LDH activity at 0.59 ± 0.10. This contrasted with cells exposed to non-parasitized erythrocytes, which had an OD of LDH activity at 0.31 ± 0.06 (*p-value* = 0.0423), STB alone at 0.27 ± 0.05 (*p-value* = 0.0148), and cytotrophoblasts (CTB) alone at 0.17 ± 0.04 (*p-value* = 0.0008) (**Figure 20**).
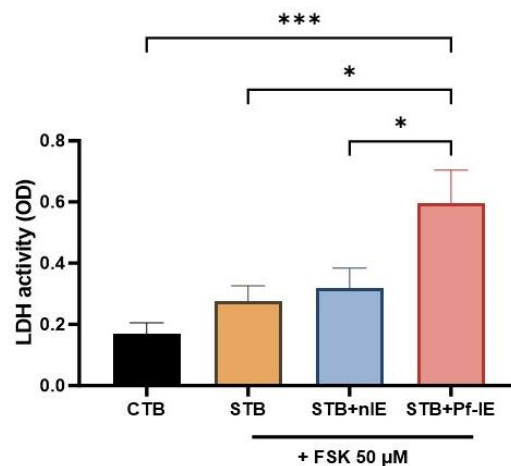
Figure 20. BeWo cells syncytiotrophoblast exhibit significant changes in LDH activity when exposed to *P. falciparum*. Control untreated cells (CTB), STB in co-culture with non-parasitized red blood cells (nIE), STB in co-culture with erythrocytes parasitized by *P. falciparum* (Pf-IE) (n=3). Test: ANOVA *p-value* < 0.05.

3.2.2.3. The production of βhCG remains unchanged in syncytiotrophoblast exposed to *Plasmodium falciparum*

The STB produce higher levels of hCG compared to CTB, used as a control in the differentiation process. A trend towards decreased hCG production was observed in STB exposed to parasitized erythrocytes, but there was no significant decrease (**Figure 21**).
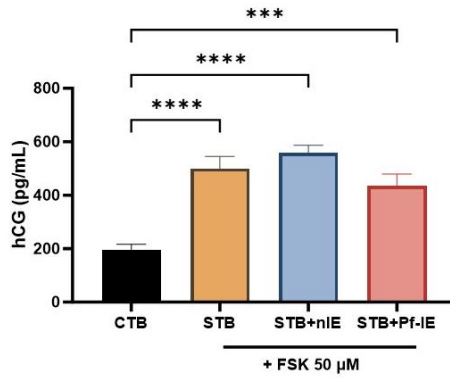
Figure 21. Measurement of hCG in syncytiotrophoblast in co-culture with erythrocytes parasitized by *P. falciparum* does not change compared to control. STB in co-culture with uninfected erythrocytes (STB+nIE), STB in co-culture with infected erythrocytes (STB+Pf-IE). (n=6). Test: ANOVA *p-value* < 0.05.

3.2.2.4.   *Plasmodium falciparum* decreases the membrane fusion of cytotrophoblast

A significant impact of *P. falciparum* on the syncytialization process was observed, specifically during the fusion process. When the CTB is simultaneously exposed to parasitized erythrocytes and FSK, the expression of E-cad increases, and the syncytialization index decreases, demonstrating a negative impact of *P. falciparum* in the process of cellular fusion (Figure 22).

Figure 22. Exposure to *P. falciparum* decreases syncytialization index in syncytiotrophoblast. A. Panel of representative photos depicting the expression of E-cadherin in CTB, STB, and STB exposed to *P. falciparum*. B. Fusion index, C. Mean fluorescence intensity of E-Cad. (n=3). ANOVA *p-value* (*): <0.05.

3.2.2.5. *Plasmodium falciparum* does not alter the proliferation rate during syncytiotrophoblast differentiation

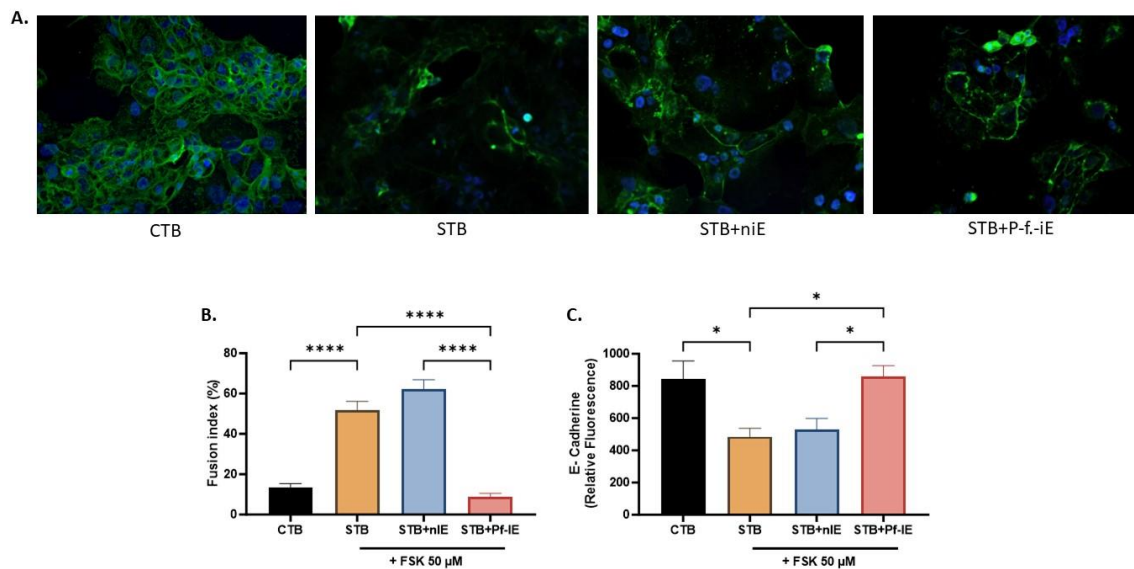The proliferation determined by the frequency of nuclei positive for Ki67 suggests that STB exhibit a lower proliferation rate compared to CTB cells. Furthermore, the exposure of STB to *P. falciparum*-iE does not affect the proliferation rate. The percentage of proliferating cells was found to be 16.99 ± 1.75% and 16.39 ± 2.02% in STB and STB exposed to parasites, respectively. (**Figure 23**).
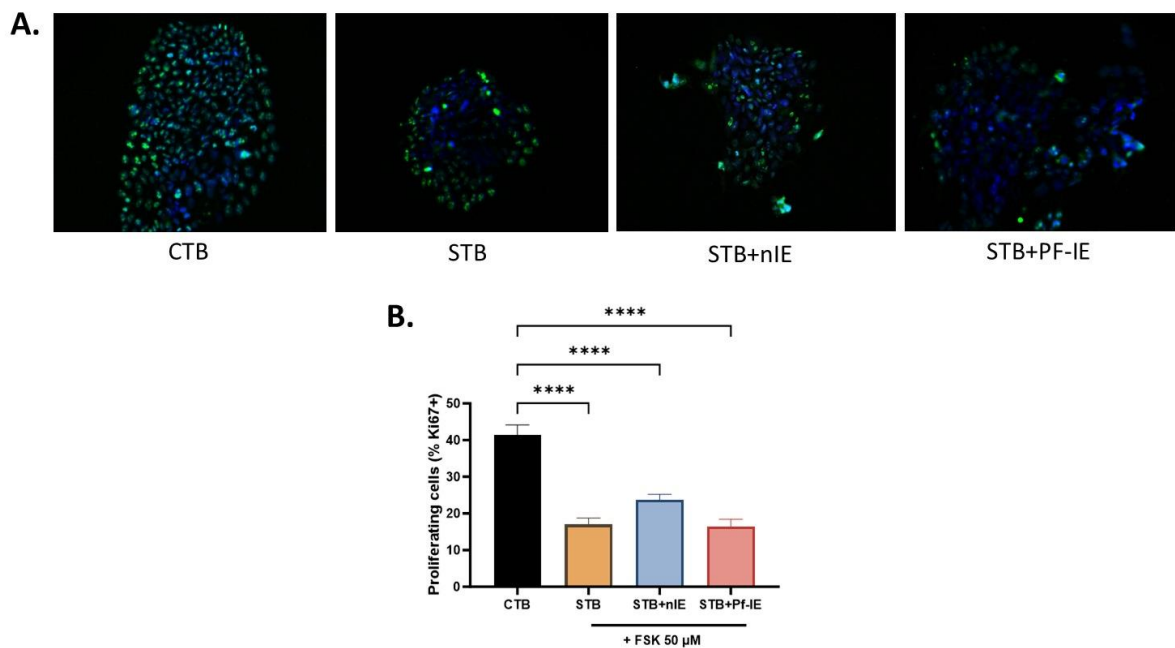
Figure 23. Frequency of Ki67-positive nuclei in syncytiotrophoblast cells exposed to *P. falciparum*-IE. Count of Ki67-positive nuclei in control cells and STB, exposed or not to *P. falciparum*. Frequency assessed systematic counting of the number of nuclei. (n=3). ANOVA *p-value*: <0.0001.

3.2.2.6. *Plasmodium falciparum* does not affect the apoptosis process during syncytiotrophoblast differentiation

The STB have a greater percentage of apoptotic cells compared to CTB cells. Additionally, the higher apoptotic rate of STB is not affected by exposure to *P. falciparum*-IE. The percentage of cells stained positive to M30 epitope was found to be 67.8 ± 4.9% and 64.82 ± 3.69% in STB and STB exposed to parasites, respectively (**Figure 24**).
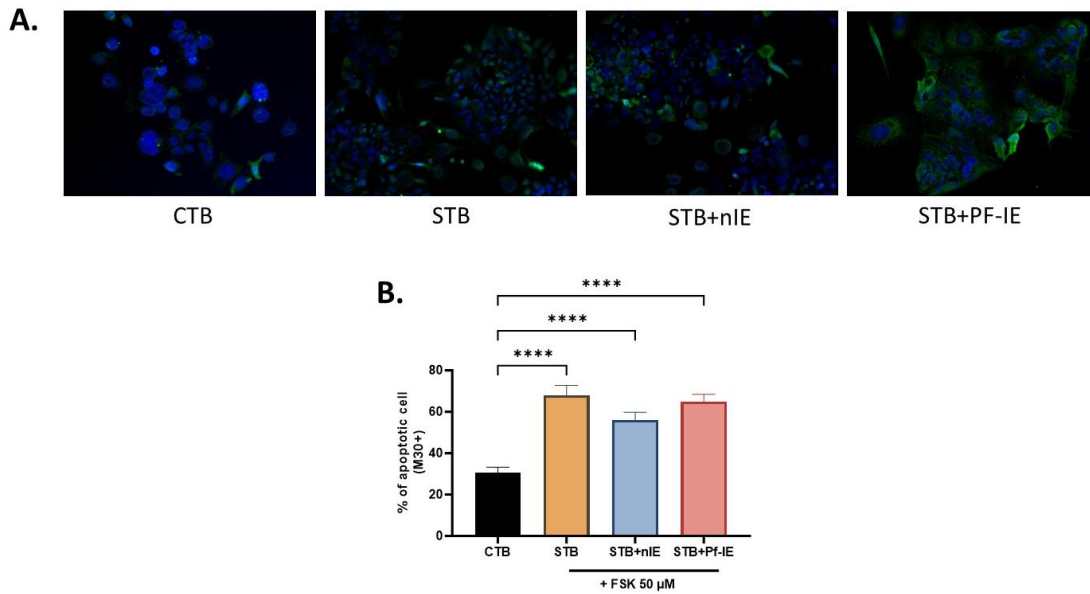
Figure 24. The expression of M30 does not change in syncytiotrophoblast cells exposed to *P. falciparum*-IE. A. Panel of photographs depicting M30 expression under different study conditions. B. Statistical analysis of the mean fluorescence intensity of M30 in control cells and STB exposed or not to *P. falciparum*. (n=3). ANOVA *p-value*: < 0.0001.

3.2.2.7.   *Plasmodium falciparum* significantly decreases the expression of syncytialization mediators in syncytiotrophoblast

A significant decrease in the expression of STB mediators, such as the SYN-1 gene, SYN-2 gene, and hCG, was observed when the STB was exposed to *P. falciparum*-iE, reaching values similar to those found in the CTB (**Figure 25**). The SYN-1 gene exhibited 3-fold decrease in STB exposed to *P. falciparum*-iE, with an expression of 0.53 ± 0.35 compared to STB alone with an expression of 3.65 ± 1.44 (*p-value* 0.0063) (**Figure 25A**). The SYN-2 gene showed 5-fold decrease in expression in STB exposed to *P. falciparum*-iE, with an expression of 1.22 ± 0.60 compared to STB alone with an expression of 6.22 ± 2.02 (*p-value* 0.0010) (**Figure 25B**). The βhCG gene demonstrated approximately 5-fold decrease in expression in STB exposed to *P. falciparum*-iE, with an expression of 1.42 ± 0.59 compared to STB alone with an expression of 6.29 ± 1.09 (*p-value* 0.0004) (**Figure 25C**).
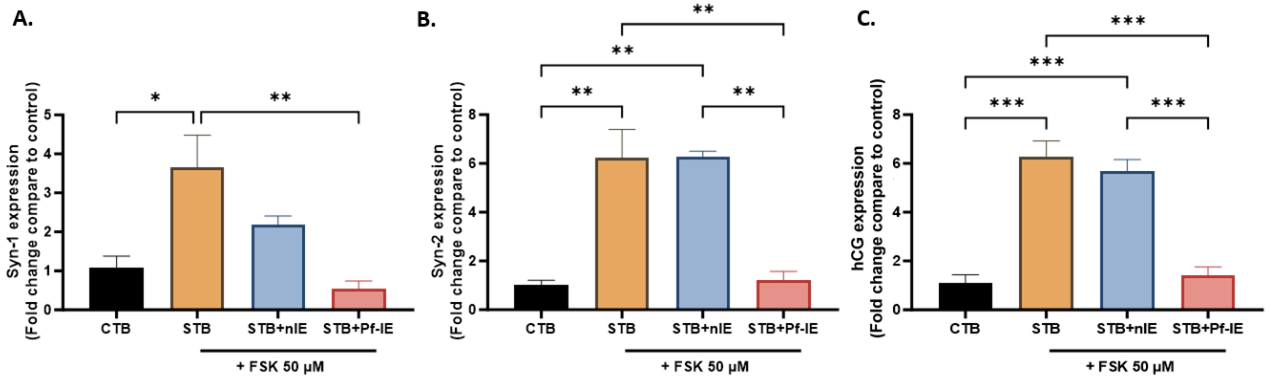
Figure 25. Expression levels of the SYN-1, SYN-2, and βhCG genes in treated cells versus control cells evaluated by qPCR. **A.** The SYN-1 gene **B.** The SYN-2 gene and **C.** The βhCG gene. (n=3). ANOVA *p-value* (***): <0.0001.

3.2.3.   Graphical summary of results
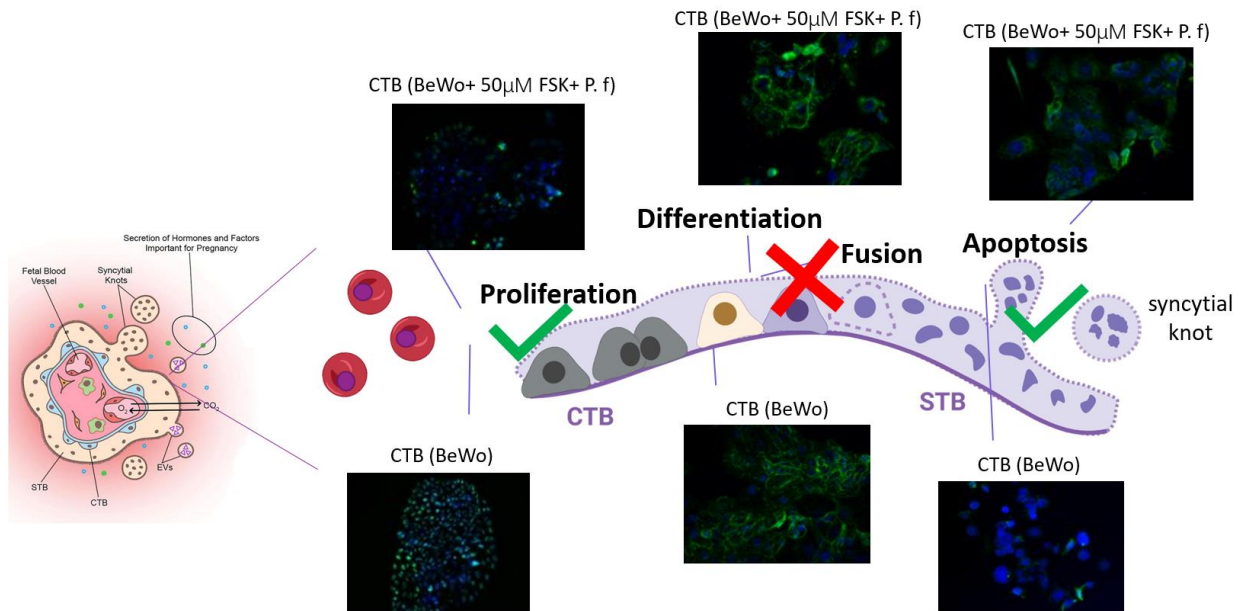
Figure 26. The process of cell fusion was not carried out properly when CTB cells were simultaneously exposed to FSK and *P. falciparum*-IE.

3.2.4.   Conclusion

Based on these results, *Plasmodium falciparum* disrupts the cellular fusion process in the CTB to STB differentiation pathway, which was evidenced by the expression of E-cadherin that increases in STB exposed to parasites, and by the low syncytialization index. It is noteworthy that a significant decrease in the expression of crucial molecular mediators in the fusion

process, such as SYN-1, SYN-2, and hCG, was observed, further emphasizing the negative impact of *P. falciparum* on the CTB differentiation process. Moreover, it was also found that *P. falciparum* cause cellular damage, as the levels of LDH in culture supernatants were higher in the STB exposed to parasites. However, there are no observed alterations in cellular proliferation and apoptosis processes induced by the infected erythrocytes.

3.3. Specific objective 3. To establish a viable and integral culture of Human Placental Explants (HPEs) from third-trimester placentas of healthy pregnant

To achieve this objective, the cultivation of HPEs was standardized, considering various parameters: morphological characteristics in macroscopic and microscopic features of placental tissues. Qualitative and semiquantitative evaluations were conducted to assess tissue integrity, viability and apoptosis were also evaluated. A well-structured protocol was established, described step by step with recommendations at each stage of the methodological strategies that were improved and established for the cultivation of HPEs for up to 72 hours. This protocol was accepted to the MDPI: *Methods and Protocols* journal on October 29 and is attached to this research work (refer to **Supplementary file 1** to see these results).

The results of this specific objective are presented in the article accepted by Methods and Protocols Journal, under the title: "**Assessment of the integrity and function of human term placental explants in short time culture**". Authors: *López-Guzmán Carolina, et al. 2024. (109)*.

Carolina López-Guzmán[1], Ana María García[1], Paula Marín[1], Ana María Vásquez[1,2]

[1] Grupo Malaria, Facultad de Medicina, Universidad de Antioquia, Medellín, Colombia. Calle 62 # 52-59 Torre 1 Laboratorio 610
[2] Escuela de Microbiología, Universidad de Antioquia, Medellín, Colombia. Calle 67 # 53-108, Bloque 5, Oficina 5-135
* Correspondence: amaria.vasquez@udea.edu.co

Abstract: Human placental explant (HPE) culture has generated significant interest as a valuable in vitro model for studying tissue functions in response to adverse conditions, such as fluctuations in oxygen levels, nutrient availability, exposure to pathogenic microorganisms, and toxic compounds. HPE offers the advantage of replicating the intricate microenvironment and cell-to-cell communication involved in this critical and transient organ. Although HPE culture conditions have been extensively discussed, a protocol for assessing the viability and function of HPE during short-term

3.3.1.   Methods

3.3.1.1.   Subjects and Samples

The placentas were donated by pregnant women aged between 23 and 33 years old, the inclusion criteria were women with uncomplicated pregnancies, without comorbidities such as hypertension, preeclampsia, or diabetes, who did not take medication, and underwent scheduled cesarean sections instead of delivery induction. These women delivered via cesarean section after reaching 37 weeks of gestation, and their babies were also in good health. Neither the pregnant women nor their children should have been actively experiencing infectious processes. Exclusion criteria included maternal, fetal, or placental pathologies. The research protocols adhered to the principles of the Declaration of Helsinki and received approval from the Bioethics Committee of the Institute of Medical Research, Faculty of Medicine, University of Antioquia (Acta No. 015, dated 24/09/2020). All participants willingly participated in the study and provided informed consent by signing the documents approved by the Bioethics Committee. A total of twelve human term placentas (>37 weeks of gestation) were included in the study.

3.3.1.2.   Collection of placentas from donors

The nursing staff at the Department of Gynecology and Obstetrics in Clinica El Rosario, Medellín, provided the research team with a database of candidates who met the inclusion criteria for placenta donation. These candidates were contacted by a member of the research team, who explained the study's purpose and requested their voluntary participation. After signing informed consent forms, the placenta and umbilical cord were placed in a red bag and stored in an airtight plastic container. Within two hours of cesarean delivery, the placenta was transported to the laboratory (BSL II) for processing.

3.3.1.3.   Human placental explants dissection and culture

Placentas were obtained under sterile conditions and processed within 1 to 3 hours. The maternal and fetal surfaces were removed, and villi tissue was extracted from central cotyledons. For each placenta, around five randomly selected 2x2 cm fragments of cotyledons from the maternal side were taken. These fragments were washed to remove maternal blood, and smaller villi dissections (about 0.5 cm3) were obtained. Three chorionic villi explants

(average of 100 mg total) were then cultured in 6-well plates with 2 ml of DMEM/F-12-Ham medium culture media supplemented with 10% fetal bovine serum, penicillin (100 U/mL), and streptomycin (100 µg/mL). The cultures were incubated for 48 hours before treatment (the processing is detailed in Figure 27). Due to biological variability among donors, the experimental design should involve donor-matched control and treatment groups. This means that each donor's tissue should be divided into control and experimental groups.
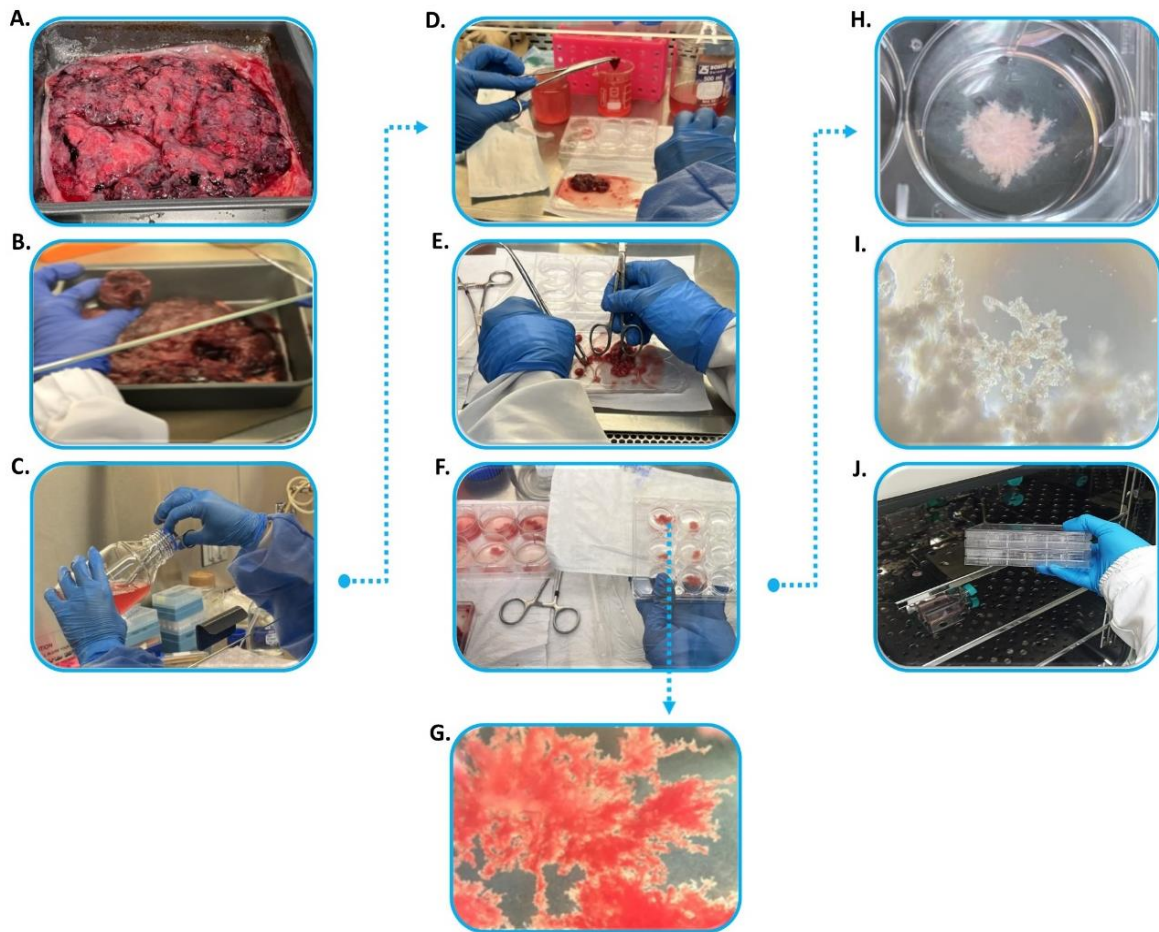
Figure 27. Procedure for isolating human placenta villous. A. Placenta lying in an aluminum tray in a maternal portion of the surface facing upwards. At this point the tissue should be weighed. **B.** Small blocks of cotyledons located on the maternal side of the placenta are dissected, with dimensions of 3x3 cm and 2 cm in depth. Depending on the purpose of the study and tissue healthy two or three cotyledons are required. **C.** Each cotyledon is washed in a PBS 1X plus antibiotic (final concentration 1%) solution to remove blood clots. **D.** Small fragments with dimensions around 4-6 mm are dissected from washed cotyledons. In this point it is important to avoid capillaries during fragments dissection. **E.** Villous from fragments are held using a blunt surface to press fragments until to obtain pieces with dimensions around 2-3mm as much. **F.** Additional washing of these small pieces is done by immersion in well plates containing PBS plus antibiotic. Two or three pieces are washed together in a six well plate and then the best tissues are selected for extra wash in a twelve well plate. **G.** Macroscopic appearance of the placental explant during washes under a stereoscope Leica S6 with 1,25x20 zoom and a 60° viewing angle. **H.** After washing villous are seeding in well containing a matrix of FBS during five to ten minutes. **I.** Then complete culture medium is added to the well plate to a final volume of 3 mL the

placental villous are confirmed under optical microscopy. **J.** The placental villous are cultured under standard conditions, with 5% CO_2 at 37°C for a period of 24 to 72 hours, with daily medium changes.

3.3.1.4. Measurement of cell viability through detection of Lactate Dehydrogenase (LDH) activity

The activity of the LDH enzyme was measured as an indicator of cellular damage. It was measured as described in the methodology of objective 1. The normalization of the obtained results was done per 100 mg of tissue, and a positive control of damage with Triton X-lysed tissue was used as a positive control for the technique, representing 100% of LDH activity.

3.3.1.5. Detection of endocrine mediators and angiogenic factors to assess Human placental explants functionality

The functionality of HPEs was assessed through the detection of endocrine mediators and angiogenic factors, including, the Human Chorionic Gonadotropin (hCG), Placental Growth Factor (PlGF), Vascular Endothelial Growth Factor (VEGF), Vascular Endothelial Growth Factor Receptor (VEGF R1/Flt-1) and Endoglin (END), by using DuoSet ELISA enzymatic immunoassay kit (R&D Systems). These kits follow the sandwich ELISA principle and detect free protein in culture supernatant. In brief, a 96-well microplate was coated with 50 µL of capture antibody and left overnight at room temperature. The plate was then washed three times with a buffer and dried with a clean towel. Next, the plate was blocked with 150 µL of blocking buffer and left to incubate for one hour at room temperature, followed by more washes. Samples were added in a 1:1 (v/v) ratio, with a final volume of 100 µL in each well and incubated for 2 hours. The plate was then washed again and 50 µL of Detection Antibody was added to each well and incubated for another 2 hours, followed by more washing. Finally, 50 µL of Streptavidin-HRP solution was added to each well and left to incubate for 20 minutes at room temperature. After that, 50 µL of substrate solution was added to each well and left to incubate for another 20 minutes at room temperature. The reaction was stopped by adding 50 µL of stop solution. The absorbances were measured in a Microplate Photometer (Multiskan™ FC Thermo Scientific™) at 450 nm OD, and the concentration was determined in pg/mL by extrapolating the OD data into a standard curve.

3.3.1.6. Histological analysis with Hematoxylin-Eosin

HPEs samples were processed as follows: they were fixed in 10% formaldehyde in 0.1 M phosphate buffer (pH 7.3) for 24 hours. Afterward, they were dehydrated in alcohol, clarified in xylene, embedded in paraffin, and sectioned into 3 µm slices. The paraffin-embedded tissue sections underwent different staining techniques for analysis. Hematoxylin-eosin (H&E) staining was used for histological examination, which assessed the presence of syncytial knots, fibrin deposits, infarction, and total fetal blood vessels (as detailed in **Table 6**). The average of these values was estimated across the observed villi in 10 microscopic fields. The slides were examined by two trained microscopists using a light microscope under 40X magnification (400-fold) and, if necessary, in 100X magnification (1000-fold) for histological confirmation.

Table 6. Scores for the analysis of the histopathological damage

Score	Histopathological damage
1	Trophoblast/Fetal connective tissue intact
2	Minor detachment of the trophoblast and/or disorganization of fetal connective tissue
3	Almost complete detachment of trophoblast and/or disorganization of fetal connective tissue
4	Complete detachment of the trophoblast/disorganization or destruction of fetal connective tissue
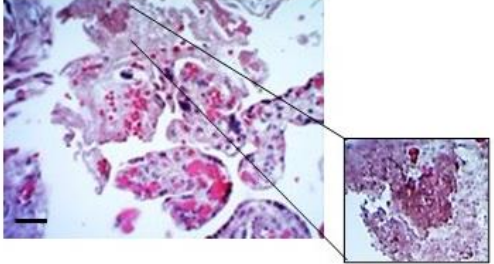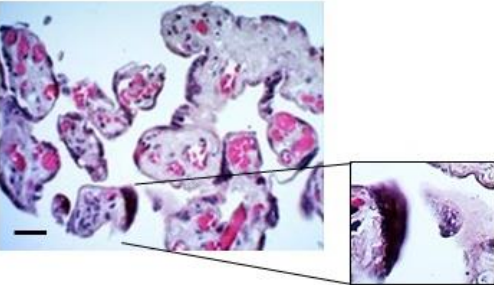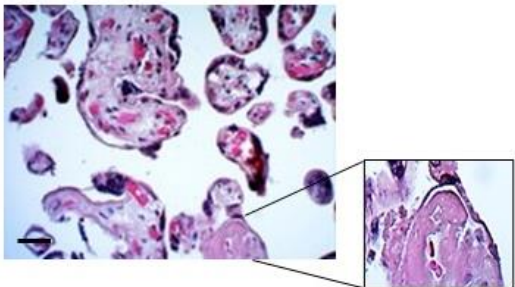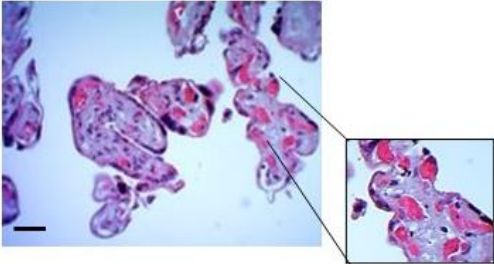
Adapted from (29).

3.3.1.7. Histochemical staining and analysis

Routine histological analysis was performed using Hematoxylin-Eosin staining (H&E), the frequency of villi with the presence of different events was determined based on the total number of villi evaluated in 10 microscopic fields (**Table 7**).

Table 7. Evaluation of placental villous integrity by histology.

Histological findings	Definition	Appearance (scale bar 25 µm)

Tissue infarction	The ischemic area of the villi due to the interruption of blood flow.	
Syncytial node	Aggregates of syncytial nuclei on the surface of the villi.	
Fibrin deposits	Accumulation of fibrin in the stroma of the villus or around it.	
Capillaries	Number of capillaries per villus.	
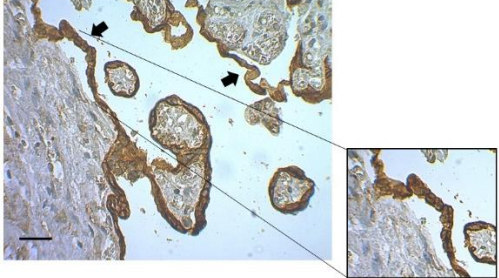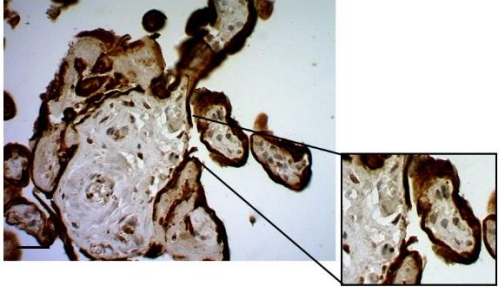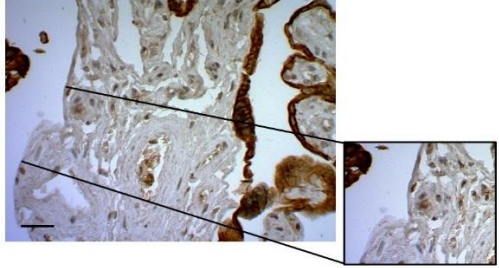
Representative images of cross-sectional sections of placental explants stained with H&E. summarizing the definitions of histological findings evaluated in cultured HPEs stained with H&E. A zoom of each finding is shown for a better understanding of the description.

3.3.1.8. Immunohistochemistry staining and analysis

Tissue samples were processed conventionally by deparaffinization in alcohol and xylene. Antigens were retrieved by incubating the samples in sodium citrate buffer in a steamer for 30 minutes. Staining for trophoblast was performed using a polyclonal anti-CK-7 IgG antibody that was diluted 1:1000. Finally, 10 random fields were analyzed to detect trophoblast detachment, denudation, and membrane rupture. (**Table 8**). The frequency of different events was

determined in the total number of villi examined across 10 microscopic fields. The slides were examined by light microscopy, under 40X magnification (400-fold).

Table 8. Evaluation of trophoblast epithelium through CK-7 staining.

Histological findings	Definition	Appearance (scale bar 25 μm)
Membrane detachment	Represents a space observed between the trophoblast membrane and the villus; there is no complete union between them.	
Membrane disrupted	Represents a membrane break, loss of continuity of the trophoblast membrane.	
Membrane denudation	Represents a villi partially or completely devoid of trophoblast membrane.	

Summarizing the definitions of histological findings evaluated in cultured HPEs stained with CK-7. A zoom of each finding is shown for a better understanding of the description.

3.3.1.9.   Histochemical to evaluate the organization of collagen fiber

For the PSR analysis, the study followed established principles for valid histopathological scoring for research (110), as described in **Table 9,** adapted from (29). Numerical values were assigned to the presence or absence of the event, (i.e., birefringence in PSR of the observed villi).

Table 9. Score for the analysis of collagen organization in the villous stroma.

Score	Organization of collagen I	Appearance

1	Absence of collagen birefringence	
2	Low collagen birefringence	
3	Moderate collagen birefringence	
4	Strong collagen birefringence	
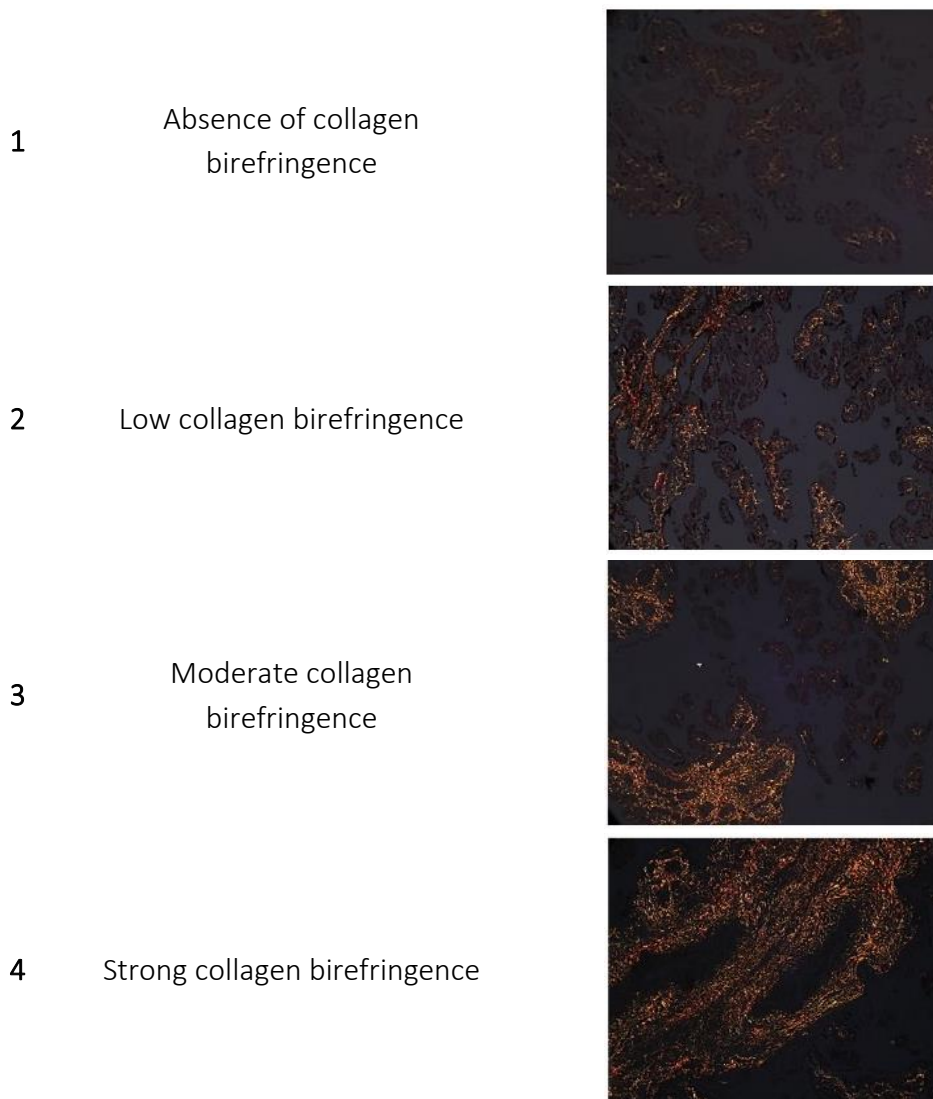
Score for the collagen organization analysis in the villous stroma of HPEs stained with PSR. Adapted from (29).

3.3.1.10. Evaluation of apoptosis using TUNEL assay

To determine the frequency of apoptotic cells in HPEs, the DeadEnd™ Fluorometric TUNEL System was employed. This system is non-reactive and quantifies the fragmented DNA of apoptotic cells by catalytically incorporating fluorescein-12-dUTP(a) at 3′-OH DNA ends, utilizing the Terminal Deoxynucleotidyl Transferase, Recombinant (rTdT) enzyme (15). To prepare the samples for analysis, 3-micron sections were cut from paraffin blocks using a microtome. These sections were then mounted onto glass microscope slides and left to dry. The slides were then placed in a 4% methanol-free formaldehyde solution in PBS (pH 7.4) and left to soak for 25 minutes at 4°C. Next, the slides were washed in fresh PBS for 5 minutes at room temperature. To permeabilize the tissue sections, 100 µL of Proteinase K was added for 5 minutes, followed by washing. Then, 50 µL of equilibration buffer was added to the slides,

which were covered with plastic coverslips and incubated at room temperature for 5 minutes. Afterward, the slides were incubated with 50 µL of the equilibration buffer containing the nucleotide Mix and rTdT Enzyme at 37°C for 1 hour in a humidified chamber, protected from light. The plastic coverslip was removed, and the slides were dipped in 40 mL of 2X stop solution (NaCL+Sodium citrate) (1:10 in deionized water) and left for 15 minutes at room temperature. A final washing step was performed to remove any unincorporated fluorescein-12-dUTP. Finally, 50 µL of DAPI nuclear stain in mounting medium (Vector Lab Cat. # H-1200) was added, and the slides were stored overnight at 4°C in the dark. Afterward, the slides were washed, and the sample was analyzed to detect localized green fluorescence of apoptotic cells (fluorescein-12-dUTP) against a blue background (DAPI) using fluorescence microscopy. A standard fluorescein filter set was used to view the green fluorescence at 520 ± 20nm. For data interpretation and comparison, a positive apoptosis control was used, consisting of HPEs treated with 20 ng/mL of TNF-α for 24 h.

3.3.1.11. Measurement of cytokines by flow cytometry

The levels of TH1/TH2/TH17 cytokine profiles were measured using the Cytometric Bead Array (CBA) Human TH1/TH2/TH17 Cytokine Kit (BD Bioscience). This assay provides a method to capture a set of analytes with known bead size and fluorescence, enabling the detection of analytes via flow cytometry. The cytokines measured were Interleukin-2 (IL-2), IL-4, IL-6, IL-10, Tumor Necrosis Factor (TNF), Interferon-γ (IFN-γ), and IL-17A. Briefly, 1:2 serial dilutions were prepared for eight points of the TH1/TH2/TH17 cytokine standard in a final volume of 300 µL. The assay diluent was used as a negative control. Next, capture beads for the seven cytokines were combined into a single vial along with the capture bead reagents (mixed capture beads). Vigorous mixing of the mixed capture beads was achieved using a vortex mixer. Then, 25 µL of mixed capture beads were added to each well of a 96-well plate. Subsequently, 25 µL of standard, negative control, and samples were added to each well, followed by the addition of 25 µL of phycoerythrin (PE)-labeled TH1/TH2/TH17 detection reagent to each well. The samples were incubated at 4°C overnight, protected from light. Next day, a washing step was performed using 500 µL of washing buffer per well, and the plate was centrifuged at 3290 rpm for 5 minutes. The supernatant was gently aspirated and discarded. Finally, 150 µL of washing buffer was added to each well, resuspended, and transferred to Falcon cytometry tubes for

analysis. The cells were analyzed using a flow cytometry instrument (Cytoflex of Beckman coulter), and the data were analyzed using FlowJo v10.8.1 Software.

3.3.2.   Summary of Results

In this study, we have developed a short-term HPEs culture protocol, specifically up to 72 hours, and have employed quantitative, semi-quantitative, and qualitative analyses to evaluate tissue viability and function over the follow-up period. Under our standardized conditions, placental villi explants began to regain their structural properties (integrity of the trophoblast and villous stroma) and the functionality of the HPEs (production of angiogenic, endocrine, and immunological factors) starting from the 48-h of culture. This restoration ensures a suitable environment for several applications. The data presented in the HPEs culture protocol developed in this study can be highly valuable for laboratories aiming to implement an HPEs model, whether in the process of standardization or seeking to enhance and optimize working conditions and timing with placental tissue. **<u>A complete version of these results is presented in Supplementary file 1 (109).</u>**

3.3.3.   Conclusion

In summary, we assessed the integrity and function of tissue samples dissected after 24, 48, and 72 h of culture. Histological evaluations of placental tissue indicated a restoration of integrity, as evidenced by a reduction in syncytial nodules and fibrin deposits, beginning at the 48-h mark after HPEs culture. The same trend was observed for trophoblast detachment, rupture, and denudation, which were more frequent during the initial 24 h but declined by the 48 h and 72 h time points evaluated. Furthermore, we observed a decrease in LDH activity after 48 h of HPEs cultivation. In summary, all the variables studied in relation to crop viability and their function served in the present study to reach the conclusion that from 48 hours onward, the crop begins to be in optimal conditions for its use, and the choice of the time at which a specific condition is to be evaluated will depend on the researcher's objectives.

3.4. Specific objective 4. To evaluate the changes in the tissue integrity and production of various physiological mediators of HPEs from healthy donors exposed to *P. falciparum ex vivo*

3.4.1. Methods

The methodology used to study viability, integrity, and functional parameters in HPEs exposed to *P. falciparum* is described previously in Section III. The parameters evaluated included:

- Cell Viability measuring LDH,
- Tissue integrity thought histology staining with H&E and immunohistochemistry staining of CK-7.
- Evaluation of collagen distribution in the villous stroma.
- Expression and quantification of inflammatory and angiogenic mediators.
- Assessment of apoptosis by TUNEL assay.

The methodologic approach followed to *P. falciparum* culture and co-incubation conditions with the cells, is outlined below.

3.4.1.1. Co-culture of human placental explants and *P. falciparum*-infected erythrocytes

All placental explants were washed three times with warm PBS 1X prior to treatment, for each placenta, three groups or conditions were tested: i. HPEs alone (Control), ii. HPEs with non-infected erythrocytes (nIE), and iii. HPEs with *P. falciparum*-IE. The infected erythrocytes with mature stages of *P. falciparum* were added at 10% parasitemia and 3% hematocrit (corresponding to 30.000 parasites/µL; this parasite density was calculated from the parasitemia value assuming that 1 µL of blood contains 5×10^6 red blood cells at 50% hematocrit) (111). Parasites were resuspended in the HPEs culture medium and incubated for 24 hours, at 37°C with HPEs culture gas mix (21% O_2, 5% CO_2). After this period, supernatants were collected for viability measurements and functionality assessment. A portion of the tissue was stored in Trizol for gene expression analysis via RNA extraction, while another part was stored in 10% neutral formalin at room temperature for HPEs histological staining and structural analysis methodology represented in **Figure 28**.
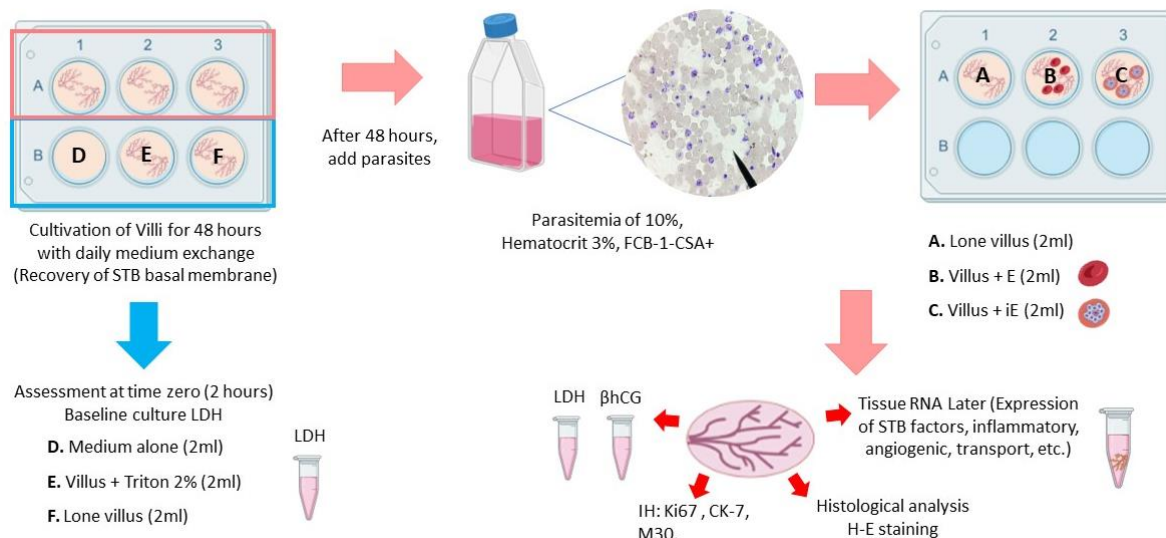
Figure 28. Graphical description of co-culture of human placental explants with infected erythrocytes. The HPEs culture begins with cultivating villi for 2 hours, that is, at time zero (blue square on the culture plate). Afterward, supernatants are collected for LDH measurement to determine the baseline conditions from which the culture starts. A portion of HPEs continues in culture for up to 48 hours, during which previously selected parasites with a CSA cytoadherence phenotype are added. The co-culture with the parasite includes an experimental control (villus alone), a biological control (villus + parasitized red blood cell), and a problem condition (villus + infected red blood cell). Once the culture conditions with explants and red blood cells, whether infected or not, are established, they are left in culture for 24 hours. After this time, supernatants are collected for LDH and hCG measurement, the tissue is stored in RNA Later for RNA extraction, and in 10% formalin for histological staining.

3.4.1.2. Quantification of differentiation and inflammatory mediators using real-time PCR (qPCR)

RNA was extracted from placental tissue using QIAGEN RNeasy columns. Subsequently, the RNA concentration was normalized, ensuring uniform RNA concentration across the experimental conditions. After normalization, cDNA synthesis was carried out using the Quantabio qScriptTM cDNA SuperMIX kit. PCR was conducted under universal amplification conditions with the HOT FIREPol® EvaGreen® qPCR Supermix (95°C for 12 minutes, 95°C for 15 seconds, 60 to 65°C for 30 seconds, and 72°C for 30 seconds) on the AriaMx Real-Time PCR System. The final reaction volume was 20 µL, comprising 2 µL of cDNA, 12.5 µL of Master mix (Solis Biodyne), and 1.125 µL of primers, adjusted with 5.25 µL of water. The relative expression was determined using the delta-delta CT method, and the normalization gene was GAPDH. Primer sequences are provided in **Table 10**.

Table 10. Primer sequences for amplifying differentiation and inflammatory mediators

Gen	Secuence (5'-3')	Tm
SYN-1_F	GCA ACC ACG AAC GGA CAT C	60.0°C
SYN-1_R	GTA TCC AAG ACT CCA CTC CAG C	60.0°C
SYN-2_F	CGG ATA CCT TCC CTA GTG CC	64.0°C
SYN-2_R	AGC TGA GGT TGC TGG TTC TG	62.0°C
βhCG_F	GCT ACT GCC CCA CCA TGA CC	66.0°C
βhCG_R	ATG GAC TCG AAG CGC ACA TC	62.0°C
ICAM-1_F	AGG CCA CCC CAG AGG ACA AC	66.0°C
ICAM-1_R	CCC ATT ATG ACT GCG GCT GCT A	60.0°C
IL-10_F	CCT GGA GGA GGT ATG CCC CCA	67.2°C
IL-10_R	CAG CGC CGT AGC CTC AGC C	66.0°C
TGF-b_F	TCA GAG CTC CGA GAA GCG GTA	63.3°C
TGF-b_R	GTT GCT GTA TTT CGT GTA CAT	55.5°C
LEP_F	TCC ACA CAC GCA GTC AGT CTC	63.3°C
LEP_R	CTG CCA GTG TCT GGT CCA	62.5°C
VEGF_F	TCT ACC TCC ACC ATG CCA AGT	61.3°C
VEGF_R	TGC GCT GAT AGA CAT CCA TGA	59.4°C
P21_F	GCA GAC CAG CAT GAC AGA TTT C	58.1°C
P21_R	CGG ATT AGG GCT TCC TCT TG	62.0°C
Fas-L_F	CTG GGG ATG TTT CAG CTC TTC	57.8°C
Fas-L_R	GTC CTG CTT TCT GGA GTG AAG	57.8°C
ZO-1_F	CAA CAT ACA GTG ACG CTT CAC A	56.3°C
ZO-1_R	CAC TAT TGA CGT TTC CCC ACT C	58.1°C
GAPDH_F	GGT GTG AAC CAT GAG AAG	51.8°C
GAPDH_R	CCA CGA TAC CAA AGT TGT C	50.9°C

3.4.1.3. Statistical analysis

The experimental data were presented as the mean ± standard error of the mean (SEM). LDH, hCG, cytokines and angiogenic factors release in culture supernatants of placental explants were normalized to tissue wet weight. A repeated measures ANOVA test was employed to compare groups. A *p-value* < 0.05 was considered statistically significant. The Tukey post hoc

test was applied to compare different conditions. Graphs and statistical analyses were performed using GraphPad Prism version 10.

3.4.2. Results and Analysis

Exposure to *Plasmodium falciparum* increases cell damage in human placental explants exposed *ex vivo*. The main objective of this set of experiments was to primarily analyze the *ex vivo* effect of *P. falciparum* on the viability and integrity of placental tissue. We previously adapted the HPEs culture of term placental tissue under conditions that guarantee the viability and structure integrity for up to 72 hours of culture (109).

3.4.2.1. Human placental explants cell viability assessed by LDH activity

Placental explants exposed to *P. falciparum* for 24 hours showed an increase in cellular cytotoxicity (1.08 ± 0.09) as compared to HPEs exposed to the control using nIEs (0.82 ± 0.12) (*p-value*= 0.0009) (**Figure 29A**). A positive control using Triton X-100 that lysates tissue was used, representing the maximum release of LDH into the medium (2.75 ± 0.72). Additionally, the analysis of βhCG secretion in the supernatant, which serves as an important biochemical marker of the endocrine activity of STB within the HPEs, did not reveal significant differences among the treatment groups. (*p-value* = 0.845) (**Figure 29B**).
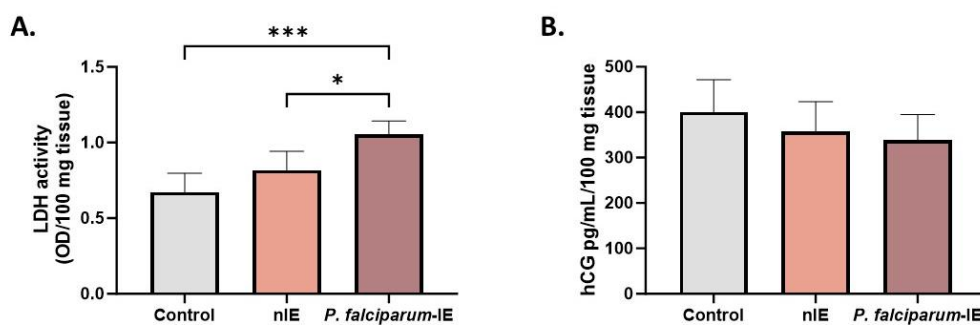
Figure 29. LDH activity and βhCG production in human placental explants exposed to *P. falciparum ex vivo*. **A.** LDH activity measured in the supernatant of HPEs, normalized per 100 mg of tissue. **B.** Production of βhCG measured in the supernatant of HPEs, normalized per 100 mg of tissue, in the study groups. Bar graphs represent means ME ± SEM. n=9. One-way ANOVA to repeated measures with a test to multiple comparisons (Tukey).

3.4.2.2. *Ex vivo* exposure to *P. falciparum* causes histological damage, disruption, and detachment of trophoblast in human placental explants

Histological analysis with H&E staining was employed to assess the impact of *P. falciparum* on tissue integrity. A notable increase was observed in the percentage of tissue damage when exposed compared to unexposed tissue, as indicated below (HPEs + *P. falciparum*-iE *vs* HPEs + niE): villi with syncytial knots (55.2 ± 18.93 *vs* 33.6 ± 15.2, *p-value* = 0.002), fibrin deposits (11.3 ± 7.18 *vs* 6.1 ± 6.01, *p-value* = 0.0003), and infarction (20.8 ± 13.36 *vs* 7.7 ± 4.47, *p-value* = 0.019) (**Figure 30 D-F**). Complementing the H&E analysis, CK-7 immunohistochemistry, a specific marker for trophoblast cells, revealed that *P. falciparum* significantly disrupted the trophoblast of the placental villi (**Figure 30 G-I**). The frequency of villi presenting detachment of trophoblasts (46.2 ± 13.4 *vs* 27.8 ± 14.3, *p-value* = 0.013), trophoblast rupture (50.0 ± 13.4 *vs* 27.3 ± 9.8, *p-value* = 0.0002), and denudation (35.3 ± 21.2 *vs* 16.8 ± 16.6, *p-value* = 0.003) (**Figure 30 J-L**).
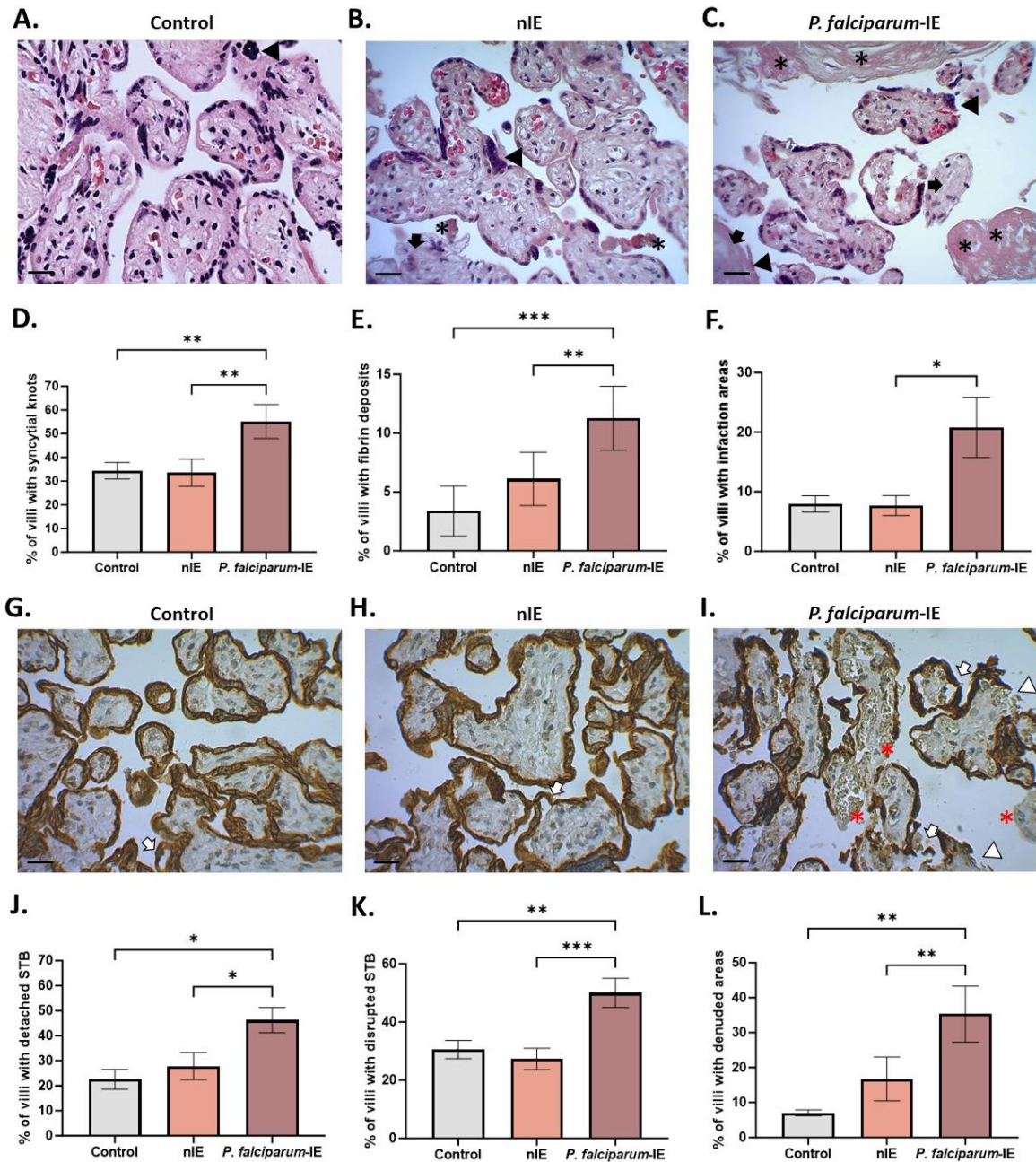
Figure 30. Exposure to *P. falciparum* causes histological damage in human placental explants exposed *ex vivo*. A-C. Panel of representative microphotographs of HPEs stained with H&E. **D-F.** Frequency of the different findings; syncytial knots (black arrowhead), fibrin deposits (black arrow) and infarction (black asterisk). **G-I.** Panel of representative microphotographs of HPEs stained with CK-7. **J-L.** Frequency of trophoblast detachment (white arrow), trophoblast rupture (white arrowhead), and trophoblast denudation (red asterisk). Bar graphs represent means ME ± SEM. n=7. One-way ANOVA to Mixed Model with test to multiple comparisons (Tukey). Scale bar: 20 µm. Total magnification (400X).

3.4.2.3. The exposure to *P. falciparum*-iE disrupts collagen organization in the villous stroma of human placental explants exposed *ex vivo* and induces an increase in areas with thickening of the basal lamina

One of the main components of the villous stroma is collagen. To assess the integrity of the villous stroma, a collagen histochemistry analysis was conducted, and the collagen distribution was examined using specific stains. TM staining was performed, facilitating the qualitative identification of collagen fibers (in blue) in the HPEs. Additionally, PRS staining allowed for the specific visualization of collagen I within the villous matrix (in orange) and collagen III within the blood vessels (in green). In the case of TM, large white spaces within the villous stroma indicated partial or complete absence of collagen in those areas (**Figure 31A-C**), aligning with the previous findings from PSR staining. Significant differences were observed in both PSR- and TM-stained sections, indicating a severe disorganization of collagen fibers when HPEs were exposed to *P. falciparum*-iE compared to the control group of HPEs. The distribution of type I collagen by PSR staining (**Figure 31D-F**) showed a substantial absence of collagen birefringence in the HPEs group exposed to *P. falciparum*-IE compared to the control samples (*p-value* =0.011) (**Figure 31G**), as indicated by the organization score that decrease from (3.36 ± 0.12) in the control group to (1.80 ± 0.26) in the parasite-treated group.

Another critical component of the villous stroma is the basement membrane, which is part of the placental barrier. PAS reagent is used for the staining regions rich in glycoproteins, typically found in connective tissues and basal lamina (112); thus, PAS staining was employed to examine this component, with an emphasis on identifying regions with thickened trophoblast basal lamina. In HPEs exposed to *P. falciparum*-IE, an increase in PAS staining was observed with an average of 1.72 ± 0.22 points of thickening of the basement membrane compared to the unexposed control (1.23 ± 0.02) (**Figure 31H-J**), which was more visible in the basal lamina. Statistical analysis showed a significant increase in the areas of basal lamina with thickening regions per villi in the *P. falciparum*-IE group compared with the nIE group (*p-value* = 0.027) (**Figure 31K**).
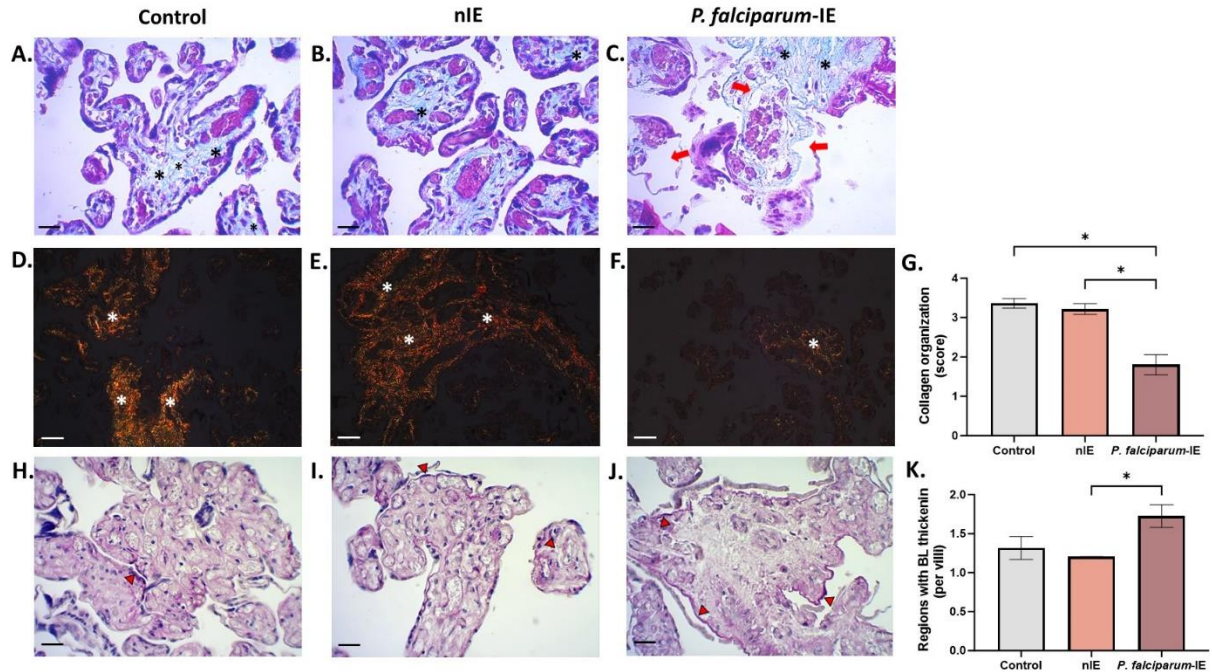
Figure 31. The exposure to *P. falciparum*-iE disrupts collagen in the villous stroma of human placental explants exposed *ex vivo* and induces an increase in regions with thickened trophoblast basal lamina. Photographic panel of cross-sections of HPEs stained with: **A-C.** TM to visualize collagen fiber organization in blue (black asterisk), areas devoid of collagen fibers (red arrows). **D-F.** PSR (white asterisk). **G.** Score of distribution of Col I with PSR. **H-J.** PAS to identify areas of basal lamina thickening (red arrowhead). **K.** Frequency of areas of basal lamina thickening using PAS. Bar graphs represent means ME ± SEM. n=3. One-way ANOVA to repeated measures with a test to multiple comparisons (Tukey). Total magnification for TM and PAS (400X) (**A-C** and **H-J**). Total magnification of PSR (200X) (**D-F**). Scale bar: 20 μm.

3.4.2.4. The exposure to *P. falciparum*-iE does not affect the cellular apoptosis of human placental explants exposed *ex vivo*

Apoptosis in HPEs exposed *ex vivo* to *P. falciparum* was evaluated using the TUNEL Assay (**Figure 32A**). No significant differences were observed among the study groups regarding the percentage of apoptotic cells per villus, likely due to data dispersion. However, the upward trend persisted in exposed HPEs, as indicated below (HPEs + *P. falciparum*-iE vs HPEs + niE): 14.13% ± 9.66 *vs* 9.25% ± 3.08 (*p-value* = 0.37) (**Figure 32B**).
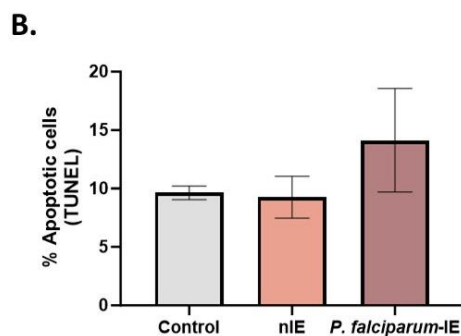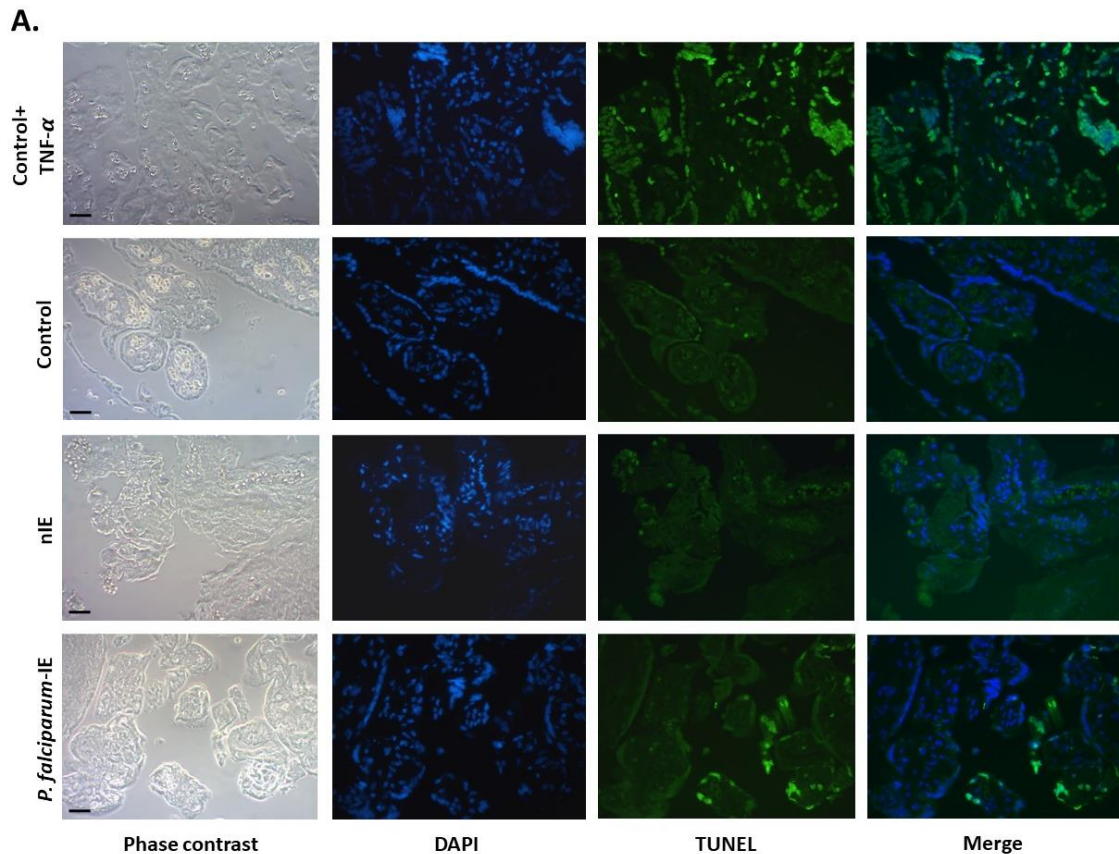
Figure 32. The exposure to *P. falciparum*-iE does not significantly affect the cellular apoptosis of human placental explants exposed *ex vivo*. A. Panel of representative photographs of HPEs exposed *ex vivo* to *P. falciparum* labeled with TUNEL. The positive control corresponds to HPEs exposed to TNF-α (20ng/mL) for 24 hours. B. Frequency of the data presented in A. There are no statistically significant differences in DNA fragmentation among the different study groups. Bar graphs represent ME ± SEM. n=3. One-way repeated measures ANOVA with multiple comparisons (Tukey) test. Scale bar: 20 µm. Total magnification 400X.

3.4.2.5. Production of cytokines and angiogenic factors by human placental explants exposed to *P. falciparum*-iE

Cytokines and angiogenic factors production by HPEs were assessed in the study groups to determine whether the exposed to *P. falciparum*-iE altered these molecules. In general, no changes were observed in any molecules across the different study groups, but a trend towards an increase in IL-6 and IL-10 was noted in the group exposed to *P. falciparum*-iE compared to the unexposed group, although it was not statistically significant (**Table 11**).

3.4.2.6.   *Table 11. Production and release of cytokines and angiogenic factors by human placental explants exposed ex vivo to P. falciparum*-iE

Cytokines [pg/mL] n=8	nIE	*P. falciparum*-IE	*p-value*
IL-6	18887 ± 4658	23034 ± 6400	0.188
IFN-*γ*	67.6 ± 6.9	76.2 ± 9.5	0.399
IL-4	62.3 ± 7.0	72.9 ± 8.6	0.257
IL-17	37.7 ± 4.2	45.62 ± 5.4	0.228
IL-10	6.1 ± 0.7	9.2 ± 1.8	0.066
IL-2	4.8 ± 0.4	5.67 ± 0.7	0.232
Angiogenic factors [pg/mL] n=5			
sFLT-1	7362 ± 991	7262 ± 1419	0.908
Endoglin	47.8 ± 1.2	55.4 ± 8.1	0.334
PIGF	52.3 ± 3.2	58.2 ± 14.4	0.694
VEGF	44.9 ± 3.8	45.9 ± 4.7	0.841

The results of cytokines and angiogenic factors production in HPEs cultured for 24 hours with *P. falciparum* and their respective controls are presented. Cytokines (n=8), angiogenic factors (n=5). Data represent the ME ± SEM, statistical analysis was the paired t-test.

3.4.3.   Conclusion

Placental infection with *P. falciparum*-iE can cause damage to the trophoblast layer in HPEs exposed *ex vivo* to parasites. This damage is accompanied by increased histological findings such as fibrin deposits, syncytial knots, and infarction. Additionally, the distribution of collagen fibers in the villous stroma was altered, indicating that *P. falciparum* may not only harm the trophoblast layer but also potentially damage the villous stroma. These alterations are linked to elevated LDH levels during infection. Moreover, HPEs exposed to parasites showed a decline in hCG synthesis, suggesting the impact of trophoblast membrane damage. Thickening of the basal lamina was also observed in the infected group, which is frequently associated with zones

where trophoblast detachment or rupture occurs, suggesting a detrimental effects of the infection on placental tissue. Furthermore, the evaluation of the immune response through the measurement of pro and anti-inflammatory mediators showed a rise in the production of all evaluated mediators, particularly IL-6 and IL-10. This elevation might be associated with a potential compensatory mechanism to regulate or balance both TH1 and TH2 responses, respectively. In summary, these findings highlight the numerous types of damage that *P. falciparum* infection can cause to placental tissue. It is worth noting that the evaluated tissue in this model is the villous tissue, representing the fetal portion of the placenta, which lacks maternal immune response or regulation factors.

3.5. Specific Objective 5: To evaluate the changes in the tissue integrity and production of various physiological mediators of HPEs from healthy donors exposed to natural hemozoin *ex vivo*

3.5.1. Methods

The methodology employed for assessing cell viability, integrity, and functional parameters in exposed to Hz has been detailed in Section III. The parameters evaluated included:

- Microscopic characterization of the effect of natural hemozoin on HPEs by SEM

- Cell viability of HPEs measuring LDH

- Tissue integrity was assessed through histology staining with H&E and immunohistochemistry staining for CK-7.

- Evaluation of collagen distribution in the villous stroma.

- Expression and quantification of inflammatory and angiogenic mediators.

The methodological approach employed for the isolation of natural hemozoin (nHz), and the treatment conditions applied to the HPEs is outlined below.

3.5.1.1. Natural Hemozoin Isolation

The hemozoin crystals were obtained from *P. falciparum* cultures using a strain called FCB1. The parasite culture conditions were previously detailed in objective 2. Samples of iE pellets obtained from cultures with 6% of parasitemia or higher were collected. These pellets underwent three cycles of freezing at -4°C and thawing at 37°C for 10 minutes each step to lyse the red blood cells. Subsequently, they were passed through a magnetic column, the paramagnetic properties of hemozoin, as described previously (113), allowed us to standardize this method so that, for hemozoin quantification, it would enable us to separate the crystals. Finally, Hz was eluted with distilled water and centrifuged at 4000 rpm. The supernatant was discarded, and the precipitate (Hz) was dried in an oven at 37°C until all moisture was eliminated. Once the dry crystals were obtained, they were weighed on an analytical balance, starting with 5μg and 10μg for the treatment with HPEs for 24 hours. After this period, supernatants were collected for LDH and hCG measurements. A portion of the tissue was

stored in 10% formalin, as previously explained, for routine histological analysis with H&E and histochemical analysis of collagen distribution. Finally, another portion of the tissue was preserved in Trizol for RNA extraction by qPCR. This procedure is illustrated in **Figure 33A**.

3.5.1.2.   Exposure of human placental explants to natural hemozoin

All placental explants were washed three times with warm PBS 1X prior to treatment, for each placenta, three groups or conditions were tested: i. HPEs alone (Control), ii. HPEs with 5µg and iii. HPEs with 10µg from natural Hz (nHz) analysis methodology represented in **Figure 33B**.
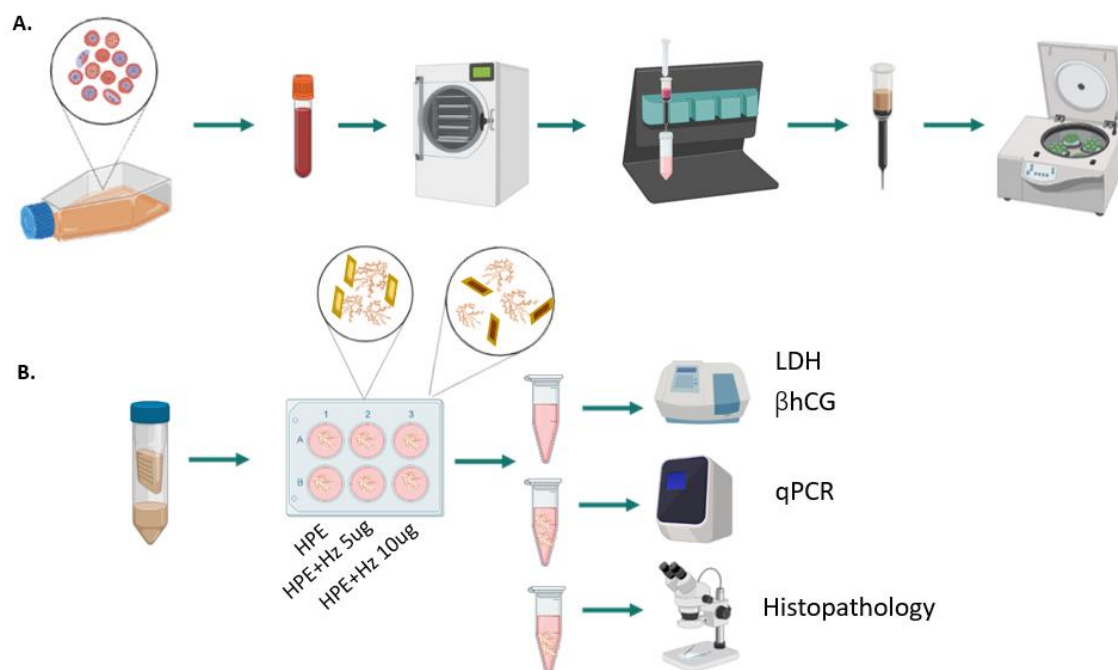
Figure 33: Process for the natural hemozoin isolation using magnetic column. A. The samples are subjected to 3 cycles of freezing and thawing to lyse the red blood cells. They are then passed through a magnetic column, where Hz becomes trapped due to its magnetism. Finally, the Hz is eluted B. The crystals are obtained for the treatment with HPEs with 5ug and 10ug for 24 hours.

3.5.1.3.   Statistical analysis

The experimental data were presented as the mean ± standard error of the mean (SEM). LDH, hCG, cytokines and angiogenic factors release in culture supernatants of placental explants were normalized to tissue wet weight. A repeated measures ANOVA test was employed to compare groups. A *p-value* < 0.05 was considered statistically significant. The Tukey post hoc

test was applied to compare different conditions. Graphs and statistical analyses were performed using GraphPad Prism version 10.

3.5.2.   Results and Analysis

3.5.2.1.   Morphological and vibrational characterization of natural hemozoin

The morphological analysis was obtained using a JEOL JSM-6490LV scanning electron microscope at magnifications of 200X. The analysis reveals that natural hemozoin crystals exhibit a needle-like morphology, with approximate measurements of 500 nm for natural hemozoin. This morphology aligns with findings from previous studies (111). **Figure 34**.
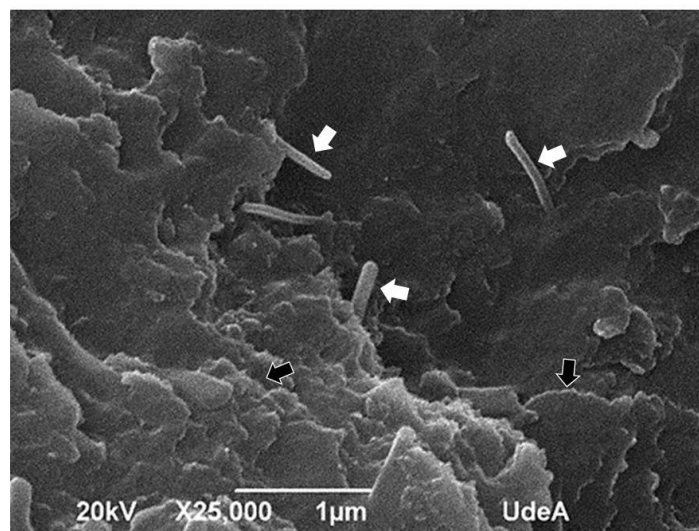
Figure 34. Morphological characterization of natural hemozoin. Scanning electron microscopy micrograph of natural hemozoin crystals separated from *P. falciparum*-IE by magnetic column. The heme group dimerizes, forming a hemozoin dimer that constitutes triclinic needle-shaped structures (white arrow). These hemozoin dimers grow together through hydrogen bridges, creating long chains of hydrogen bonds that shape the various crystal terraces of hemozoin (black arrow). (*Collaborative work with Herrera-J, PhD student in chemistry*).

3.5.2.2.   The natural hemozoin neither affected the production of hCG nor the activity of lactate dehydrogenase in ex vivo-exposed human placental explants

Although a downward trend in hCG production was observed in HPEs exposed to nature Hz at both concentrations (5 µg/mL and 10 µg/mL) compared to unexposed or control HPEs, No statistically significant differences were found in these data, with an average production of 200 pg/mL in HPEs, whether exposed to 5 µg/mL or 10 µg/mL of natural Hz. This may be attributed

to the variability in results within the control group (**Figure 35A**). On the other hand, no significant changes were observed in the LDH activity of HPEs, with an average OD of 0.22, whether exposed or unexposed to natural Hz (**Figure 35B**).
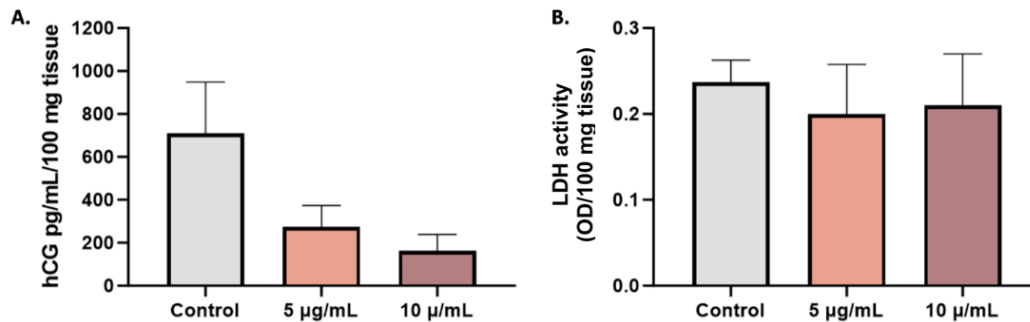
Figure 35. Natural hemozoin induces a downward trend in hCG but does not alter LDH activity in *ex vivo*-exposed Human placental explants. Frequency of the measurement of hCG production (**A**) and LDH activity (**B**) in HPEs exposed and unexposed to natural Hz.

3.5.2.3. Natural hemozoin induces histological damage and disruption of trophoblast in Human placental explants exposed *ex vivo*

Histological analysis with H&E staining was performed on human placental explants exposed to two concentrations of natural hemozoin (5 µg/mL) and (10 µg/mL) (**Figure 36A**). Analysis of overall histopathological damage is presented, which provides a comprehensive overview of tissue damage, Additionally, significant tissue damage was observed with 5 µg/mL treatment, mainly with an increase in syncytial nodes compared to control HPEs (**Figure 36B**). Analysis using CK-7 immunohistochemistry revealed that natural hemozoin significantly disrupted the trophoblast of the placental villi (**Figure 36C**). Predominantly, detachment and denudation of the trophoblast were observed, exposing the villous stroma (**Figure 36D**).

Figure 36. Natural hemozoin increases histological damage in *ex vivo*-exposed human placental explants. **A.** Panel of representative photographs of HPEs exposed *ex vivo* to nature Hz with H&E staining **B.** Frequency of the data presented in A. Histological damage was significantly greater in HPEs exposed to natural Hz compared to unexposed HPEs (Control) (**Table 7**). **C.** Panel of representative photographs of HPEs exposed *ex vivo* to nature Hz with CK-7 staining. **D.** The detachment, rupture, and denudation of the trophoblast are observed in HPEs exposed to natural hemozoin (**Table 8**). Bar graphs represent ME ± SEM. n=3. One-way repeated measures ANOVA with multiple comparisons (Tukey) test. Scale bar: 20 µm. Total magnification 400X.

3.5.2.4. Natural hemozoin disrupts the collagen distribution in the villous stroma of *ex vivo* exposed Human placental explants

A qualitative assessment of the distribution of type IV collagen was conducted using TCM. An increase in collagen fiber-deprived areas was observed in the villous stroma of HPEs exposed to natural Hz compared to non-exposed control HPEs, where fibers were regularly observed

covering the villous stroma. Additionally, a semiquantitative evaluation of the distribution of type I collagen on the villous stroma was performed using PRS staining. It was found that these collagen types significantly decrease in HPEs exposed to natural Hz compared to the control HPEs results represented in **Figure 37**.
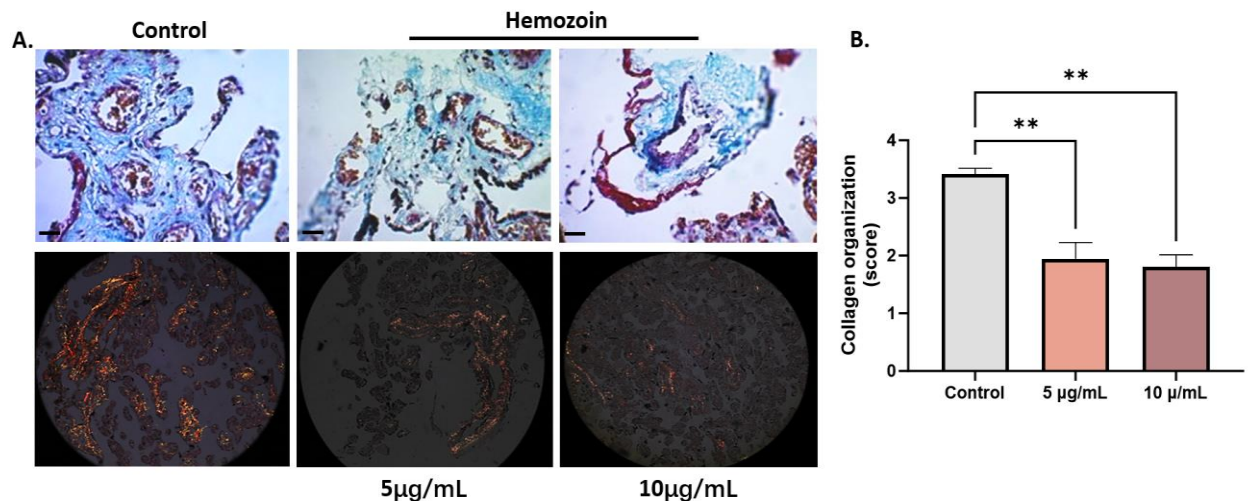
Figure 37. Natural hemozoin disrupts the collagen distribution in the villous stroma of *ex vivo* exposed Human placental explants. **A.** Photographic panel of cross-sections of HPEs stained with TM to visualize type IV collagen fiber organization in blue and PSR to visualize type I collagen fiber organization (**Table 9**). **B.** Frequency of the distribution of Col I with PSR. Bar graphs represent means ME ± SEM. n=3. One-way ANOVA to repeated measures with a test to multiple comparisons (Tukey). Total magnification for TM (400X) and Total magnification of PSR (200X). Scale bar: 20 μm.

3.5.2.5. Natural hemozoin significantly increases cellular apoptosis in *ex vivo* exposed human placental explants

A notable increase in cellular apoptosis (cells in green fluorescence) was observed when HPEs were exposed to natural hemozoin. This phenomenon suggests a dose-dependent pattern: as HPEs were exposed to higher concentrations of natural hemozoin (10 μg/mL), cellular death in these HPEs increased by 35% compared to 27% when HPEs were exposed to 5 μg/mL of natural hemozoin and by 15% in control HPEs. (**Figure 38**).
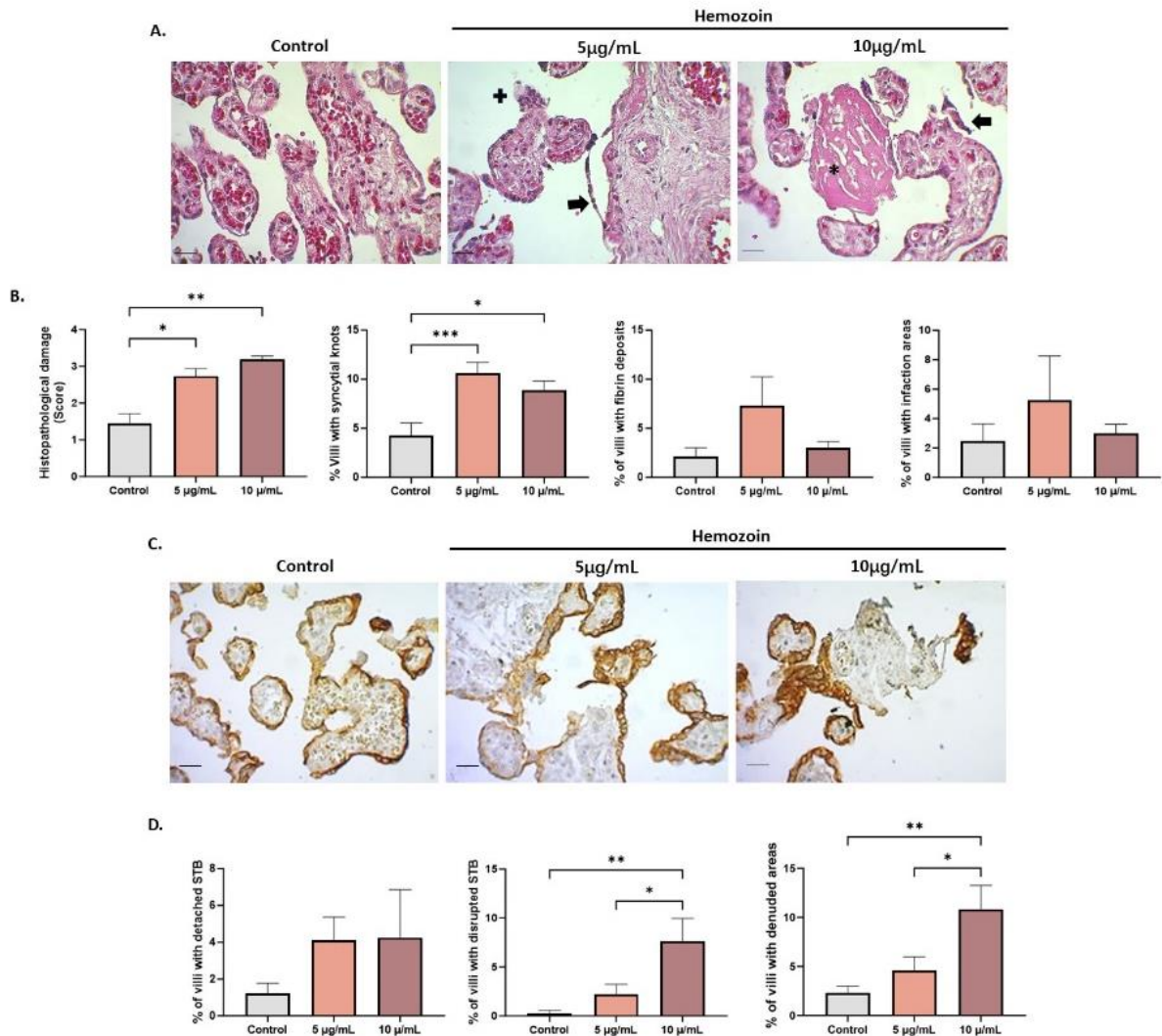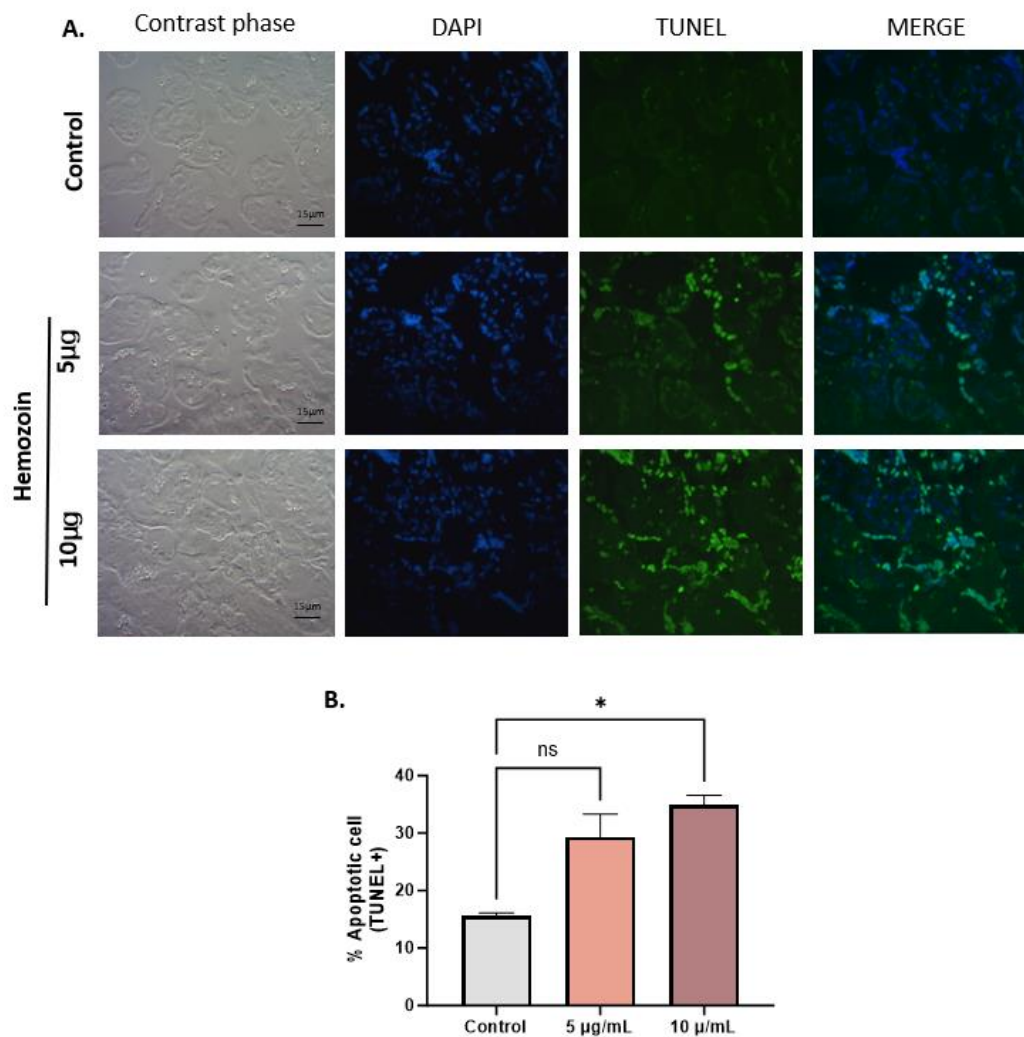
Figure 38. Natural hemozoin increases cellular apoptosis in *ex vivo* exposed human placental explants. A. Panel of representative photographs of HPEs exposed *ex vivo* to *P. falciparum* labeled with TUNEL. The positive control corresponds to HPEs exposed to TNF-α (20ng/mL) for 24 hours. **B.** Frequency of the data presented in A. There are no statistically significant differences in DNA fragmentation among the different study groups. Bar graphs represent ME ± SEM. n=3. One-way repeated measures ANOVA with multiple comparisons (Tukey) test. Scale bar: 15 μm. Total magnification 400X.

3.5.3.   Conclusion

Hemozoin plays a crucial role in the pathogenesis of *P. falciparum* infection, and by assessing the effect of this crystal separated from the parasite, it was revealed that it independently acts as a significant mediator in the increased histological damage, as evidenced by routine histological analyses using H&E staining. Trophoblast staining further revealed detachment and denudation in HPEs exposed to Hz compared to non-exposed control HPEs. While these

87

findings indicated tissue deterioration, no difference was observed in LDH activity under different study conditions. This suggests that, although there is structural damage to the tissue, cellular viability is preserved and not altered to the extent observed with the complete parasite, as found in the results analysis from the previous chapter. On the other hand, apoptosis was a process increased in HPEs exposed to Hz, as also observed with the parasite. This suggests that different mechanisms involving the parasite and Hz deposits may exert distinctive effects on cellular viability or death, indicating that these processes may not be exclusive to a single component of the parasite or a single pathway.

3.6. Specific Objective 6: To compare the effect of *P. falciparum*-iE *ex vivo* exposure of HPEs with placentas from pregnant women with malaria (*in vivo* exposure), using histological and immunohistochemical analysis

3.6.1. Methods

The methodology used to study cell viability, integrity, and functional parameters in placentas from pregnant women with malaria has been described previously in Section III. The parameters evaluated in this chapter include:

- Tissue integrity thought histology staining with H&E and immunohistochemistry staining of CK-7.
- Evaluation of collagen distribution in the villous stroma.

3.6.1.1. Collection of placentas naturally exposed to *P. falciparum* infection

To validate the results observed in HPEs exposed to *P. falciparum in vitro*, analyses of placentas from pregnant women with malaria by *P. falciparum* were included. Paraffin-embedded tissues were obtained from pregnant women who had previously participated in a study conducted in the Urabá-Antioquia region during 2005-2007. The selection criteria for these tissues included and analyzed in this study was the availability of samples in paraffin blocks. Paraffin-embedded tissues from pregnant women with *P. falciparum* infection were processed as previously described for histological and histochemical analyses with H&E, TM, PSR, PAS, and immunohistochemical analyses with CK-7, as well as for apoptosis assessment using the TUNEL technique.

The selected tissues, which were used to validate the *ex vivo* analyses carried out in this study, were categorized into three groups (see **Figure 39**), each with a sample size (n) of 6, based on both sample availability and infection status: Group 1 (Control) consisted of pregnant women without malaria, Group 2 included individuals with a history of past placental malaria, and Group 3 comprised women with active placental malaria.
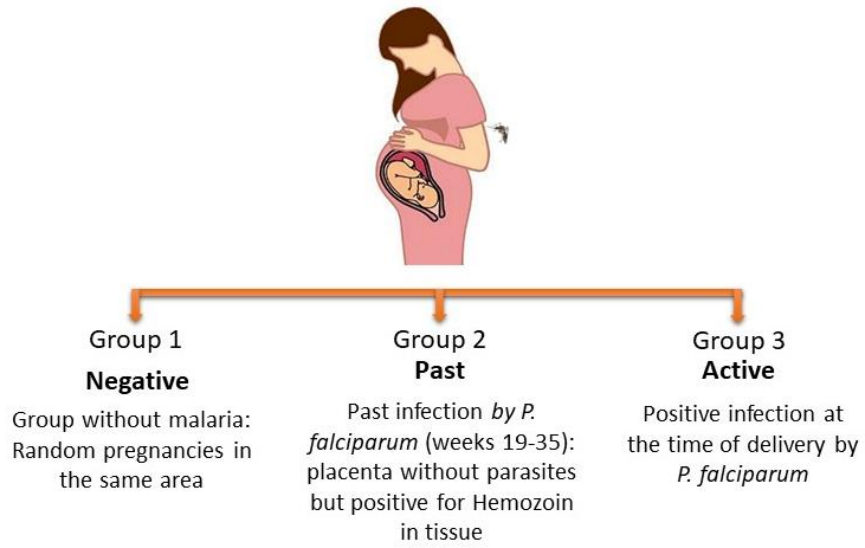
Group 1
Negative

Group without malaria: Random pregnancies in the same area

Group 2
Past

Past infection *by P. falciparum* (weeks 19-35): placenta without parasites but positive for Hemozoin in tissue

Group 3
Active

Positive infection at the time of delivery by *P. falciparum*

Figure 39. Description of study groups formed with tissues from naturally exposed pregnant women.

3.6.2. Results and Analysis

3.6.2.1. Collection of placentas naturally exposed to *P. falciparum* infection for the validation of the *ex vivo* results

To confirm the observed in HPEs exposed *ex vivo* to *P. falciparum*, placentas of women naturally exposed to infection, hereafter referred to as *in vivo* exposure to infection, were included. An overview of the characteristics of the pregnant women from whom paraffin-embedded tissues were included is summarized in **Table 12**.

Characteristics	Control n=6	Past infection n=6	Active infection n=6
Maternal age (years)	21.5±3.4	20.3±3.5	25.8±3.6
Multigravid	6 (100%)	6 (100%)	6 (100%)
Previous pregnancies (#)	2.3±1	3.3±2	4.0±1.5
Gestational age (weeks)	40.2±0.7	39.4±2.1	38.3±1.6
Preterm delivery	0	0	0
Placental weight (mg)	488±77	490±90	590±86
Birth weight (kg)	3.45±0.24	3.37±0.70	3.41±0.48
Parasites and immune cells in the IVS			
PMNN	14.8±9.0	18.7±9.7	9.8±4.9
Monocytes	12.6±3.2	11.0±5.5	17.8±7.5
Infected erythrocytes (total in 100 HPF)	NA	NA	32.2±49

Table 12. Characteristics of the pregnant women from the malaria-endemic region of Urabá included in the placental histology analysis. Parasites and immune cells were counted in 100 fields at 100×. Immune cells are presented as the mean number per field and parasite as the total of infected erythrocytes counted in the 100 HPF. IVS: Intervillous space, PMNN: Polymorphonuclear neutrophils, HPF: High-power field.

For a better understanding of the tissue characteristics included in this study of pregnant women naturally exposed to *P. falciparum* infection, representative photos are shown in **Figure 40**. Keeping in mind the classification by Rogerson et al (20).

| Negative | Active Acute | Active Chronic | Past |
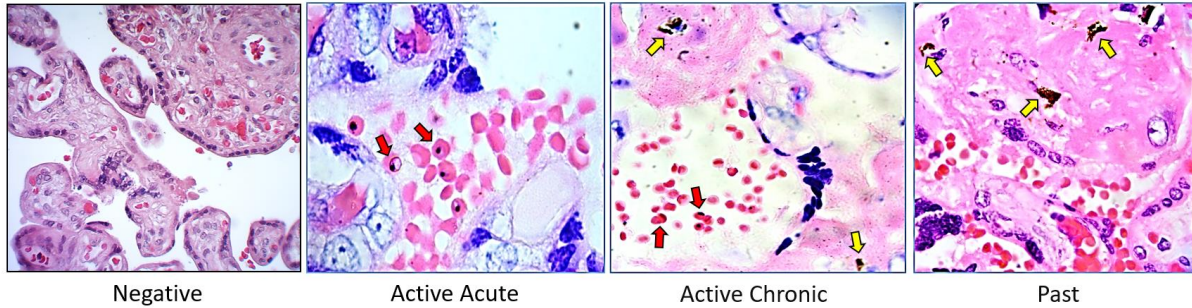
Figure 40. Classification of *P. falciparum* infection in the placenta. *P. falciparum*-infected erythrocytes can be observed in the intervillous space and adhered to the surface of the syncytiotrophoblast (red arrows); Deposits of hemozoin are observed in the fibrin of the villous stroma (yellow arrows) Photos taken by Ana María Vásquez of the donated placentas from the Urabá project used for this study.

3.6.2.2. Presence of *P. falciparum* in placenta from pregnant women is associated with tissue damage determined by histological parameters

Histological analysis with H&E showed a significant increase in histological damage in pregnant with both past (2.31 $\pm$ 0.15) and active (2.49 $\pm$ 0.17) infection compared to the control group (1.22 $\pm$ 0.07) (*p-value* <0.0001) (**Figure 41A-B**). This damage was reflected in the increased syncytial knots in past infection versus the negative control (63.68 $\pm$ 9.52 vs 35.18 $\pm$ 4.64) (*p-value* = 0.0242) (**Figure 41C**), increased fibrin deposits in active (27.52 $\pm$ 4.41) and past infection (22.42 $\pm$ 2.43) versus control (8.42 $\pm$ 2.36) (*p-value* = 0.0022) (**Figure 41D**), and infarction, with an average for active and past infection of (24.17 $\pm$ 1.44) versus negative control with (6.93 $\pm$ 1.94) (*p-value* = 0.1313) (**Figure 41E**). This was consistently higher in women with active *P. falciparum* infection in the placenta at the time of delivery. On the other hand, the results obtained with CK-7 staining (**Figure 41F**) revealed minimal damage to the trophoblast, with no significant changes observed on average for the different conditions in terms of detachment (2.18 $\pm$ 0.50, *p-value* = 0.92), rupture (1.26 $\pm$ 0.23, *p-value* = 0.12), and denudation (2.50 $\pm$ 0.44, *p-value* = 0.31) between the study groups (**Figure 41G-I**).
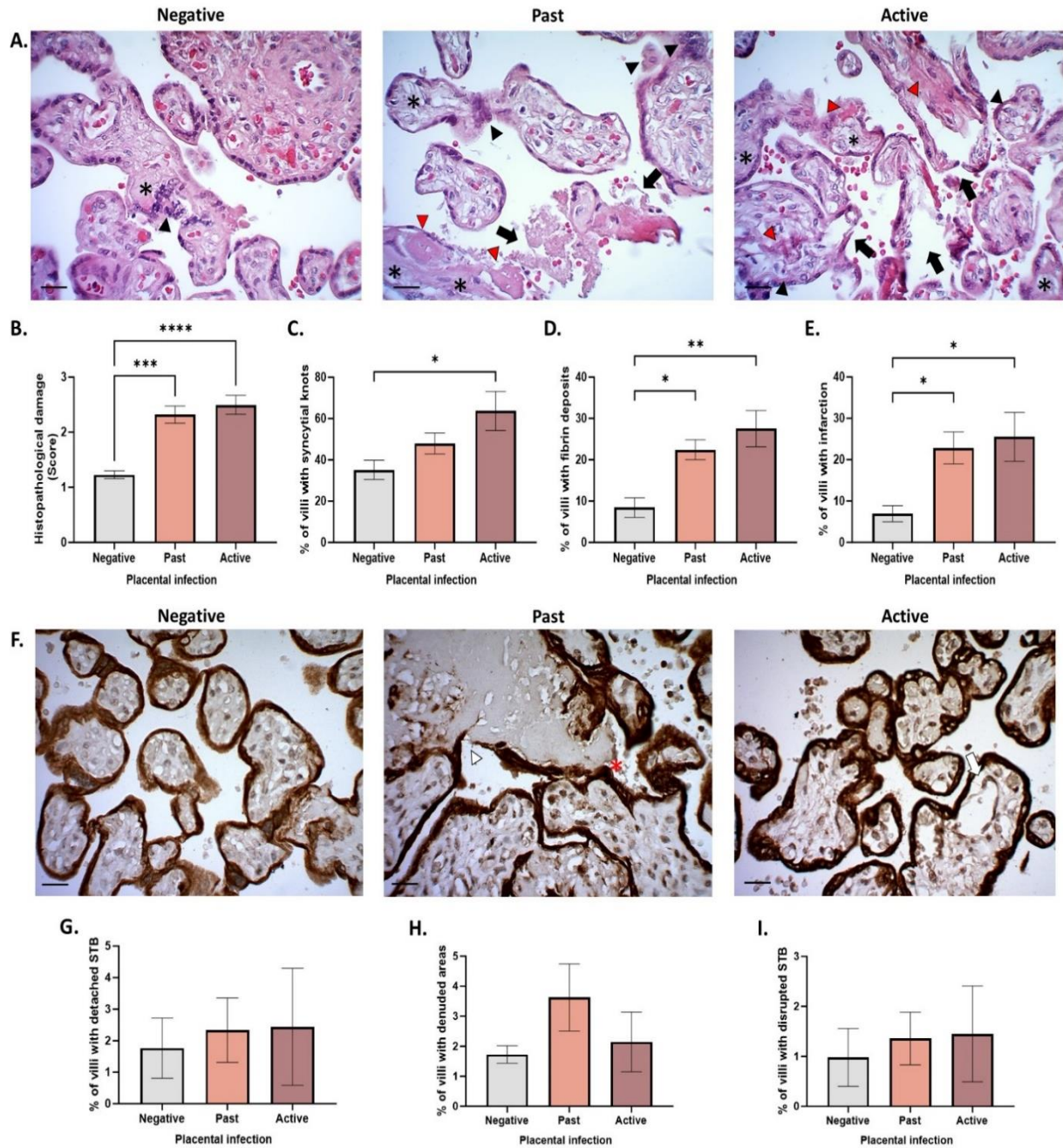
Figure 41. The exposure to *P. falciparum*-iE causes histological damage in Human placental exposed *in vivo*. **A.** Panel of representative photographs of HPEs exposed *in vivo* to *P. falciparum* labeled with H&E. **B-E.** Statistical analysis panel to determine the frequency of the different findings; histological damage (black arrow), syncytial knots (black arrowhead), fibrin deposits (red arrowhead) and infarction (black asterisk). **F.** Panel of representative photographs of HPEs stained with CK-7. **G-I.** Frequency of; Trophoblast detachment (white arrow), Trophoblast rupture (white arrowhead), and Trophoblast denudation (red asterisk). Bar graphs represent ME ± SEM. n=6. One-way repeated measures ANOVA with multiple comparisons (Tukey) test. Scale bar: 20 μm. Total magnification 400X.

3.6.2.3. The exposure to *P. falciparum*-iE disrupts collagen in the stroma of placental villi

The qualitative analysis of collagen organization using the TM technique revealed a greater number of areas in the villous stroma devoid of collagen fibers (red arrows) in the group with both past and active infection compared to the control group (**Figure 42A-C**). This difference could be quantified using the PSR technique (**Figure 42D-F**), where a clear reduction in collagen fibers (in orange) was more pronounced in the group with both past (2.06 + 0.15) and active infection (1.86 + 0.09) than in the control group (3.45 + 0.11) (*p-value* = <0.0001) (**Figure 42G**). Regarding the thickening regions of the basement membrane evaluated with PAS staining (**Figure 42H-J**), no statistical difference was observed. On average for all groups, it measured (1.27 + 0.06) (**Figure 42K**).
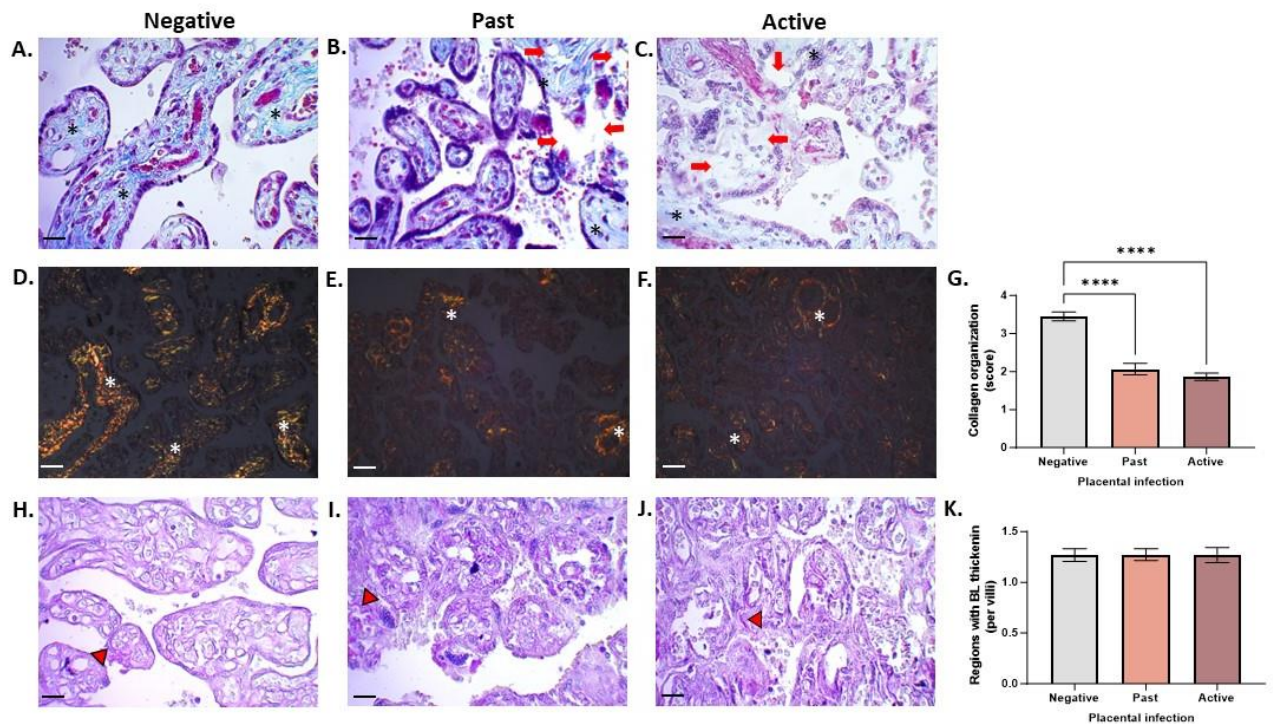
Figure 42. The exposure to *P. falciparum*-iE disrupts collagen in the stroma of human placental exposed *in vivo*. Photographic panel of cross-sections of HPEs stained with: **A-C.** TM to visualize collagen fiber organization in blue (black asterisk), areas devoid of collagen fibers (red arrows). **D-F.** PSR (white asterisk). **G.** Statistical analysis of distribution of Col I with PSR. **H-J.** PAS to identify areas of basal lamina thickening (red arrowhead). **K.** Frequency of areas of basal lamina thickening with PAS. Bar graphs represent means ME ± SEM. n=6. One-way ANOVA to repeated measures with test to multiple comparisons (Tukey). Total magnification for TM and PAS (400X) (**A-C** and **H-J**). Total magnification for PSR (200X) (**D-F**). Scale bar: 20 μm.

3.6.2.4.   The exposure to *P. falciparum*-iE increases cellular apoptosis of human placenta

A significant increase in the percentage of cells undergoing apoptosis was observed in the active (24.28 $\pm$ 1.88) and past infection (21.13 $\pm$ 3.01) group compared to the control group (10.36 $\pm$ 1.93) (*p-value* = 0.0019) (**Figure 43**).
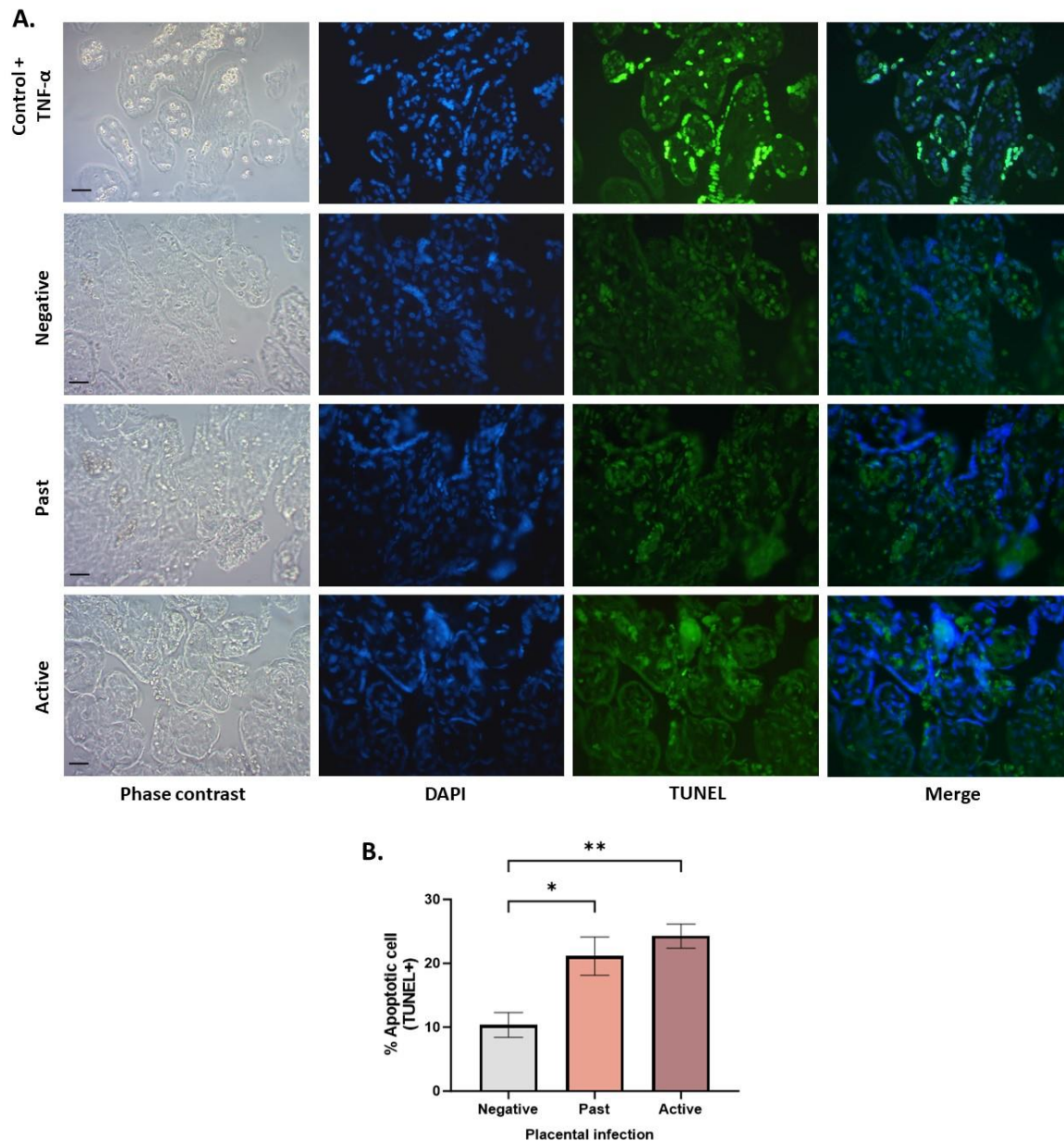
Figure 43. The exposure to *P. falciparum*-iE affects the cellular apoptosis of human placental exposed *in vivo*. A. Panel of representative photographs of HPEs exposed *in vivo* to *P. falciparum* labeled with TUNEL. The positive control corresponds to HPEs exposed to TNF-α (20ng/mL) for 24 hours. **B.** Statistical analysis of the data presented in A. Frequency of differences in DNA fragmentation among the different study groups, with a higher percentage of apoptotic cells in tissues from pregnant women with active and past infection compared to the control. Bar graphs represent ME ± SEM. n=6. One-way repeated measures ANOVA with multiple comparisons (Tukey) test. Scale bar: 20 μm. Total magnification 400X.

3.6.3.   Conclusion

The examination of tissues from pregnant individuals naturally exposed to *P. falciparum*, classified according to Rogerson et al., revealed that the concurrent presence of parasites and hemozoin in active infection is significantly associated with tissue damage, characterized by an increase in syncytial knots, fibrin deposits, and infarction. Interestingly, the trophoblast layer remained intact, as assessed with CK-7, despite the observed tissue damage. Evaluation of the villous stroma showed disorganization and decreased collagen distribution in placental tissue from women with both past and active infections. No thickening of the basement membrane was observed in any group. Apoptosis was notably more frequent in infected groups, indicating the pathophysiological impact of *P. falciparum*, as discussed in previous chapters. It is crucial to exercise caution in interpreting results, considering cumulative effects of variables influencing tissue alterations. Factors such as immune responses, tissue healing, and repair mechanisms, which involve not only specific cell components but also maternal factors, play a crucial role in understanding the impact of *P. falciparum* infection on placental tissue. The intact trophoblast layer in this *in vivo* study suggests potential repair mechanisms during prolonged exposures to infection, an important consideration when contrasting with short-term *ex vivo* exposures. Within the potential cellular repair effects possibly associated with these recent findings in the *in vivo* study of naturally exposed tissues, it is noteworthy to observe the intact trophoblast layer in the various study groups. Furthermore, the basement membrane did not show regions of thickening, contrasting with observations in HPEs exposed *ex vivo* to *P. falciparum*.

The role of Hz in the pathogenesis of infections is significant and should be considered. However, when it comes to pregnant women who have been naturally exposed to infections in the past, it is challenging to attribute any observed damage solely to Hz. This is because the pregnant woman may have experienced an active infectious process and an inflammatory response, both of which are decisive factors in the harmful effects of the infection. Therefore, it is important to consider the interplay between these factors and the role of Hz in the development of infections in pregnant women.

4. General Discussion

The mechanism behind placental malaria by *P. falciparum* is mainly due to the ability of infected erythrocytes to adhere to the placental tissue, through the interaction between the VAR2CSA and the CSA on the surface of the STB, and the inflammatory response characterized by the infiltration of monocytes and macrophages into the placenta, with subsequent production of cytokines and other inflammatory mediators. It is important to note that this mechanism has been extensively studied for several years (41, 114, 115); however, little research has been conducted on the direct impact of *P. falciparum* on the STB, which are the target cells of cytoadherence. (16, 116).

In this research, the impact of *P. falciparum* on trophoblast cells and placental tissue was investigated, using various study models to elucidate alterations in the integrity and function of this tissue during infection, the combination of the *in vitro* model with BeWo cells, the *ex vivo* model using HPEs, and the *in vivo* study involving placental tissue from naturally *P. falciparum*-iE exposed pregnant women provides a more comprehensive insight for understanding the pathophysiology of placental malaria. The aim was to propose mechanisms of pathogenesis and potential therapeutic targets. Firstly, considering that the STB is the target cell for cytoadherence, we studied how the parasite can affect the differentiation process of these cells and found that *P. falciparum* infection has an adverse impact on the cell fusion process in BeWo cells exposed to infected erythrocytes. These results were validated by a reduction in the cell fusion index, as determined by E-Cad expression, and a significant decrease in the expression of Syn-1 and Syn-2, which are crucial regulators in mediating cell fusion. The observed effects align with the findings of Liu Mingli et al (117), which indicated an altered cell fusion process in BeWo cells exposed to Hz and the heme group. Furthermore, these findings align with earlier descriptions of the fusion process, illustrating that the negative regulation of genes led to cell cycle arrest and subsequent cell-cell fusion (118, 119), primarily affecting Syn 1 and 2 (120, 121). At the same time, it has been demonstrated that changes in fusion impede syncytial regeneration. In summary, the decline in the cell fusion index and the number of nuclei in the STB are associated with placentas from pregnancies complicated, for instance, by intrauterine growth restriction (122).

On the other hand, focusing on functional assessment, a notable decrease in hCG expression and a downward trend in its supernatant levels from cells cultured with *P. falciparum* were observed. This suggests potential issues with the function of the CTB, which does not differentiate properly into the STB, the main producer of this hormone.

The co-culture of BeWo and *P. falciparum*-iE did not show any associations with alterations in proliferation and apoptosis processes, which are linked to syncytialization as the preliminary and final steps, respectively. Contrary to these results and related to the apoptosis process in a mouse model, it was found that *Plasmodium* increases oxidative stress, activating the mitochondrial apoptosis pathway (intrinsic pathway) in the maternal-fetal exchange system, resulting in placental damage and malfunctioning (123).

In summary, it is important to highlight that the *in vitro* model with BeWo cells allowed for the identification of a negative effect of *P. falciparum* on trophoblast cell fusion. In the placenta the trophoblast fusion is a crucial event for maintaining a healthy pregnancy, as it is essential for the STB layer's preservation, the direct interface between maternal blood and fetal tissues (124).

On the other hand, this study considered two types of models: *ex vivo* and *in vivo*, which, in turn, considered different time-points of the *P. falciparum* infection. The short exposure model (*ex vivo*) considered only 24 hours of infection, while the long exposure model (*in vivo* exposition) in the context of naturally exposed pregnant women considered more than 24 hours of infection, and it should be considered, in addition to parasite exposure, that a maternal inflammatory response would also be active. Having the opportunity to include these two models allowed for a more comprehensive set of results, obtained *in vitro* and *ex vivo* findings are complemented by *in vivo* observations of the effects of *P. falciparum* on placental tissue. *P. falciparum* disrupts the integrity of the villi, inducing changes in the epithelial barrier and the villous stroma. These alterations could potentially impact the proper functioning of the villi, which constitute the functional units of the placenta.

In general, poor placental outcomes associated with histopathological lesions were observed with H&E staining in both *ex vivo* and *in vivo* infection models, including infarcts, increased syncytial knots, and fibrin deposits, which have been associated with arterial wall atherosis, accelerated villous maturation, and calcifications in cases of placental malaria (11, 125). These findings have been reported previously and reflect an association with uteroplacental malperfusion (63) and hypoxia (126). Fibrin deposits are associated with STB damage, and ultrastructural damage in placentas affected by placental malaria (127). Infarction has been associated with poor blood flow perfusion to the fetus (128) and is explained as a pathological change that can contribute to adverse birth outcomes and increased perinatal mortality and morbidity (127). Additionally, placentas affected by preeclampsia or fetal growth retardation often exhibit increased apoptosis (129), a higher presence of syncytial knots (125), and thickening of the basal lamina (130), all potential outcomes of tissue impairment. These findings align closely with what we observed in the current study with HPEs exposed *ex vivo* to *P. falciparum*.

In the HPEs exposed to *P. falciparum ex vivo,* evident alterations were found in the integrity of the trophoblast, such as detachment from the stroma and areas of rupture. Collagen disruption in the villous stroma was also observed, leading to increased areas devoid of collagen fibers. The dysregulation of placental collagen and stroma is associated with several negative impacts, including: 1. Structural deterioration, affecting its ability to provide adequate support and nutrition to the fetus; 2. Compromise of barrier function, as the integrity of these barriers is compromised, allowing the entry of unwanted or harmful substances; 3. Alterations in vascularization, potentially leading to insufficient nutrients and oxygen for the fetus; and 4. Triggering of the immune response, contributing to inflammation and possibly complications such as preeclampsia (131-133). However, it is important to note that optical microscopy alone may not be sufficient to provide comprehensive structural evidence of the effects induced by the parasite. Complementary methodological strategies are needed to analyze the damage caused by the parasite. These findings are related to the damage observed in LDH release to HPEs supernatant culture, during the exposure to the parasite. Regions with thickening of the trophoblast basement membrane increased in the exposed HPEs compared to the unexposed group, which is related to previous findings in naturally exposed placentas (134).

The thickening of the basement membrane can be seen from two angles: one from the perspective of a consequence of the infection and a possible pathogenic mechanism that explains the decrease in nutrient and oxygen transport through the placental barrier, and second, from the host's perspective, where it could be hypothesized as a possible defense mechanism that prevents infection in regions without trophoblast (135). Interestingly, it has been suggested that the production of non-chemotactic cytokines may be associated with thickening of the trophoblast basement membrane and may cause a mechanical blockage in the transport of oxygen and nutrients in the placenta (136).

On the other hand, significant changes were observed in trophoblast damage and villous stroma organization in tissues from naturally exposed placentas, validating and corroborating what was found in the *ex vivo* model. Apoptosis, which did not show significant differences in the *ex vivo* model, showed a significant increase in placentas from pregnant women with an active infection by *P. falciparum,* suggest that the exposure time in one model or another may reveal aspects related to tissue regeneration capacity (137). The *ex vivo* exposure of explants to hemozoin suggests an important role in the pathogenesis of this crystal on the PM, and its involvement in histological damage to the placenta should not be disregarded. Although some previous studies have not found an association between the presence of this crystal and the complication of PM (138), it is pertinent to consider including additional studies to further elucidate its specific role in pathogenesis due to its significant impact on the immune response. While not conclusively demonstrated in this study, others have reported its positive effect on the elevation of cytokines that mediate the proinflammatory response during infection (139).

In the *in vivo* study no changes were observed in the trophoblast, suggesting that the epithelial layer is constantly replaced, ensuring that there is always trophoblast covering the villous, as previously described (137). This was not observed in the *ex vivo* model, possibly due to the short evaluation period, which did not allow for sufficient time to replenish the STB that detached during infection. In the villous stroma, similar observations were made in both the *ex vivo* and *in vivo* study, with disorganization of collagen fibers. This suggests that even if the trophoblast is replenished *in vivo*, stromal damage persists in the tissue, or the complete recovery is slower (140).

Another interesting observation is related to apoptosis, which in the *ex vivo* exposure model for 24 hours showed a slight increase but was not significant, while placentas from pregnant women with active *P. falciparum* infection showed a clear increase in apoptosis, suggesting that to demonstrate the effect of apoptosis *ex vivo*, more time may be needed due to the complex process involving various factors (141). This was corroborated in the *in vivo* exposition of prolonged exposure, where apoptosis in tissues with active infection was significantly higher. It is necessary to mention that the increase in apoptosis may also be related to the formation of syncytial knots and constant trophoblast regeneration (64, 137).

The production of cytokines and angiogenic factors were only evaluated in the *ex vivo* infection model because in this model, we can study the specific production of cytokines in villous cells by removing maternal blood before culturing and examining the products secreted by the villi into the medium. A trend toward an increase in all evaluated cytokines was observed in the *P. falciparum*-IE group, which aligns with previous reports, especially the significant increase in IL-6 (24, 95). This may be related to the imbalance in the immune response induced by *P. falciparum* infection in the human placenta (142). However, angiogenic factors did not show changes between the evaluated groups, which may be due to the exposure time, which may need to be longer to generate an effect related to angiogenic function, as has been observed in placentas naturally exposed, with a significant increase in anti-angiogenic factors such as sFLT-1 (143, 144).

Ex vivo infection of human placental chorionic villi explants has primarily focused on the effects of *Trypanosoma cruzi* and *Toxoplasma gondii*. This approach has proven to be a suitable model for studying tissue damage during vertical transmission, yielding interesting results (28, 29, 145). These findings provide an opportunity to address unresolved issues related to another significant protozoan parasite that has received limited attention in this model, such as *P. falciparum*. These findings reinforce the need to delve deeper into the pathogenesis mechanisms of these infectious agents and the possible preventive measures to mitigate the harmful effects on maternal and infant health.

In general, taken together, the results obtained allow the identification of extensive disruption of placental histology and function, which may result in fetal loss or impaired intrauterine

growth (146). Which are clinical symptoms that can be recognized in cases of congenital malaria (147). The frequency of cells undergoing apoptosis has been reported to be significantly higher in the presence of congenital infection, even in asymptomatic and submicroscopic infections (98). This cell death could partly explain the intrauterine growth restriction as previously described (148) and in other infectious processes the cell death could be increased such as cytomegalovirus (149) and *Toxoplasma gondii* (150) and *Trypanosoma cruzi* in *ex vivo* infected human chorionic villi (112).

The HPEs model offers the advantage of maintaining intact microarchitecture and preserving cell-cell interactions and paracrine communications. Furthermore, this model also encompasses variability among donors. This encourages the search for models that are close to what happens *in vivo* but, at the same time, are reproducible. Therefore, the contribution of mesenchymal and endothelial cells in metabolic processes and their effects on tissue integrity should be considered (103, 151). Interestingly, findings reflected characteristics specific to each model, mainly the exposure time to infection and the participation of extracellular matrix components and other factors present in the *in vivo* environment versus *ex vivo* as mechanisms of tissue repair or maternal immune response to damage. These are factors that possibly allowed some findings to be different (67).

Despite the greater understanding of placental malaria pathology, the exact mechanisms leading to placental changes and impairment of maternal-fetal exchange are not fully understood. However, it has been suggested that the parasites alone are unlikely to be directly responsible for placental pathology. Host factors, placental tissue-specific factors, stromal cells, or maternal immune response may contribute to the observed histological changes. This is the first study to include three models of *P. falciparum* infection and that consolidates the results the effect on tissue integrity. It is also the first to provide evidence in both models of damage at the trophoblast and villous stroma level, using specific techniques that offer descriptive and semi-quantitative information on this histological damage.

5. General Conclusions

The syncytialization model with BeWo cells revealed that *P. falciparum* affects cell fusion and the formation of STB without significantly impacting cell proliferation and apoptosis. This finding suggests that the parasite impacts the structure of the STB, which maintains characteristics of CTB but fails to fulfill necessary functions such as mediating the transport of nutrients and oxygen. This could be linked to the occurrence of adverse effects during placental malaria, such as low birth weight.

On the other hand, the reduction in the STB formation may suggest an anti-parasitic response from the villous tissue by reducing the production and availability of the CSA receptor for parasite cytoadherence. It is worth noting that this *in vitro* model with BeWo cells allows the observation of alterations caused by the contact of two specific cell types (BeWo and iE) without the intervention of inflammatory mediators produced by the mother or fetus. Interpretation of these findings should consider the context of *ex vivo* or *in vivo* studies.

In the *ex vivo* model, it was evident that *P. falciparum* significantly alters the production of endocrine mediators such as hCG, which is crucial in the syncytialization process. The parasite also increases trophoblast damage, as indicated by elevated levels of trophoblast rupture, denudation, and detachment, as evidenced by increased LDH activity. In the same model, apoptosis did not show a significantly increased effect, but there was a trend towards an increase in HPEs exposed to *P. falciparum*. This suggests that apoptosis may not be the sole mechanism activated by the parasite to induce cell death in this model. However, it is important to note that this HPEs model provides a broader perspective of the tissue, considering not only CTB cells or STB but also incorporating components of the stroma (137) and fetal factors that are worth considering in cellular repair processes.

The distribution of collagen as a key component to assess the integrity of the villous structure revealed that *P. falciparum* not only compromises the integrity of the superficial layer of the villi related to the bi-stratified epithelium (CTB-STB) but also, like other protozoa like *T. cruzi*, can also disrupt the integrity of the villous stroma. This suggests a pathophysiological

mechanism independent of the cytoadherence process, extending to possible interactions with extracellular matrix components, a mechanism not yet fully evaluated.

This work allows us propose an overview of the possible pathways through which *P. falciparum* may cause damage to placental tissue, affecting two newly identified processes in this study: non-fusion of BeWo STB cells and damage to the integrity of the extracellular matrix, primarily collagen. These two processes, along with those previously described by other authors, contribute to the generation of placental malaria damage by *P. falciparum* through various mechanisms (**Figure 44**).

Finally*, P. falciparum* induces damage to the trophoblast in the *ex vivo* infection model, which was not observed in the *in vivo* exposition. This discrepancy may be attributed to the limited exposure time in the *ex vivo* model, preventing the syncytial regeneration seen in the *in vivo* tissue. The alteration in the villous stroma was a common finding in both exposure models, and it is of particular significance as it could indicate irreversible damage that persists regardless of the duration of exposure. This alteration may serve as a mechanism that disrupts placental barrier function. The basement membrane, another critical component of the placental barrier, was affected in the *ex vivo* model but remained intact in the *in vivo* exposition. This suggests that it might serve as a defense mechanism when the trophoblast is detached, damaged, or exposed.

Further studies exploring the impact of *P. falciparum* could provide additional insights to complement the findings presented here. Incorporating additional components in the functional assessment of tissues, such as protein transport, may help uncover other specific mechanisms underlying impaired tissue function. Understanding the physiopathology of malaria is crucial for developing effective prevention and treatment strategies, including the use of antimalarial drugs, vector control, and the development of malaria vaccines. The findings of this study could have implications for future management guidelines in regions endemic to malaria.
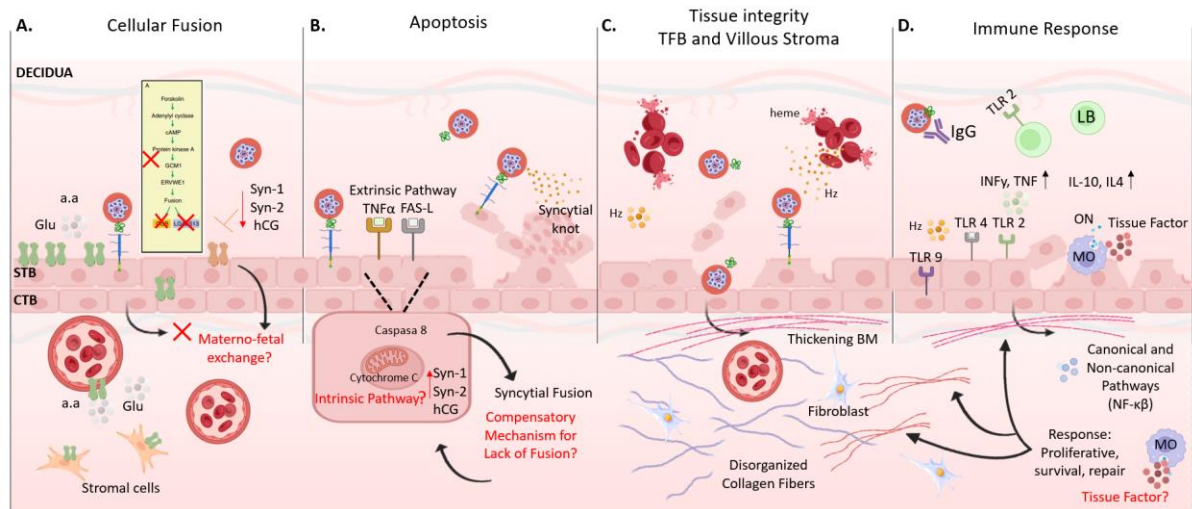
Figure 44. Possible mechanism of *P. falciparum* placental pathogenesis built from results obtained using various methodological approaches and supported by evidence from previous studies. **A.** At the onset of parasite-tissue interaction, *P. falciparum*-iE alters cell fusion, possibly by inhibiting the signaling cascade for the expression of mediators associated with cellular syncytialization processes. This, in turn, may regulate functions of the syncytiotrophoblast (STB) related to maternal-fetal metabolic exchange. **B.** This altered function, evidenced by the failure of STB fusion, could induce cellular apoptosis as a possible response mechanism to direct exposure to *P. falciparum*-iE, thus activating both extrinsic and intrinsic pathways of cellular apoptosis in non-fused cells, accompanied by an increase in the release of apoptotic material or syncytial knots. **C.** Regions devoid or stripped of STB are exposed to direct contact with various pro-inflammatory factors, not only infected erythrocytes but also deposits of Hemozoin (Hz), free heme groups, endotoxins, all of which induce the activation of stromal cells and fibroblasts in the tissue. **D.** These, in turn, respond to signals from immune cells such as macrophages and collectively trigger a cellular repair response and tissue factors to induce the formation of villous and perivillous fibrin with thickening of the basement membrane (BM) in areas devoid of STB that are more exposed to the parasite.

6. Limitations and Strengths

6.1. Limitations

Isolated CTB cells in primary culture could provide a useful system for studying individual trophoblast dynamics over the course of pregnancy. However, it has been argued that this approach has disadvantages, including the isolation of cells from significant interactions with other components of the villous structure.

The variability among donors implies a notable constraint in interpreting the obtained results, suggesting a possible lack of change in specific inflammatory or angiogenic mediators measured as part of the secretory function of placental tissue. However, this suggests that what happens *in vivo* under normal circumstances is that organisms respond differently to an infection.

It is essential to expand the sample size further to assess the findings presented here more clearly. This consideration also applies to the group of individuals naturally exposed to infection, which was limited to only 6 tissues per group. In a future opportunity, it may be possible to include more tissues in each group and observe discernible trends in damage and tissue function when infected with *P. falciparum*.

6.2. Strengths

The first study demonstrating the direct negative impact of *P. falciparum* infection on the non-fusion of BeWo cells (that do not syncytialize) and components of the extracellular matrix and histoarchitecture (basal lamina and collagen), providing an additional pathway in the pathophysiological context of the infection.

Including different types of models and being able to gather all the results together allowed for a more comprehensive understanding of the effect of *P. falciparum*, not only on the STB, the target of cytoadherence, but also on components of the chorionic villus, whether accompanied or not by the maternal component, encompassing the intricate network of components of the villous stroma inherent to the placental barrier.

This is the first study that involves a comprehensive analysis of *in vitro*, *ex vivo*, and *in vivo* results regarding the effect of *P. falciparum* on cells and the placental villi. The work employed specific techniques for the identification of different components of the placental barrier, revealing the negative impact of *P. falciparum* not only on the trophoblast membrane but also on the villous stroma of the placenta.

Qualitative, semi-quantitative, and quantitative analyses were included in this study, utilizing various methodological strategies previously validated in other studies. This approach provided sufficient experimental and analytical support to formulate potential hypotheses and draw general conclusions about the processes affected by *P. falciparum* on placental tissue.

7. Perspectives

To continue studying the effect of *Plasmodium* spp on the placenta using complementary models such as organoids is considered a challenge, as it allows the implementation of new methodological strategies in the laboratory. Not only assessing the effect of *P. falciparum* but also the effect of *P. vivax* would be interesting, as it is one of the species that generates a high number of infectious cases. Similar to *P. falciparum*, *P. vivax* is associated with maternal and fetal health detriment.

Conducting more detailed studies on cellular integrity and villous stroma, for instance, through the specific use of markers for Hofbauer cells, fibroblasts cells, STB, or indicators such as fibronectin and vimentin, among others, would provide complementary insights into collagen redistribution. This approach helps elucidate more precisely how infection can alter tissue integrity specifically and the elements contributing to such damage. It allows for a thorough understanding of how infection adversely affects not only the cellular environment but also the structural aspects of the tissue.

Elucidating the role of hemozoin will pose a future challenge and being able to assess it. Expanding the analyses in this regard will provide a more certain understanding of the impact of this parasitic material, which may persist even after the resolution of the Plasmodial infection.

Claim of Originality

All the results recorded in this work, as well as the tables and figures, are the student's own creation with the supervisor's endorsement, arising from the experimental processes conducted during the doctoral work. Figures borrowed from other works, used to illustrate certain aspects of the theoretical framework more clearly, are appropriately referenced with the respective source and author from which they were obtained or modified.

References

1.   White NJ, Pukrittayakamee S, Hien TT, Faiz MA, Mokuolu OA, Dondorp AM. Malaria. Lancet. 2014;383(9918):723-35.
2.   Zakama AK, Ozarslan N, Gaw SL. Placental Malaria. Curr Trop Med Rep. 2020:1-10.
3.   WHO. World malaria report 2022. Geneva: World Health Organization; 2022. Licence: CC BY-NC-SA 3.0 IGO. 2022.
4.   Campos IM, Uribe ML, Cuesta C, Franco-Gallego A, Carmona-Fonseca J, Maestre A. Diagnosis of gestational, congenital, and placental malaria in Colombia: comparison of the efficacy of microscopy, nested polymerase chain reaction, and histopathology. Am J Trop Med Hyg. 2011;84(6):929-35.
5.   Burton G, Kaufmann, Peter, Huppertz, Berthold. Anatomy and Genesis of the Placenta. 3rd edn Amsterdam, The Netherlands: Academic Press ed: Knobil and Neill's Physiology of Reproduction; 2006. p. 189-243.
6.   Kurt Benirschke GJB, Rebecca N Baergen. Pathology of the Human Placenta. 6 ed: Springer Berlin, Heidelberg; 2012. p. XVIII, 941.
7.   Megli CJ, Coyne CB. Infections at the maternal-fetal interface: an overview of pathogenesis and defence. Nat Rev Microbiol. 2022;20(2):67-82.
8.   Fried M, Domingo GJ, Gowda CD, Mutabingwa TK, Duffy PE. Plasmodium falciparum: chondroitin sulfate A is the major receptor for adhesion of parasitized erythrocytes in the placenta. Exp Parasitol. 2006;113(1):36-42.
9.   Chua CLL, Khoo SKM, Ong JLE, Ramireddi GK, Yeo TW, Teo A. Malaria in Pregnancy: From Placental Infection to Its Abnormal Development and Damage. Front Microbiol. 2021;12:777343.
10.   Obiri D, Erskine IJ, Oduro D, Kusi KA, Amponsah J, Gyan BA, et al. Histopathological lesions and exposure to Plasmodium falciparum infections in the placenta increases the risk of preeclampsia among pregnant women. Sci Rep. 2020;10(1):8280.
11.   Chaikitgosiyakul S, Rijken MJ, Muehlenbachs A, Lee SJ, Chaisri U, Viriyavejakul P, et al. A morphometric and histological study of placental malaria shows significant changes to villous architecture in both Plasmodium falciparum and Plasmodium vivax infection. Malar J. 2014;13:4.
12.   Moormann AM, Sullivan AD, Rochford RA, Chensue SW, Bock PJ, Nyirenda T, et al. Malaria and pregnancy: placental cytokine expression and its relationship to intrauterine growth retardation. J Infect Dis. 1999;180(6):1987-93.
13.   Silver KL, Zhong K, Leke RG, Taylor DW, Kain KC. Dysregulation of angiopoietins is associated with placental malaria and low birth weight. PLoS One. 2010;5(3):e9481.
14.   SPITZ AJ. Malaria infection of the placenta and its influence on the incidence of prematurity in eastern Nigeria. Bull World Health Organ. 1959;21(2):242-4.
15.   Menendez C, Ordi J, Ismail MR, Ventura PJ, Aponte JJ, Kahigwa E, et al. The impact of placental malaria on gestational age and birth weight. J Infect Dis. 2000;181(5):1740-5.
16.   Vásquez AM, Segura C, Blair S. Induction of pro-inflammatory response of the placental trophoblast by Plasmodium falciparum infected erythrocytes and TNF. Malar J. 2013;12:421.
17.   Feeney ME. The immune response to malaria in utero. Immunol Rev. 2020;293(1):216-29.
18.   Lucchi NW, Koopman R, Peterson DS, Moore JM. Plasmodium falciparum-infected red blood cells selected for binding to cultured syncytiotrophoblast bind to chondroitin sulfate A and induce tyrosine phosphorylation in the syncytiotrophoblast. Placenta. 2006;27(4-5):384-94.
19.   Lucchi NW, Sarr D, Owino SO, Mwalimu SM, Peterson DS, Moore JM. Natural hemozoin stimulates syncytiotrophoblast to secrete chemokines and recruit peripheral blood mononuclear cells. Placenta. 2011;32(8):579-85.
20.   Rogerson SJ, Hviid L, Duffy PE, Leke RF, Taylor DW. Malaria in pregnancy: pathogenesis and immunity. Lancet Infect Dis. 2007;7(2):105-17.
21.   Bakken L, Iversen PO. The impact of malaria during pregnancy on low birth weight in East-Africa: a topical review. Malar J. 2021;20(1):348.

22.   Boström S, Ibitokou S, Oesterholt M, Schmiegelow C, Persson JO, Minja D, et al. Biomarkers of Plasmodium falciparum infection during pregnancy in women living in northeastern Tanzania. PLoS One. 2012;7(11):e48763.

23.   Silver KL, Conroy AL, Leke RG, Leke RJ, Gwanmesia P, Molyneux ME, et al. Circulating soluble endoglin levels in pregnant women in Cameroon and Malawi--associations with placental malaria and fetal growth restriction. PLoS One. 2011;6(9):e24985.

24.   Chêne A, Briand V, Ibitokou S, Dechavanne S, Massougbodji A, Deloron P, et al. Placental cytokine and chemokine profiles reflect pregnancy outcomes in women exposed to Plasmodium falciparum infection. Infect Immun. 2014;82(9):3783-9.

25.   Lucchi NW, Peterson DS, Moore JM. Immunologic activation of human syncytiotrophoblast by Plasmodium falciparum. Malar J. 2008;7:42.

26.   McGready R, Davison BB, Stepniewska K, Cho T, Shee H, Brockman A, et al. The effects of *Plasmodium falciparum* and *P. vivax* infections on placental histopathology in an area of low malaria transmission. Am J Trop Med Hyg. 2004; 70(4):398-407.

27.   López-Guzmán C, Carmona-Fonseca J. Submicroscopic placental malaria: histopathology and expression of physiological process mediators. Rev Peru Med Exp Salud Publica. 2020;37(2):220-8.

28.   Castillo C, Muñoz L, Carrillo I, Liempi A, Gallardo C, Galanti N, et al. Ex vivo infection of human placental chorionic villi explants with Trypanosoma cruzi and Toxoplasma gondii induces different Toll-like receptor expression and cytokine/chemokine profiles. Am J Reprod Immunol. 2017;78(1).

29.   Liempi A, Castillo C, Medina L, Galanti N, Maya JD, Parraguez VH, et al. Comparative ex vivo infection with Trypanosoma cruzi and Toxoplasma gondii of human, canine and ovine placenta: Analysis of tissue damage and infection efficiency. Parasitol Int. 2020;76:102065.

30.   Crocker IP, Tansinda DM, Baker PN. Altered cell kinetics in cultured placental villous explants in pregnancies complicated by pre-eclampsia and intrauterine growth restriction. J Pathol. 2004;204(1):11-8.

31.   Hoo Regina RE, Kelava Iva, et al. Early infection response of the first trimester human placenta at single-cell scale. bioRxiv preprint ed: bioRxiv preprint; 2023. p. 2-44.

32.   Wice B, Menton D, Geuze H, Schwartz AL. Modulators of cyclic AMP metabolism induce syncytiotrophoblast formation in vitro. Exp Cell Res. 1990;186(2):306-16.

33.   Sheridan MA, Fernando RC, Gardner L, Hollinshead MS, Burton GJ, Moffett A, et al. Establishment and differentiation of long-term trophoblast organoid cultures from the human placenta. Nat Protoc. 2020;15(10):3441-63.

34.   Dellicour S, Tatem AJ, Guerra CA, Snow RW, ter Kuile FO. Quantifying the number of pregnancies at risk of malaria in 2007: a demographic study. PLoS Med. 2010;7(1):e1000221.

35.   Desai M, ter Kuile FO, Nosten F, McGready R, Asamoa K, Brabin B, et al. Epidemiology and burden of malaria in pregnancy. Lancet Infect Dis. 2007;7(2):93-104.

36.   Cardona-Arias JA, Carmona-Fonseca J. Frequency of placental malaria and its associated factors in northwestern Colombia, pooled analysis 2009-2020. PLoS One. 2022;17(5):e0268949.

37.   Cardona-Arias JA, Carmona-Fonseca J. Meta-analysis of the prevalence of malaria associated with pregnancy in Colombia 2000-2020. PLoS One. 2021;16(7):e0255028.

38.   Ashley EA, Pyae Phyo A, Woodrow CJ. Malaria. Lancet. 2018;391(10130):1608-21.

39.   Venugopal K, Hentzschel F, Valkiūnas G, Marti M. Plasmodium asexual growth and sexual development in the haematopoietic niche of the host. Nat Rev Microbiol. 2020;18(3):177-89.

40.   Duffy PE. Plasmodium in the placenta: parasites, parity, protection, prevention and possibly preeclampsia. Parasitology. 2007;134(Pt 13):1877-81.

41.   Duffy MF, Maier AG, Byrne TJ, Marty AJ, Elliott SR, O'Neill MT, et al. VAR2CSA is the principal ligand for chondroitin sulfate A in two allogeneic isolates of *Plasmodium falciparum.* Mol Biochem Parasitol. 2006; 148(2):117-24.

42.   Beeson JG, Amin N, Kanjala M, Rogerson SJ. Selective accumulation of mature asexual stages of Plasmodium falciparum-infected erythrocytes in the placenta. Infect Immun. 2002;70(10):5412-5.

43.   Dasari P, Reiss K, Lingelbach K, Baumeister S, Lucius R, Udomsangpetch R, et al. Digestive vacuoles of *Plasmodium falciparum* are selectively phagocytosed by and impair killing function of polymorphonuclear leukocytes. Blood. 2011;118(18):4946-56.

44.   Shio MT, Kassa FA, Bellemare MJ, Olivier M. Innate inflammatory response to the malarial pigment hemozoin. Microbes Infect. 2010;12(12-13):889-99.

45.   Hempelmann E. Hemozoin biocrystallization in Plasmodium falciparum and the antimalarial activity of crystallization inhibitors. Parasitol Res. 2007;100(4):671-6.

46.   Fried M, Kurtis JD, Swihart B, Pond-Tor S, Barry A, Sidibe Y, et al. Systemic Inflammatory Response to Malaria During Pregnancy Is Associated With Pregnancy Loss and Preterm Delivery. Clin Infect Dis. 2017;65(10):1729-35.

47.   Aplin JD. Implantation, trophoblast differentiation and haemochorial placentation: mechanistic evidence in vivo and in vitro. J Cell Sci. 1991;99 (Pt 4):681-92.

48.   J James. Overview of Human Implantation. Linda M. McManus, Richard N. Mitchell ed: Pathobiology of Human Disease, Academic Press; 2014. p. 2293-307.

49.   Ander SE, Rudzki EN, Arora N, Sadovsky Y, Coyne CB, Boyle JP. Human Placental Syncytiotrophoblasts Restrict. mBio. 2018;9(1).

50.   Gauster M HB. Fusion of Cytothrophoblast with Syncytiotrophoblast in the Human Placenta: Factors Involved in Syncytialization. J. Reproduktionsmed. Endokrinol; 2008. p. 76-82.

51.   Jaremek A, Jeyarajah MJ, Jaju Bhattad G, Renaud SJ. Omics Approaches to Study Formation and Function of Human Placental Syncytiotrophoblast. Front Cell Dev Biol. 2021;9:674162.

52.   Huppertz B, Gauster M. Trophoblast fusion. Adv Exp Med Biol. 2011;713:81-95.

53.   West RC, Ming H, Logsdon DM, Sun J, Rajput SK, Kile RA, et al. Dynamics of trophoblast differentiation in peri-implantation-stage human embryos. Proc Natl Acad Sci U S A. 2019;116(45):22635-44.

54.   Orendi K, Gauster M, Moser G, Meiri H, Huppertz B. The choriocarcinoma cell line BeWo: syncytial fusion and expression of syncytium-specific proteins. Reproduction. 2010;140(5):759-66.

55.   RICHART R. Studies of placental morphogenesis. I. Radioautographic studies of human placenta utilizing tritiated thymidine. Proc Soc Exp Biol Med. 1961;106:829-31.

56.   Garcia-Lloret MI, Morrish DW, Wegmann TG, Honore L, Turner AR, Guilbert LJ. Demonstration of functional cytokine-placental interactions: CSF-1 and GM-CSF stimulate human cytotrophoblast differentiation and peptide hormone secretion. Exp Cell Res. 1994;214(1):46-54.

57.   Tug E, Yirmibes Karaoguz M, Nas T. Expression of the syncytin-1 and syncytin-2 genes in the trophoblastic tissue of the early pregnancy losses with normal and abnormal karyotypes. Gene. 2020;741:144533.

58.   Napso T, Zhao X, Lligoña MI, Sandovici I, Kay RG, George AL, et al. Placental secretome characterization identifies candidates for pregnancy complications. Commun Biol. 2021;4(1):701.

59.   Sarah L. Berga JFN, Glenn D. Braunstein. Chapter 21 - Endocrine Changes in Pregnancy. Williams Textbook of Endocrinology (Thirteenth Edition) ed2016. p. 831-48.

60.   Huppertz B, Kadyrov M, Kingdom JC. Apoptosis and its role in the trophoblast. Am J Obstet Gynecol. 2006;195(1):29-39.

61.   da Silva Castro A, Angeloni MB, de Freitas Barbosa B, de Miranda RL, Teixeira SC, Guirelli PM, et al. BEWO trophoblast cells and Toxoplasma gondii infection modulate cell death mechanisms in THP-1 monocyte cells by interference in the expression of death receptor and intracellular proteins. Tissue Cell. 2021;73:101658.

62.   Al-Nasiry S, Spitz B, Hanssens M, Luyten C, Pijnenborg R. Differential effects of inducers of syncytialization and apoptosis on BeWo and JEG-3 choriocarcinoma cells. Hum Reprod. 2006;21(1):193-201.

63.   Loukeris K, Sela R, Baergen RN. Syncytial knots as a reflection of placental maturity: reference values for 20 to 40 weeks' gestational age. Pediatr Dev Pathol. 2010;13(4):305-9.

64.   Burton GJ, Jones CJ. Syncytial knots, sprouts, apoptosis, and trophoblast deportation from the human placenta. Taiwan J Obstet Gynecol. 2009;48(1):28-37.

65.   Fogarty NM, Ferguson-Smith AC, Burton GJ. Syncytial knots (Tenney-Parker changes) in the human placenta: evidence of loss of transcriptional activity and oxidative damage. Am J Pathol. 2013;183(1):144-52.

66.   Kidima WB. Syncytiotrophoblast Functions and Fetal Growth Restriction during Placental Malaria: Updates and Implication for Future Interventions. Biomed Res Int. 2015;2015:451735.

67.   Nelson DM, Crouch EC, Curran EM, Farmer DR. Trophoblast interaction with fibrin matrix. Epithelialization of perivillous fibrin deposits as a mechanism for villous repair in the human placenta. Am J Pathol. 1990;136(4):855-65.

68.   Crocker IP, Strachan BK, Lash GE, Cooper S, Warren AY, Baker PN. Vascular endothelial growth factor but not placental growth factor promotes trophoblast syncytialization in vitro. J Soc Gynecol Investig. 2001;8(6):341-6.

69.   Mor G, Cardenas I. The immune system in pregnancy: a unique complexity. Am J Reprod Immunol. 2010;63(6):425-33.

70.   Yockey LJ, Iwasaki A. Interferons and Proinflammatory Cytokines in Pregnancy and Fetal Development. Immunity. 2018;49(3):397-412.

71.   Mayhew TM, Charnock-Jones DS, Kaufmann P. Aspects of human fetoplacental vasculogenesis and angiogenesis. III. Changes in complicated pregnancies. Placenta. 2004;25(2-3):127-39.

72.   Rodríguez-Cortésa Y, Mendieta-Zeróna H. La placenta como órgano endocrino compartido y su acción en elembarazo normoevolutivo.: Revista de Medicina e Investigación. ELSEVIER; 2014. p. 28-34.

73.   Schumacher A, Costa SD, Zenclussen AC. Endocrine Factors Modulating Immune Responses in Pregnancy. Front Immunol.   2014;5:196.

74.   Caniggia I, Taylor CV, Ritchie JW, Lye SJ, Letarte M. Endoglin regulates trophoblast differentiation along the invasive pathway in human placental villous explants. Endocrinology. 1997;138(11):4977-88.

75.   Kaufmann P, Mayhew TM, Charnock-Jones DS. Aspects of human fetoplacental vasculogenesis and angiogenesis. II. Changes during normal pregnancy. Placenta. 2004;25(2-3):114-26.

76.   Shibuya M. Vascular endothelial growth factor receptor-1 (VEGFR-1/Flt-1): a dual regulator for angiogenesis. Angiogenesis. 2006;9(4):225-30.

77.   Yang D, Dai F, Yuan M, Zheng Y, Liu S, Deng Z, et al. Role of Transforming Growth Factor-β1 in Regulating Fetal-Maternal Immune Tolerance in Normal and Pathological Pregnancy. Front Immunol. 2021;12:689181.

78.   Goyal P, Brünnert D, Ehrhardt J, Bredow M, Piccenini S, Zygmunt M. Cytokine IL-6 secretion by trophoblasts regulated via sphingosine-1-phosphate receptor 2 involving Rho/Rho-kinase and Rac1 signaling pathways. Mol Hum Reprod. 2013;19(8):528-38.

79.   Geremia A, Jewell DP. The IL-23/IL-17 pathway in inflammatory bowel disease. Expert Rev Gastroenterol Hepatol. 2012;6(2):223-37.

80.   Wang Y, Zhao S. Vascular Biology of the Placenta. 2010.

81.   Demir-Weusten AY, Seval Y, Kaufmann P, Demir R, Yucel G, Huppertz B. Matrix metalloproteinases-2, -3 and -9 in human term placenta. Acta Histochem. 2007;109(5):403-12.

82.   Amenta PS, Gay S, Vaheri A, Martinez-Hernandez A. The extracellular matrix is an integrated unit: ultrastructural localization of collagen types I, III, IV, V, VI, fibronectin, and laminin in human term placenta. Coll Relat Res. 1986;6(2):125-52.

83.   Korhonen M, Virtanen I. The distribution of laminins and fibronectins is modulated during extravillous trophoblastic cell differentiation and decidual cell response to invasion in the human placenta. J Histochem Cytochem. 1997;45(4):569-81.

84.   Castellucci M, Kaufmann P, Bischof P. Extracellular matrix influences hormone and protein production by human chorionic villi. Cell Tissue Res. 1990;262(1):135-42.

85.   Sati L, Demir AY, Sarikcioglu L, Demir R. Arrangement of collagen fibers in human placental stem villi. Acta Histochem. 2008;110(5):371-9.

86.   Vizza E, Goranova V, Heyn R, Correr S, Motta PM. Extracellular fibrillar matrix architecture of human placental villi at term. Ital J Anat Embryol. 2001;106(2 Suppl 2):317-23.

87.   Oefner CM, Sharkey A, Gardner L, Critchley H, Oyen M, Moffett A. Collagen type IV at the fetal-maternal interface. Placenta. 2015;36(1):59-68.

88.   Demir R, Kosanke G, Kohnen G, Kertschanska S, Kaufmann P. Classification of human placental stem villi: review of structural and functional aspects. Microsc Res Tech. 1997;38(1-2):29-41.

89.   Koi H, Zhang J, Parry S. The mechanisms of placental viral infection. Ann N Y Acad Sci. 2001;943:148-56.

90.   Friedman JF, Mital P, Kanzaria HK, Olds GR, Kurtis JD. Schistosomiasis and pregnancy. Trends Parasitol. 2007;23(4):159-64.

91.   Correa D, Cañedo-Solares I, Ortiz-Alegría LB, Caballero-Ortega H, Rico-Torres CP. Congenital and acquired toxoplasmosis: diversity and role of antibodies in different compartments of the host. Parasite Immunol. 2007;29(12):651-60.

92.   Rocha G, Martins A, Gama G, Brandão F, Atouguia J. Possible cases of sexual and congenital transmission of sleeping sickness. Lancet. 2004;363(9404):247.

93.   Rogerson SJ, Pollina E, Getachew A, Tadesse E, Lema VM, Molyneux ME. Placental monocyte infiltrates in response to Plasmodium falciparum malaria infection and their association with adverse pregnancy outcomes. Am J Trop Med Hyg. 2003;68(1):115-9.

94.   Suguitan AL, Leke RG, Fouda G, Zhou A, Thuita L, Metenou S, et al. Changes in the levels of chemokines and cytokines in the placentas of women with Plasmodium falciparum malaria. J Infect Dis. 2003;188(7):1074-82.

95.   Fried M, Muga RO, Misore AO, Duffy PE. Malaria elicits type 1 cytokines in the human placenta: IFN-gamma and TNF-alpha associated with pregnancy outcomes. J Immunol. 1998;160(5):2523-30.

96.   Tomlinson A, Semblat JP, Gamain B, Chêne A. VAR2CSA-Mediated Host Defense Evasion of. Front Immunol. 2020;11:624126.

97.   Steketee RW, Wirima JJ, Hightower AW, Slutsker L, Heymann DL, Breman JG. The effect of malaria and malaria prevention in pregnancy on offspring birthweight, prematurity, and intrauterine growth retardation in rural Malawi. Am J Trop Med Hyg. 1996;55(1 Suppl):33-41.

98.   Agudelo-García OM, Arango-Flórez EM, Carmona-Fonseca J. Submicroscopic and Asymptomatic Congenital Infection by *Plasmodium vivax* or *P. falciparum* in Colombia: 37 Cases with Placental Histopathology and Cytokine Profile in Maternal and Placental Blood. J Trop Med. 2017; 2017:368078.

99.   McGready R, Brockman A, Cho T, Levesque MA, Tkachuk AN, Meshnick SR, et al. Haemozoin as a marker of placental parasitization. Trans R Soc Trop Med Hyg. 2002;96(6):644-6.

100.   Tyberghein A, Deroost K, Schwarzer E, Arese P, Van den Steen PE. Immunopathological effects of malaria pigment or hemozoin and other crystals. Biofactors. 2014;40(1):59-78.

101.   Drewlo S, Baczyk D, Dunk C, Kingdom J. Fusion assays and models for the trophoblast. Methods Mol Biol. 2008;475:363-82.

102.   Sheridan MA, Zhao X, Fernando RC, Gardner L, Perez-Garcia V, Li Q, et al. Characterization of primary models of human trophoblast. Development. 2021;148(21).

103.   Miller RK, Genbacev O, Turner MA, Aplin JD, Caniggia I, Huppertz B. Human placental explants in culture: approaches and assessments. Placenta. 2005;26(6):439-48.

104.   Jebbink J, Keijser R, Veenboer G, van der Post J, Ris-Stalpers C, Afink G. Expression of placental FLT1 transcript variants relates to both gestational hypertensive disease and fetal growth. Hypertension. 2011;58(1):70-6.

105.   Orendi K, Kivity V, Sammar M, Grimpel Y, Gonen R, Meiri H, et al. Placental and trophoblastic in vitro models to study preventive and therapeutic agents for preeclampsia. Placenta. 2011;32 Suppl:S49-54.

106.   ATCC. BeWo is a cell line CCL-98 ™.

107.   Matsuura K, Jigami T, Taniue K, Morishita Y, Adachi S, Senda T, et al. Identification of a link between Wnt/β-catenin signalling and the cell fusion pathway. Nat Commun. 2011;2:548.

108.   Trager W, Jenson, J. Cultivation of malarial parasites. *Nature*; 1978. p. 621-2.

109.   López-Guzmán C, García AM, Marín P, Vásquez AM. Assessment of the Integrity and Function of Human Term Placental Explants in Short-Term Culture. Methods Protoc. 2024;7(1).

110.   Gibson-Corley KN, Olivier AK, Meyerholz DK. Principles for valid histopathologic scoring in research. Vet Pathol. 2013;50(6):1007-15.

111.   Orbán A, Butykai Á, Molnár A, Pröhle Z, Fülöp G, Zelles T, et al. Evaluation of a novel magneto-optical method for the detection of malaria parasites. PLoS One. 2014;9(5):e96981.

112.   Duaso J, Rojo G, Cabrera G, Galanti N, Bosco C, Maya JD, et al. Trypanosoma cruzi induces tissue disorganization and destruction of chorionic villi in an ex vivo infection model of human placenta. Placenta. 2010;31(8):705-11.

113.   Roch A, Prodéo J, Pierart C, Muller RN, Duez P. The paramagnetic properties of malaria pigment, hemozoin, yield clues to a low-cost system for its trapping and determination. Talanta. 2019;197:553-7.

114.   Salanti A, Staalsoe T, Lavstsen T, Jensen AT, Sowa MP, Arnot DE, et al. Selective upregulation of a single distinctly structured var gene in chondroitin sulphate A-adhering Plasmodium falciparum involved in pregnancy-associated malaria. Mol Microbiol. 2003;49(1):179-91.

115.   Muthusamy A, Achur RN, Bhavanandan VP, Fouda GG, Taylor DW, Gowda DC. Plasmodium falciparum-infected erythrocytes adhere both in the intervillous space and on the villous surface of human placenta by binding to the low-sulfated chondroitin sulfate proteoglycan receptor. Am J Pathol. 2004;164(6):2013-25.

116.   Salanti A, Dahlbäck M, Turner L, Nielsen MA, Barfod L, Magistrado P, et al. Evidence for the involvement of VAR2CSA in pregnancy-associated malaria. J Exp Med. 2004;200(9):1197-203.

117.   Liu M, Hassana S, Stiles JK. Heme-mediated apoptosis and fusion damage in BeWo trophoblast cells. Sci Rep. 2016;6:36193.

118.   Baczyk D, Satkunaratnam A, Nait-Oumesmar B, Huppertz B, Cross JC, Kingdom JC. Complex patterns of GCM1 mRNA and protein in villous and extravillous trophoblast cells of the human placenta. Placenta. 2004;25(6):553-9.

119.   Lin C, Lin M, Chen H. Biochemical characterization of the human placental transcription factor GCMa/1. Biochem Cell Biol. 2005;83(2):188-95.

120.   Mi S, Lee X, Li X, Veldman GM, Finnerty H, Racie L, et al. Syncytin is a captive retroviral envelope protein involved in human placental morphogenesis. Nature. 2000;403(6771):785-9.

121.   Lu X, Wang R, Zhu C, Wang H, Lin HY, Gu Y, et al. Fine-Tuned and Cell-Cycle-Restricted Expression of Fusogenic Protein Syncytin-2 Maintains Functional Placental Syncytia. Cell Rep. 2018;23(13):3979.

122.   Zhou H, Zhao C, Wang P, Yang W, Zhu H, Zhang S. Regulators involved in trophoblast syncytialization in the placenta of intrauterine growth restriction. Front Endocrinol (Lausanne). 2023;14:1107182.

123.   Sharma L, Kaur J, Shukla G. Role of oxidative stress and apoptosis in the placental pathology of Plasmodium berghei infected mice. PLoS One. 2012;7(3):e32694.

124.   Huppertz B, Bartz C, Kokozidou M. Trophoblast fusion: fusogenic proteins, syncytins and ADAMs, and other prerequisites for syncytial fusion. Micron. 2006;37(6):509-17.

125.   Staff AC, Dechend R, Pijnenborg R. Learning from the placenta: acute atherosis and vascular remodeling in preeclampsia-novel aspects for atherosclerosis and future cardiovascular health. Hypertension. 2010;56(6):1026-34.

126.   Heazell AE, Moll SJ, Jones CJ, Baker PN, Crocker IP. Formation of syncytial knots is increased by hyperoxia, hypoxia and reactive oxygen species. Placenta. 2007;28 Suppl A:S33-40.

127.   Walter PR, Garin Y, Blot P. Placental pathologic changes in malaria. A histologic and ultrastructural study. Am J Pathol. 1982;109(3):330-42.

128.   McDermott M, Gillan JE. Chronic reduction in fetal blood flow is associated with placental infarction. Placenta. 1995;16(2):165-70.

129.   Ishihara N, Matsuo H, Murakoshi H, Laoag-Fernandez JB, Samoto T, Maruo T. Increased apoptosis in the syncytiotrophoblast in human term placentas complicated by either preeclampsia or intrauterine growth retardation. Am J Obstet Gynecol. 2002;186(1):158-66.

130.   Sankar KD, Bhanu PS, Kiran S, Ramakrishna BA, Shanthi V. Vasculosyncytial membrane in relation to syncytial knots complicates the placenta in preeclampsia: a histomorphometrical study. Anat Cell Biol. 2012;45(2):86-91.

131.   Shi JW, Lai ZZ, Yang HL, Yang SL, Wang CJ, Ao D, et al. Collagen at the maternal-fetal interface in human pregnancy. Int J Biol Sci. 2020;16(12):2220-34.

132.   Teodoro WR, Andreucci D, Palma JA. Short communication: placental collagen and premature rupture of fetal membranes. Placenta. 1990;11(6):549-51.

133.   Feng Y, Chen X, Wang H, Lan Z, Li P, Cao Y, et al. Collagen I Induces Preeclampsia-Like Symptoms by Suppressing Proliferation and Invasion of Trophoblasts. Front Endocrinol (Lausanne). 2021;12:664766.

134.   Bulmer JN, Rasheed FN, Morrison L, Francis N, Greenwood BM. Placental malaria. II. A semi-quantitative investigation of the pathological features. Histopathology. 1993;22(3):219-25.

135.   Ismail MR, Ordi J, Menendez C, Ventura PJ, Aponte JJ, Kahigwa E, et al. Placental pathology in malaria: a histological, immunohistochemical, and quantitative study. Hum Pathol. 2000;31(1):85-93.

136.   Matteelli A, Caligaris S, Castelli F, Carosi G. The placenta and malaria. Ann Trop Med Parasitol. 1997;91(7):803-10.

137.   Simán CM, Sibley CP, Jones CJ, Turner MA, Greenwood SL. The functional regeneration of syncytiotrophoblast in cultured explants of term placenta. Am J Physiol Regul Integr Comp Physiol. 2001;280(4):R1116-22.

138.   López ML, Arango EM, Arias LR, Carmona-Fonseca J, Silvia B. Intraleucocytic hemozoine as an indicator of malaria complicated by *Plasmodium falciparum*. Acta Médica Colombiana. 2004;29(2):80-7.

139.   Moore JM, Chaisavaneeyakorn S, Perkins DJ, Othoro C, Otieno J, Nahlen BL, et al. Hemozoin differentially regulates proinflammatory cytokine production in human immunodeficiency virus-seropositive and -seronegative women with placental malaria. Infect Immun. 2004;72(12):7022-9.

140.   Chen CP, Aplin JD. Placental extracellular matrix: gene expression, deposition by placental fibroblasts and the effect of oxygen. Placenta. 2003;24(4):316-25.

141.   Fuchs Y, Steller H. Programmed cell death in animal development and disease. Cell. 2011;147(4):742-58.

142.   Fievet N, Moussa M, Tami G, Maubert B, Cot M, Deloron P, et al. Plasmodium falciparum induces a Th1/Th2 disequilibrium, favoring the Th1-type pathway, in the human placenta. J Infect Dis. 2001;183(10):1530-4.

143.   J. L-GCC-F. Malaria placentaria submicroscópica: histopatología y expresión de mediadores de procesos fisiológicos. Revista Peruana de Medicina Experimental y Salud Publica; 2020. p. 220-8.

144.   Nevo O, Soleymanlou N, Wu Y, Xu J, Kingdom J, Many A, et al. Increased expression of sFlt-1 in in vivo and in vitro models of human placental hypoxia is mediated by HIF-1. Am J Physiol Regul Integr Comp Physiol. 2006;291(4):R1085-93.

145.   Mezzano L, Sartori MJ, Lin S, Repossi G, de Fabro SP. Placental alkaline phosphatase (PLAP) study in diabetic human placental villi infected with Trypanosoma cruzi. Placenta. 2005;26(1):85-92.

146.   Seitz J, Morales-Prieto DM, Favaro RR, Schneider H, Markert UR. Molecular Principles of Intrauterine Growth Restriction in Plasmodium Falciparum Infection. Front Endocrinol (Lausanne). 2019;10:98.

147.   Menendez C, Mayor A. Congenital malaria: the least known consequence of malaria in pregnancy. Semin Fetal Neonatal Med. 2007;12(3):207-13.

148.   Smith SC, Baker PN, Symonds EM. Increased placental apoptosis in intrauterine growth restriction. Am J Obstet Gynecol. 1997;177(6):1395-401.

149.   Chan G, Guilbert LJ. Ultraviolet-inactivated human cytomegalovirus induces placental syncytiotrophoblast apoptosis in a Toll-like receptor-2 and tumour necrosis factor-alpha dependent manner. J Pathol. 2006;210(1):111-20.

150.   Abbasi M, Kowalewska-Grochowska K, Bahar MA, Kilani RT, Winkler-Lowen B, Guilbert LJ. Infection of placental trophoblasts by Toxoplasma gondii. J Infect Dis. 2003;188(4):608-16.

151.   Sooranna SR, Oteng-Ntim E, Meah R, Ryder TA, Bajoria R. Characterization of human placental explants: morphological, biochemical and physiological studies using first and third trimester placenta. Hum Reprod. 1999;14(2):536-41.